

THE ROLE OF SUSTENTACULAR CELLS IN ADULT NEUROGENESIS

by

Burak Bali

B.S., Molecular Biology and Genetics, Boğaziçi University, 2013

Submitted to the Institute of Graduate Studies in
Science and Engineering in partial fulfillment of
the requirements for the degree

Master of Science

Graduate Program in Molecular Biology and Genetics

Boğaziçi University

2015

ACKNOWLEDGEMENTS

The story of my master studies has started on the day that I went to talk my future supervisor who told me that a scientific research is like a story. It has chapters that are related to each other and that have an order, which explain different aspects of the whole story. This thesis, or the story of my master's years, would not have been written without Dr. Stefan Fuss whom I thank for his guidance through these years, for teaching me how a scientist should think and for introducing me to the colorful world of Neurosciences.

This story would not be created without the superheroes in it. I thank captain of 'Team Neurogenesis' Xalid Bayramlı for his valuable contributions to my experiments and for his mentorship. A great portion of my thanks is for Büşra Çoban and Serdar Çapar who are not just colleagues but the ones making it possible to me to have a kind of friendship that I've never tasted before. I'm grateful to them that we share laughter and wipe tears together, and I also thank Büşra Çoban for her illustrations.

I want to thank our precious collaborators Dr. Ivan Manzini and his team members Dr. Thomas Hassenklöver and Katharina Dittrich for hosting me in their group to teach calcium imaging and single-cell EP. I would also like to thank old and new members of the FishLab; Gizem Sancer, Burak Kaya, Yusuf Kazçı, Metin Özdemir, Mehmet Can Demirler, for providing a nice working environment and for having jokes together. I also present my thanks to our sister lab 'FlyLab' member, Çağrı Çevrim, for his technological support. I also want to thank Ayşe Candayan for bringing me joy with her little surprises in my depressed moments. Oğuz Arı and Esra Yıldız deserve thanks for their lunch companionship. Without my parents, I could not be where I am now. This work is a little present for their priceless efforts on me.

I wish to thank TUBITAK for supporting me by '2210-E Doğrudan Yurt İçi Yüksek Lisans Burs Programı (2013-2)'. The work on this project was supported by TUBITAK project 113T038 to Dr. Stefan H. Fuss.

ABSTRACT

THE ROLE OF SUSTENTACULAR CELLS IN ADULT NEUROGENESIS

The olfactory epithelium (OE) provides a unique exception to the limited ability of the nervous system to regenerate itself. Olfactory sensory neurons (OSN) are directly exposed to the outside world, prone to environmental insult, and need to be replaced continuously to maintain a sense of smell. An open question is, how proliferation of neuronal progenitors is regulated at the tissue level. Generally, the vertebrate olfactory sensory tissue is composed of OSN, sustentacular cells (Sus), which is a unique type of olfactory glia, as well as neuronal stem cell and precursor populations. However, olfactory stem cells and Sus have not been described in zebrafish. To gain more insight into the cellular architecture and physiological role of different cell types in the zebrafish OE, immunohistochemical stainings with cell type-specific markers and physiological studies of intercellular signaling were performed. Immunohistochemistry against the intermediate filament cytokeratin II, for the first time, visualizes the entire population of zebrafish Sus. Sus are abundant, span the entire apicobasal dimension of the tissue and are regularly spaced throughout the sensory region of the epithelium. Interestingly, Sus also appear to be positive for the progenitor marker Sox2. Thus, Sus may contribute to olfactory sensory neuron regeneration in two, not necessarily exclusive ways. Sus could dedifferentiate and reacquire neuronal progenitor cell identity or they could communicate signals from OE tissue to basal stem cell / progenitor populations. To investigate these possibilities, cytokeratin II immunohistochemistry was combined with BrdU cell proliferation assays and immunohistochemistry for neuronal progenitor markers, such as nestin and sox2. To examine if Sus can communicate between the tissue and stem cells, functional Ca^{2+} -imaging and pharmacological manipulation was performed on olfactory tissue slices upon purine stimulation. The outcome of these experiments suggests that both Sus and a basal cell population respond to purine stimulation but may utilize different receptors to mediate responses, supporting the possibility of direct signaling Sus onto basal neuronal precursors.

ÖZET

DESTEK HÜCRELERİNİN YETİŞKİN NÖROGENEZDEKİ ROLÜ

Koku alma dokusu, sinir sisteminin sınırlı yenilenme yeteneğinin benzersiz bir örneğidir. Koku duyu nöronları, doğrudan dış dünyaya maruz kaldığından, çevresel müdahaleye açıktır ve koku duyusunun devamlılığı için sürekli olarak yenilenmesi gereklidir. Ancak, nöronal öncü hücrelerin çoğalmasının doku düzeyinde nasıl düzenlendiği sorgulanmaya açıktır. Omurgalı koku alma dokusu, nöronal kök hücre, öncü hücre topluluğu ve koku alma nöronları ile birlikte, destek hücresi de denilen özel bir tip koku-glia hücrelerinden oluşur. Buna karşın, koku dokusu kök hücreleri ile belirtilen destek hücreleri zebribalığında henüz tanımlanmamıştır. Bu çalışmada zebribalığı koku epitelinin hücresel yapısına ve farklı hücre tiplerinin fizyolojik rollerine dair daha geniş bir bakış açısı kazanmak için, zebribalığı koku dokusunu oluşturan farklı hücre tiplerinin moleküller ve fizyolojik karakterizasyonlarını gösterdik. Zebribalığı destek hücrelerini ara iplik sitokeratin II'yi hedef alan boyama yöntemi kullanarak, ilk defa olarak gözlemleyebildik. Destek hücrelerinin, dokunun duyusal bölgesi boyunca, bol miktarda, düzenli aralıklarla bulunduğu ve dokunun apiko-bazal yüzeyini kapladığını gösterdik. İlginç bir şekilde, destek hücrelerinin, öncü hücre belirteci, Sox2 için pozitif olduğunu gözlemledik. Bu sebeple destek hücrelerinin koku duyusu nöronlarının yenilenmesine, birbirini dışlamayan iki şekilde katkı sağladığını söyleyebilir. Destek hücreleri ters-farklılaşmayla nöronal öncü hücre kimliğini yeniden kazanabilir ya da koku epители dokusundan aldığı sinyallerin basal kök hücre/öncü hücre topluluklarına iletilmesini sağlar. Bu olasılıkların araştırılması için, sitokeratin II boyaması, çoğalma analizi olan BrdU analizi ve nöronal öncü belirteci olan Nestin ve Sox2 boyaması ile birleştirildi. Destek hücrelerinin doku ve kök hücreler arasındaki iletişimini sağladığı tezini incelemek için koku dokusu mikro-kesiti üzerinde pürin uyarımı ve farmakolojik uygulamalar ile birlikte işlevsel Ca^{2+} görüntülemesi yöntemine başvuruldu. Deneylerimizin sonucu, destek hücreleri ile basal olarak yerleşmiş öncü hücreler arasındaki doğrudan iletişimini destekler şekilde, hem destek hücrelerinin hem de basal olarak yerleşmiş hücre popülasyonunun pürin uyarımına yanıt verdiği, fakat yanıtların geliştirilmesinde farklı almaçların kullanılabileceğini göstermektedir.

TABLE OF CONTENTS

ACKNOWLEDGEMENTS	iii
ABSTRACT	iv
ÖZET	v
LIST OF FIGURES	viii
LIST OF TABLES	ix
LIST OF ACRONYMS / ABBREVIATIONS	x
1. INTRODUCTION	1
1.1. Adult neurogenesis	1
1.2. Neurogenesis in adult zebrafish CNS	2
1.3. Neurogenesis in olfactory epithelium	2
1.4. Organization of the olfactory epithelium	3
1.5. Sustentacular cells in the OE	4
1.6. Glial cells in adult neurogenesis	5
1.7. Possible progenitor cells in OE	6
1.8. Molecular mechanisms governing neurogenesis in OE	7
2. PURPOSE	9
3. MATERIALS AND METHODS	10
3.1. Materials	10
3.1.1. Model organism	10
3.1.2. Equipment and supplies	10
3.1.3. Buffers and solutions	10
3.2. Methods	11
3.2.1. Maintenance of fish	11
3.2.2. Dissection of zebrafish	11
3.2.3. Sectioning of the OE	11
3.2.4. Immunohistochemistry and nuclear staining	12
3.2.5. BrdU incorporation assay	13
3.2.6. Tissue dissociation assay	13
3.2.7. Single-cell electroporation	14

3.2.8. Functional calcium imaging.....	14
4. RESULTS	15
4.1. A synopsis	15
4.2. A Cytokeratin II antibody labels sustentacular cells in zebrafish OE	15
4.3. Neuronal progenitor markers are expressed in sustentacular cells.....	22
4.3.1. Expression of nestin on zebrafish olfactory epithelium.....	22
4.3.2. Individual cells are both cytokeratin type II and nestin immunoreactive ...	24
4.3.3. Expression of Sox2 on zebrafish olfactory epithelium	27
4.3.4. Individual cells are both cytokeratin type II and Sox2 immunoreactive	30
4.4. Cytokeratin positive cells can divide.....	30
4.5. A pharmacological approach to sustentacular cell function.....	32
4.5.1. Ca^{2+} signal is sourced from intracellular endoplasmic reticulum	36
4.5.2. Sus and basally located cells can express differential purinergic receptor subtypes	36
4.5.3. Differential response to varying purine analogs supports the existence of two purinergically inducible cell types in zebrafish olfactory epithelium ..	38
5. DISCUSSION	42
5.1. Zebrafish Sus show an inverted morphology	44
5.2. Sus can potentially be neurogenic progenitors	46
5.3. The basal OE, which cells to expect?	49
5.4. Sus and intraepithelial signaling.....	49
5.5. ATP evokes Ca^{2+} responses in Sus.....	50
5.6. Identification of purinergic receptor subtypes.....	51
5.7. Is there a role for purinergic signaling in response to injury?	52
APPENDIX A: EQUIPMENT	54
APPENDIX B: SUPPLIES	55
APPENDIX C: RESULTS FOR INDIVIDUAL EXPERIMENTS.....	57
REFERENCES.....	70

LIST OF FIGURES

Figure 1.1. General organization of the mouse olfactory epithelium.	4
Figure 4.1. Cytokeratin II antibody labels zebrafish sustentacular cells.	17
Figure 4.2. Cytokeratin II antibody labels zebrafish sustentacular cells.	18
Figure 4.3. Detailed morphology of individual sustentacular cells.	19
Figure 4.4. Cytokeratin II IHC marks a second cell population in the OE.	20
Figure 4.5. The pattern of CYKII-immunoreactivity varies across the lamella.	21
Figure 4.6. The expression motif of nestin on the OE.	23
Figure 4.7. Nestin filaments also span the apicobasal axis and can be found in Sus.	24
Figure 4.8. Cell morphologies in the dissociation assay.	25
Figure 4.9. Cell dissociation assay to detect co-localization of CYKII and nestin.	26
Figure 4.10. Expression motif of Sox2 on the OE.	28
Figure 4.11. The expression motif of Sox2 on the OE.	29
Figure 4.12. Sustentacular cells are Sox2-immunoreactive.	29
Figure 4.13. Cell dissociation assay to detect CYKII and Sox2 colocalization.	31
Figure 4.14. Profiling of the dissociated CYK II, nestin and Sox2-positive cells.	32
Figure 4.15. Ca^{2+} imaging on zebrafish OE vibratome sections.	34
Figure 4.16. Activated columnar regions are possibly the Sus.	35
Figure 4.17. Ca^{2+} signal is mainly dependent on intracellular reservoirs.	37
Figure 4.18. Two different cell populations with distinct purinergic receptor repertoire.	39
Figure 4.19. Varying analogs evoke different response.	40

LIST OF TABLES

Table A.1. List of equipments.	54
Table B.1. List of supplies.	54
Table B.1. List of supplies (cont.).	54
Table C.1. Cell numbers expressing different markers using IHC on tissue dissociation assay.	57
Table C.2. CYKII and BrdU temporal profiling.	58
Table C.2. CYKII and BrdU temporal profiling (cont.).	59
Table C.2. CYKII and BrdU temporal profiling (cont.).	60
Table C.3. Abundance and thickness of the cells expressing nestin.	60
Table C.4. Distance of the basal and columnar cells to neighboring cells.	61
Table C.4. Distance of the basal and columnar cells to neighboring cells (cont.).	62
Table C.5. Duct/gland cells morphometry.	63
Table C.6. Distance obtained from Ca^{2+} imaging.	64
Table C.6. Distance obtained from Ca^{2+} imaging (cont.).	65
Table C.7. Ca^{2+} imaging data obtained from CPA treatment.	66
Table C.8. Ca^{2+} imaging data obtained from suramin treatment.	67
Table C.9. Ca^{2+} imaging data obtained from purines treatment.	68
Table C.10. Distance of the Sox2-positive cells to apical layer.	69

LIST OF ACRONYMS / ABBREVIATIONS

ACSF	Artificial Cerebrospinal Fluid
BMP4	Bone Morphogenic Protein 4
CMZ	Ciliary Marginal Zone
CNS	Central Nervous System
CPA	Cyclopiazonic Acid
CYKII	Cytokeratin Type-2
FGF	Fibroblast Growth Factor
GBC	Globose Basal Cells
HBC	Horizontal Basal Cells
IHC	Immunohistochemistry
ILC	Interlamellar Curve
iOSN	Immature Olfactory Sensory Neuron
ir	Immunoreactive
LIF	Leukemia Inhibitory Factor
LP	Lamina Propria
MHB	Midbrain Hindbrain Border
OB	Olfactory Bulb
OE	Olfactory Epithelium
OMP	Olfactory Marker Protein
OR	Olfactory Receptor
OSN	Olfactory Sensory Neuron
PFA	Paraformaldehyde
S/NS	Sensory/Non-sensory
Sus	Sustentacular Cells
TRPC2	Trans Receptor Potential Channel 2

1. INTRODUCTION

1.1. Adult neurogenesis

It has long been thought that a loss of neurons is irreversible in the adult human brain and that dying neurons cannot be replaced (Cajal, 1913). This inability to replace nerve cells is an important cause or complication of neurological disease and impairment. In most brain regions, the generation of neurons is confined to a discrete developmental period (Bhardwaj *et al.*, 2006) but exceptions have been found with the dentate gyrus and the subventricular zone (SVZ) of central nervous system (CNS) in several mammalian species. Those unique neurogenic regions in the adult brain of mammals have been identified from mice to humans (Eriksson *et al.*, 1998; Gage, 2000; Zhao *et al.*, 2008). The olfactory bulb (OB) of the forebrain represent another important neurogenic niche, where migrating neuroblasts from the SVZ differentiate and mature into granule cell interneurons (Lepousez *et al.*, 2013). In addition, the hippocampus represents another neurogenic niche in the adult mammalian CNS (Kokoeva *et al.*, 2005; Lee *et al.*, 2012), important for the formation of new memories (Deng *et al.*, 2010).

Thus, neuronal stem cells must exist that maintain CNS homeostasis, although to a limited extent. This limitation in the generation of new neurons bears severe consequences for certain neural disorders such as neurodegenerative diseases, stroke, epilepsy or depression (Sahay and Hen, 2007; Parent and Murphy, 2008). Cell proliferation and neurogenesis in the adult brain can be modulated by diverse signals and, interestingly, recapitulate some of the molecular and cellular mechanisms that are active during embryonic development of the CNS (Bjornsson *et al.*, 2015). Therefore, it is not surprising that many growth factors, morphogens, hormones and signaling molecules, which play a role during embryonic development, also have been shown to regulate the expansion and fate of neural progenitors in the adult mammalian brain.

1.2. Neurogenesis in adult zebrafish CNS

The ability to generate neurons at adult age appears to become more restricted over evolution with lower-evolved species showing greater potential for regeneration (Kaslin *et al.*, 2008). Because adult proliferation and neurogenesis seem to recapitulate the molecular and cellular mechanisms of embryonic development it appears to be beneficial to study adult neurogenesis in model organisms of developmental biology, such as zebrafish. These species also display abundant adult neurogenesis and a great capacity to repair brain injuries.

The zebrafish, *Danio rerio*, has been reported to contain at least 16 neurogenic niches along the CNS (Grandel *et al.*, 2006). For instance, the OB, telencephalon, thalamus, epithalamus, preoptic region, hypothalamus, tectum, cerebellum, rhombencephalon and spinal cord, contain neuronal progenitors that have been shown to proliferate and maintain the corresponding neuroepithelium (Zupanc and Horschke, 1995; Zupanc *et al.*, 2005; Ekström *et al.*, 2001; Grandel *et al.*, 2006). Interestingly, the neurogenic potential of the zebrafish is not only restricted to regular renewal of the neural tissue but can regenerate and reconstitute large areas of certain neural tissues if damage destroys the tissue (Goldshmit *et al.*, 2015).

1.3. Neurogenesis in olfactory epithelium

In addition to neurogenic niches in CNS, the olfactory neuroepithelium represents perhaps the most dramatic example of lifelong neurogenesis in the adult vertebrate nervous system. (Graziadei and Graziadei 1979; Schwob 2002). The OE is in direct contact with the external environment and prone to damage by inhaled chemicals. It has been estimated that OSNs have a limited lifetime of 30 to 90 days (Mackay-Sim and Kittel, 1991; Tsai and Barnea, 2014). As a consequence, the OE has evolved a remarkable ability to regenerate sensory neurons that are lost by natural turnover or by lesions and traumatic injuries (Schwob, 2002). This ongoing adult neurogenesis is essential for maintaining olfactory sensory function. Therefore, OE has been an attractive zone for studying neurogenesis, its

progenitors and underlying mechanisms (Altman, 1969; Graziadei and Graziadei, 1979; Farbman, 1990; Carr and Farbman, 1992; Luskin, 1993; Roskams *et al.*, 1996; Calof *et al.*, 1998; Huard *et al.*, 1998; Schwob, 2002; Bauer *et al.*, 2003). The stem cell populations that underlie this highly regulated neurogenic process, however, remain controversial (Leung *et al.*, 2007).

1.4. Organization of the olfactory epithelium

The rodent OE can be divided into two parts, the OE proper and the stratum close to the lamina propria, respectively. The OE contains layers of cells that can be distinguished with respect to their morphology, location, and marker expression, with mature neurons occupying more apical positions (Iwema and Schwob, 2003). Generally, the OE consists of two major differentiated cell types, the olfactory sensory neurons (OSNs) and glial-like sustentacular cells (Calof *et al.*, 2002). Additionally, Bowman's glands and ducts extend through the OE and secrete mucus to the apical surface of the epithelium (Beites *et al.*, 2005).

Progenitor cells and stem cells are located in the basal OE close to the lamina propria (Carter *et al.*, 2004; Roskams *et al.*, 1996; Krishna *et al.*, 1996; Goldstein and Schwob, 1996; Guillemot *et al.*, 1993; Cau *et al.*, 2000; Tietjen *et al.*, 2003), while immature OSNs are situated above these progenitors (Illing *et al.*, 2002; Roskams *et al.*, 1994; Roskams *et al.*, 1998). Mature OSNs occupy even more apical positions and extend a dendrite towards the apical surface (Illing *et al.*, 2002; Roskams *et al.*, 1998). There are four known subtypes of chemosensory neurons in the zebrafish OE; ciliated cells, microvillous cells, kappe cells and crypt cells, classified based on their cell morphology, expression of different type of receptors and characteristic molecular markers in OE proper in zebrafish (Sato *et al.*, 2005; Ahuja *et al.*, 2014; Hansen *et al.*, 2000; Parisi *et al.*, 2014; Catania *et al.*, 2003). In terms of the morphology, ciliated cells have longer dendrites and more basally located cell bodies compared to the other cell types and express olfactory marker protein (OMP) as their cellular marker while the second major type of OSN, microvillous cells, express transient receptor potential channel C2 (TRPC2; Sato *et al.*, 2005). The remaining

chemosensory neurons, crypt cells and kappe cells, are less well explored, but kappe cells are immunoreactive to Gao whereas crypt cells can be stained with TrkA and S100 antibodies (Parisi *et al.*, 2014; Catania *et al.*, 2003; Ahuja *et al.*, 2014; Figure 1.1).

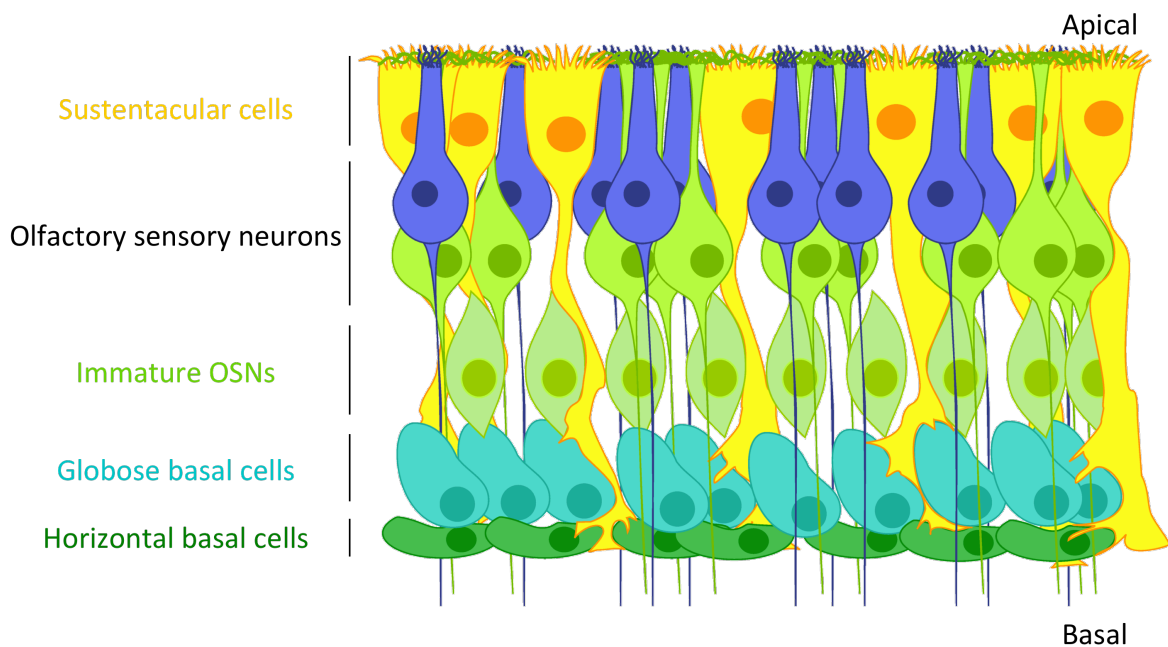


Figure 1.1. General organization of the mouse olfactory epithelium. Layers of the cells are stacked on apicobasal dimension. Most basally, stem cells HBCs and GBCs reside. Apical to these two layers, in the mid-range cell bodies of immature and mature OSNs locate. Apical borderline is decorated by Sus cell bodies (adopted from Paschaki *et al.*, 2013).

On the other hand, a layer of supporting cells or sustentacular cells aligns side by side and constitutes a type of olfactory-specific glia (Carson *et al.*, 2006; Davis and Reed, 1996; Asson- Batres and Smith, 2006; Piras *et al.*, 2003; Murray *et al.*, 2003). In most basal layers of the OE axon bundles, olfactory ensheathing cells (OEC), Bowman's glands, connective tissue and blood vessels can be found (Au and Roskams, 2003; Ramer *et al.*, 2004; Carson *et al.*, 2006).

1.5. Sustentacular cells in the OE

In rodents, Sus cell bodies are located in a single layer at the apical border of the OE

and possess thin cytoplasmic projections that terminate in basal endfeet (Farbman, 1992). This self-renewing, non-neuronal cell type expresses enzymes involved in metabolizing foreign compounds such as cytochrome p450, glutathione-S-transferase mu 2, and carbonyl reductase 2, suggesting a role for Sus in detoxifying many of the toxic substances present in the surrounding environment of the OE (Yu *et al.*, 2005). Sus may also phagocytose dead OSNs (Suzuki *et al.*, 1996) and probably provide structural support to OSNs similar to astroglia in the brain.

It remains controversial whether Sus share a common cellular lineage with OSNs (Doetsch, 2003). For instance, the intermediate filament protein nestin that is a commonly used neuronal stem cell marker, appears to label the endfeet of Sus, although it is restricted to adult tissues (Dahlstrand *et al.*, 1995; Doyle, 2001). However, nestin antibodies also label Bowman's gland cells, which lie close to the lamina propria, suggesting that Bowman's gland epithelial cells and Sus may share a common progenitor (Calof *et al.*, 1989; Huard, 1998). Other reports also indicate that Sus and respiratory epithelium share some antigenic properties (Yu *et al.*, 2005), suggesting that Sus may not be part of the OE neural lineage (Figure 1.1).

1.6. Glial cells in adult neurogenesis

The signals that trigger and coordinate adult neurogenesis are not well understood. Similarly, the exact population of cells that is able to expand by proliferation is not always well characterized. Yet, glia cells appear to have a prominent role in nervous tissue responses to damage or degeneration (Schmidt *et al.*, 2013). In this regard, two models have been suggested; the first model proposes that a subpopulation of glia cells themselves could function as neuronal precursors and generate neurons directly by dedifferentiation or transdifferentiation, whereas the alternative model suggests that glia cells convey signals about tissue damage to independent stem cell populations.

A subpopulation of radial glia cells in the zebrafish forebrain has been shown to

behave as a precursor population that expands and generates new cells upon damage (Kizil *et al.*, 2013; Kaslin *et al.*, 2013). This ability is similar to Müller glia in the vertebrate retina (Goldman, 2014). In the *Xenopus* and murine OE, however, SUs have been proposed to signal between apical regions of the OE tissue and basally located stem cell populations (Jia *et al.*, 2009; Hassenklöver *et al.*, 2009; Hayoz *et al.*, 2012). Thus, olfactory glia cells may play an essential role in the observed neurogenesis or damage responses.

1.7. Possible progenitor cells in OE

The OE most probably harbors more than one kind of progenitor cells (Calof *et al.*, 1998; Schwob, 2002; Carter *et al.*, 2004). Cells that contribute to neurogenesis lie near the basal lamina (Caggiano *et al.*, 1994; Mackay-Sim, 1991) and have been classically described as globose basal cells (GBCs) and horizontal basal cells (HBCs; Calof *et al.*, 2002).

GBCs are the major proliferating population in the olfactory neuroepithelium (Caggiano *et al.*, 1994). They are a heterogeneous population of fast cycling multipotent progenitors that give rise to neurons (Schwob, 2002). The progenitors in the OSN lineage that reside among the GBC population sequentially express the proneural genes achaete-scute-like homologue 1 (Ascl1) and Neurogenin 1 (Caudet *et al.*, 2004). Ascl1-positive GBCs are the earliest OSN precursors identified (Calof *et al.*, 2002) and their dynamics indicate that they are transit-amplifying progeny of a putative olfactory neuroepithelium stem cell (Gordon *et al.*, 1995). One model suggests that; OE stem cells reside among the GBC population (Huard, 1998; Jang, 2003), but definitive evidence to establish whether there are distinct subpopulations of the GBC or HBC participating in different cellular mechanism is lacking.

On the other hand, as a secondary precursor cell population, HBCs invade the OE after birth from the neighboring respiratory epithelium (Holbrook *et al.*, 1995). Therefore, they can clonally expand contributing to generate both neuronal and glial cell types upon

damage rather than maintenance or contributing embryonic development, while the GBCs are responsible for the maintenance of the tissue (Chen *et al.*, 2004; Leung *et al.*, 2007; Carter *et al.*, 2004). HBCs are slow cycling and they are defined by their presence as a single-cell layer below the GBCs, by their specific expression of keratin 5 and keratin 14 and by their direct contact with the basal lamina. They are thought to replenish the pool of GBCs in response to injury. However, not all GBC cell populations may be derived from HBCs (Leung *et al.*, 2007).

1.8. Molecular mechanisms governing neurogenesis in OE

Spatial and developmental regulations on OE should be strict to maintain the integrity of the olfactory mucosa. Therefore, a balance between positive regulatory factors sensing the dying cells and negative ones conveying a feedback from mature OSNs should control OSN generation (Shou *et al.*, 2000; Bauer *et al.*, 2003; Wu *et al.*, 2003). Some of the positive factors that have been described are leukemia inhibitory factor (LIF) (Satoh and Yoshida, 1997; Nan *et al.*, 2001; Getchell *et al.*, 2002 ; Bauer *et al.*, 2003 ; Carter *et al.*, 2004) and fibroblast growth factor FGF2 acting on GBCs (Goldstein *et al.*, 1997; Chuah and Teague, 1999; Hsu *et al.*, 2001), or TGF- α and EGF activating HBCs (Holbrook *et al.*, 1995; Farbman and Buchholz, 1996; Ezeh and Farbman, 1998; Carter *et al.*, 2004). On the other hand, negative regulators, such as TGF- β , arrest the cell cycle in progenitors (Wu *et al.*, 2003) and bone morphogenetic factor 4 (BMP4) inhibits cell proliferation in high concentrations (Shou *et al.*, 1999; 2000; Calof *et al.*, 1998).

Here it is investigated if and how Sus could contribute to neurogenesis in the zebrafish OE. Sus can be visualized by immunohistochemistry against the cytoskeletal marker type 2 cytokeratin. To establish a possible role of Sus in neurogenesis, co-labeling of CYKII-positive cells with the neurogenic progenitor markers nestin and Sox2 was performed in addition to a pharmacological analysis of purinergic signaling by functional Ca^{2+} imaging. Neurogenic markers co-localize with a subpopulation of CYKII-positive cells, in line with a potential role of these cells in OSN differentiation. Cells with Sus morphology can also be activated by purinergic stimuli, suggesting a candidate role for

active signaling in Sus. Taken together, expression of neuronal stem cells markers in Sus can signify that Sus might contribute to neurogenesis via de-differentiation into pluripotent neurogenic progenitors or they can signal cell death to true progenitors found on the basal lamina.

2. PURPOSE

This study aimed to investigate the neurogenic progenitor capacity of the sustentacular cells in adult zebrafish olfactory epithelium where neurogenesis is remarkably a life-long continuous phenomenon. Thus, initially, we wanted to identify and characterize the prospective sustentacular cells and basal progenitors in the zebrafish olfactory epithelium using immunohistochemistry against cytokeratin type II filament.

Following the identification of the Sus, main focus of this research concentrated on which possible role(s) Sus have in neurogenesis. Thus, we wanted to answer following question: Do sustentacular cells express neurogenic progenitor marker proteins that are nestin and Sox2? To shed light onto this question, we wanted to conduct co-labeling of the progenitor markers with CYKII either on intact olfactory epithelium or on dissociated one.

Besides direct contribution to the neurogenesis as a main progenitor component, another possible role of Sus mediating neurogenesis by signaling pathways, like purinergic signaling, was also aimed to study by utilizing functional calcium imaging. Thus, we wanted to construct a purinergic response profile of sustentacular cells along with the other cell populations participating in neurogenesis in the zebrafish olfactory epithelium. To this end, the profile of the cell responding to both purinergic activators and inhibitors was analyzed.

3. MATERIALS AND METHODS

3.1. Materials

3.1.1. Model organism

Wild type zebrafish, *Danio rerio*, of the AB or Tü genetic background obtained from the Zebrafish International Resource Center (ZIRC) or zebrafish from a local pet shop were used in immunohistochemical experiments. Fish were kept at the fish facility of the Boğaziçi University Life Sciences Center. Wild type Tüpfel-longfin zebrafish obtained from zebrafish facility at the University of Göttingen were used for all functional calcium imaging.

3.1.2. Equipment and supplies

A detailed list of equipments and supplies including manufacturers' information can be found in Appendix A and Appendix B, respectively.

3.1.3. Buffers and solutions

All solutions, media, and buffers used for zebrafish studies were prepared according to Westerfield (2007). Buffers and solutions for general molecular biology techniques were prepared according to Sambrook and Russell (2001). A detailed list of buffers and reagent can be found in Appendix A.

3.2. Methods

3.2.1. Maintenance of fish

Zebrafish were kept at 28°C under a 14/10 hours light/dark cycle. The fish were kept in 1-, 3- and 10-liter tanks for providing appropriate housing densities. Habitat water of the fish was prepared artificially (per 100 liters of reverse osmosis water: 2 g sea salt (Instant Ocean), 7.5 g sodium bicarbonate, and 0.84 g calcium sulfate (Sigma). A professional housing system (Stand Alone System, Aquatic Habitats) was used for proper aeration, sterilization, and filtering of the system water and individual tanks were connected to the system. Adult fish were fed twice a day with either flake food (TetraMin, Sera Vipan) or live brine shrimp larvae (*Artemia sp.*).

3.2.2. Dissection of zebrafish

For dissection of olfactory epithelia, zebrafish were euthanized by rapid chilling in ice water, avoiding direct contact with ice, for 10 minutes after the gills stopped moving. Then fish were decapitated at the level of the gills with a sterile surgical blade. First the lower jaw was removed under a dissection microscope (Olympus) using dissection scissors in ice-cold 1x phosphate buffer saline (PBS; Sigma). After removing the eyes and residual connective tissue using forceps, the two OEs attached to the bones forming the nasal cavity were transferred to a new dissection plate and finely dissected to remove all tissue.

3.2.3. Sectioning of the OE

For immunohistochemistry, cryosections of the OE were taken using a cryostat (Leica). Dissected OEs were embedded into optimal cutting temperature medium (OCT; Sakura Technologies) and frozen at -20°C for one hour. For long-term storage, the tissues were kept at -80°C. Sections were cut at 14 µm thickness in pre-cooled cryostat chamber (-

19°C), by keeping the tissue temperature at -21°C, and collected onto positively charged microscope slides for further experiments.

For functional calcium imaging, vibratome sections were taken on a Leica VT1200S vibratome. The dissected OEs were embedded into warm 2% agarose and immediately cooled down to room temperature. The agarose block was placed into the vibratome chamber containing artificial cerebrospinal fluid (ACSF) solution and 140 µm thick cross-sections were cut and placed into specially designed imaging plates containing ACSF solution.

3.2.4. Immunohistochemistry and nuclear staining

For immunohistochemistry, cryosections were dried in a ventilated oven for 30 min at 65°C. For rehydration of the sections, 1x PBS (Sigma) was applied onto the slide and the sections were fixed with 4% paraformaldehyde (PFA; pH 7.4) for 10 min. Following fixation, sections were washed 3 times with 0.2% Triton-X 100 (Sigma) in 1x PBS for 15 min in glass Coplin jars (VWR, The Netherlands), at room temperature while shaking. Then, tissue sections were blocked with 2% normal donkey serum (NDS) in 1x PBS containing 0.2% Triton-X 100 for 1 hour at room temperature. Primary antibodies, mouse anti-cytokeratin type II (1:1000; Developmental Studies Hybridoma Bank), rabbit anti-nestin (1:1000; Abcam), rabbit anti-Sox2 (1:1000, GeneTex), mouse anti-HuC/D (1:200, Abcam), mouse anti-BrdU (1:250, Becton-Dickinson), rat anti-BrdU (1:250, Abcam) were prepared in fresh blocking solution and sections were incubated over night at 4°C in a humid incubation chamber. After incubation with primary antibody, sections were washed 3 times with pre-cooled (4°C) 0.2% Triton-X 100 in 1x PBS, for 15 min at 4°C under agitation. Secondary antibodies, anti-mouse Alexa Fluor 488, anti-mouse Alexa Fluor 633, anti-rabbit Alexa Fluor 633, anti-rat Alexa Fluor 633 (Life Sciences) were prepared as 1:800 dilutions in blocking solution and sections were incubated for 1.5 hour at room temperature. To eliminate excessive secondary antibody, sections were washed with 1x PBS. To visualize nuclei, the sections were incubated in either ToPro-3 or DAPI (1:1000,

Invitrogen) in 1x PBS for 30 min at room temperature. The sections were imaged by laser-scanning confocal microscopy (Leica).

3.2.5. BrdU incorporation assay

To visualize proliferating cells, fish were incubated for 24 hours in artificial system water containing 30 mg/L BrdU in a dark chamber at 28°C. Dissection and cryosectioning of the OE was conducted as explained above. Essentially the same immunohistochemistry protocol was followed including an additional 10 min incubation in 4 M HCl to denature DNA followed by 3 washes in 0.2% Triton-X 100 in 1x PBS for 15 min after 4% PFA fixation.

3.2.6. Tissue dissociation assay

To dissociate OE tissue the OE was placed in pre-cooled (4°C) low- Ca^{2+} Ringer's solution (in mM: 140 NaCl, 5 KCl, 10 HEPES, 1 EDTA, 10 glucose, 1 cysteine, pH 7.2) and the tissue was minced with a razor blade. The minced tissue was treated with 1 U/ml papain (Sigma) in low- Ca^{2+} Ringer's solution for 4 min at room temperature and stopped in Ringer's solution (in mM: 140 NaCl, 5 KCl, 1 CaCl_2 , 1 MgCl_2 , 10 HEPES, 10 glucose, pH 7.2) supplemented with 0.1 mg/ml BSA. To further dissociate the tissue and to break up larger chunks, the suspension was gently triturated using a glass Pasteur pipette. The suspension was plated on poly-L-lysine coated slides (Electron Microscopy Sciences, USA) cells were allowed to settle and dried at 55°C overnight. The immunohistochemistry was carried out as described above.

3.2.7. Single-cell electroporation

Vibratome sections through the OE were used for single-cell electroporation, and individual cells were electroporated with 10 kDa dextran-coupled Alexa Fluor 488 (Life Technologies). The electroporation settings were as follows: 50-100 mΩ resistance, +50 mV voltage, +0.3V DC offset, square pulses, 550 ms train, 300 Hz frequency, 300 μs width. Microinjection needles (Warner Instruments) were prepared from glass capillaries with an outer diameter of 1.5 mm and inner diameter of 0.86 mm.

3.2.8. Functional calcium imaging

For functional imaging, acute OE vibratome slices were loaded with the Ca^{2+} -sensitive dye Fluo4-AM (excitation wavelength 488, Life Technologies) for 35 min at room temperature under gentle agitation in the dark. To remove excessive indicator dye, sections were washed with ACSF solution for 5 min. Slices were mounted onto a stage of a LSM 780/Axio Examiner confocal microscope and connected to a constant stream (1-2 drops per second) of ACSF solution. Changes in fluorescence were imaged at 1 Hz imaging speed over 60 frames upon injection of stimulating agents into the perfusion stream. The first 10 frames were taken as baseline fluorescence and purinergic stimuli (100 μM , 500 μL) or high potassium (80 mM, 500 μl) were applied at the 11th frame. For inhibitor experiments, 10 μM cyclopiazonic acid (CPA, Sigma) and 100 μM suramin (Sigma) were prepared in ACSF and applied by switching the perfusion stream from normal ACSF to inhibitor solution.

The data analysis was performed using Fiji bioanalysis software (Schindelin *et al.*, 2012). $\Delta\text{F/F}$ values were calculated as $(\text{F}_{\text{in}} - \text{F}_{\text{base}}) / \text{F}_{\text{in}}$; F_{in} : Fluorescence intensity after stimulus application for a region of interest, F_{base} : Average fluorescence intensity of first ten frames before stimulus application for a region of interest).

4. RESULTS

4.1. A synopsis

The aim of this study was to identify and to characterize the population of sustentacular cells in the zebrafish OE based on their glia-like properties and to examine their potential role in adult neurogenesis. First, a reliable molecular marker to label zebrafish Sus had to be established because such a marker had not been specified before. Cytokeratin type II, similar to the rodent and amphibian OE appears to specifically be expressed in Sus in the zebrafish as well (Hassenklöver *et al.*, 2008; Satoh and Yoshida, 2000). Thus, for the first time, the population of zebrafish Sus could be characterized by immunohistochemistry against CYKII. Because of their potential role in neurogenesis of the relationship between the CYKII-positive cell population and cells staining positive for established neurogenic progenitor markers, such as nestin and Sox2, was examined. Similar markers are expressed in other neurogenic progenitors like radial and Müller glia (Hsieh, 2012; Murdoch and Roskams, 2008; Lenkowski and Raymond, 2014). Both markers, nestin and Sox2 appear to be expressed in subpopulations of CYKII-positive cells in the zebrafish OE. Because it has been suspected that Sus can trigger neurogenesis through purinergic signaling (Weissmann *et al.*, 2004), purinergic response profile of the Sus in zebrafish OE was investigated.

4.2. A Cytokeratin II antibody labels sustentacular cells in zebrafish OE

Sus constitute a major fraction of cells in the rodent OE and have been implicated in developmental and regenerative processes. A variety of immunohistochemical and molecular markers have been identified for Sus in the rodent OE, such as cytokeratin 18, Hes1, Sox2, Sus1 or Sus4 (Suzuki and Takeda, 1991; Manglapus *et al.*, 2002; Guo *et al.*, 2010; Goldstein and Schwob, 1996; Hempstead and Morgan, 1983), yet have not been described in the zebrafish OE before. To enable further studies on zebrafish Sus, it was essential to first identify a reliable marker that allows characterizing these cells within the tight and complex cellular mosaic of the zebrafish OE. Members of the group of

cytokeratins, which are cytoskeletal proteins, typically are reliable markers of various cell populations in the rodent OE (Satoh and Yoshida, 2000). Yet, it is difficult to identify functional orthologues in zebrafish due to the third, incomplete genome duplication in the teleost lineage (Robinson-Rechavi *et al.*, 2001). A polyclonal antibody (1h5, Developmental Studies Hybridoma Bank, Iowa City, USA) raised against *Xenopus laevis* Cytokeratin type II robustly and specifically label Sus in the amphibian OE (Hassenklöver *et al.*, 2008) and was therefore tested as a first candidate to visualize zebrafish Sus.

Immunohistochemistry using the 1h5 anti-CYKII antibody labels a unique cell population in the zebrafish OE, which on the cross-sections through the OE is distributed across the entire tissue, ranging from the center of the interlamellar curves into the surrounding non-sensory tissue (Figure 4.1). CYKII-positive cells are spaced evenly ($6.99 \mu\text{m} \pm 0.15 \mu\text{m}$ distance between neighboring cells, $n = 233$ cells on 4 sections from 2 fish) along the sensory region of each hemi-lamella, resembling the mammalian and the amphibian organization of Sus (Hassenklöver *et al.*, 2008; Farbman, 1992). However, morphological deviations from this pattern are evident within the surrounding non-sensory region of the lamella (Figure 4.1). Here, CYKII-positive cells are spaced less evenly, do not traverse the entire apicobasal dimension and are stacked on top of each other adopting a stratified organization spanning the thickness of the entire hemi-lamella. This disarray at the border between the sensory and non-sensory section of the lamellae might either indicate labeling of a different cell type that also stains positive for the CYKII antibody or of a functional specialization of Sus subsets (Figure 4.1).

Interestingly, the CYKII antibody appears to recognize intracellular filament but does not allow a visualization of the shape of the CYKII-positive cells directly. The cellular architecture of the labeled cells, however, makes it likely that the CYKII antibody recognizes Sus in the zebrafish OE as well for the following reasons. Individual CYKII-positive cells span the entire apicobasal dimension of the OE, similar to rodent Sus. On the apical side of each lamella, CYKII-positive cells branch out and form cilia-like apical tufts that appear to seal the spaces between the dendritic processes of sensory neurons extending

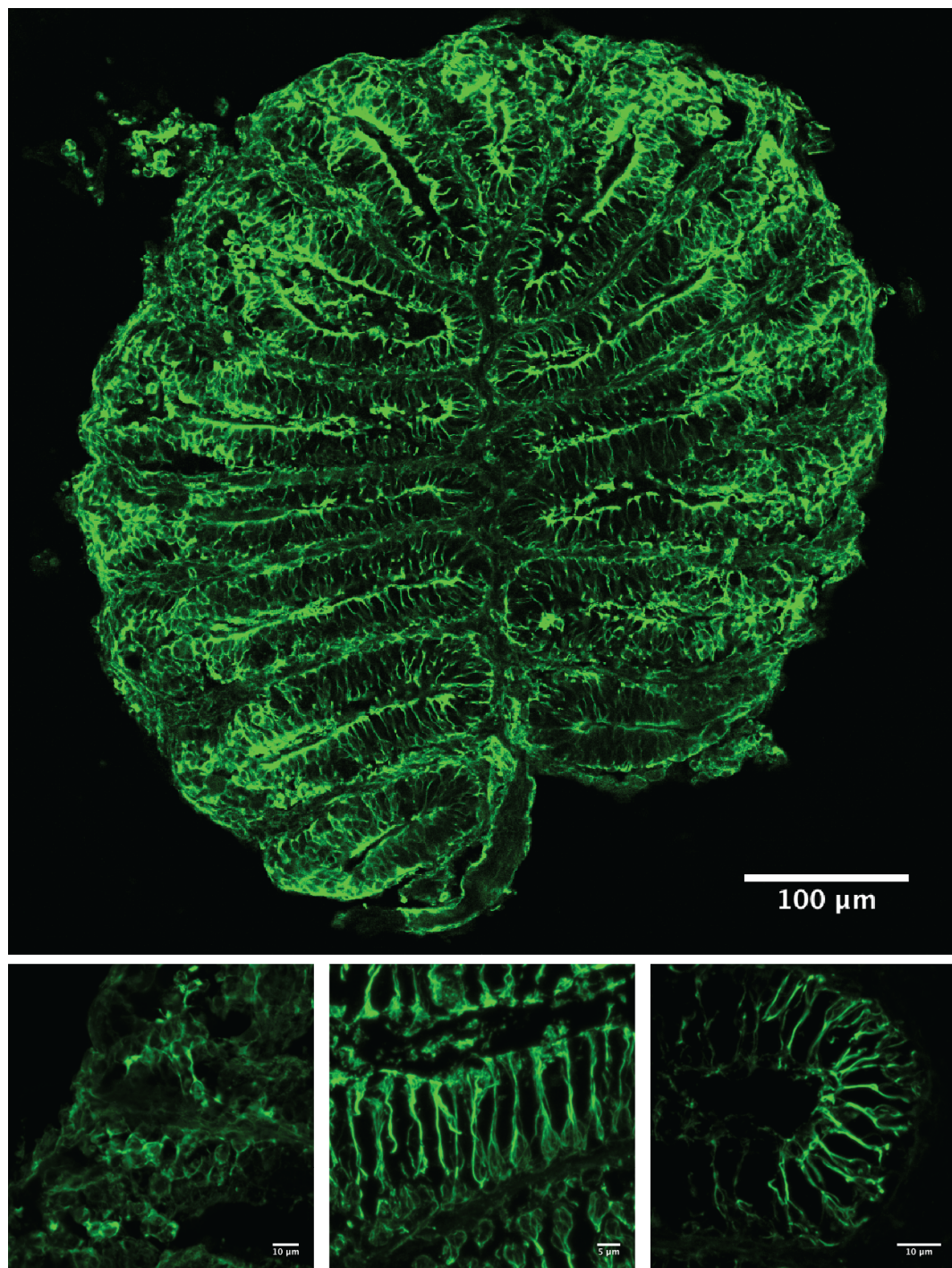


Figure 4.1. Cytokeratin II antibody labels zebrafish sustentacular cells. Confocal stacks of cryosections through the zebrafish olfactory epithelium labeled with anti-cytokeratin IHC. Top row: full sections through the OE. Bottom row: detail structure of the cytokeratin II of the periphery (left), sensory region (middle) and interlamellar curve of one lamella of a single lamella.

to the apical border. On the basal end, CYKII-positive structures arborize as well and form bulb-shaped processes that surround a central cavity (Figure 4.2; 3). To understand the nature of these empty spaces surrounded by protrusions of CYKII-positive fibers, the tissue was counterstained with the nuclear label TO-PRO 3 to visualize nuclei. Double-labeled sections reveal that the bulb-shaped protrusions of CYKII-positive cells enclose a single central nucleus. Yet, because CYKII antibody staining does not allow visualization of the entire cell, it remains unclear whether these basal nuclei belong to Sus or whether Sus systematically surround another cell type that is located in the basal OE (Figure 4.2).

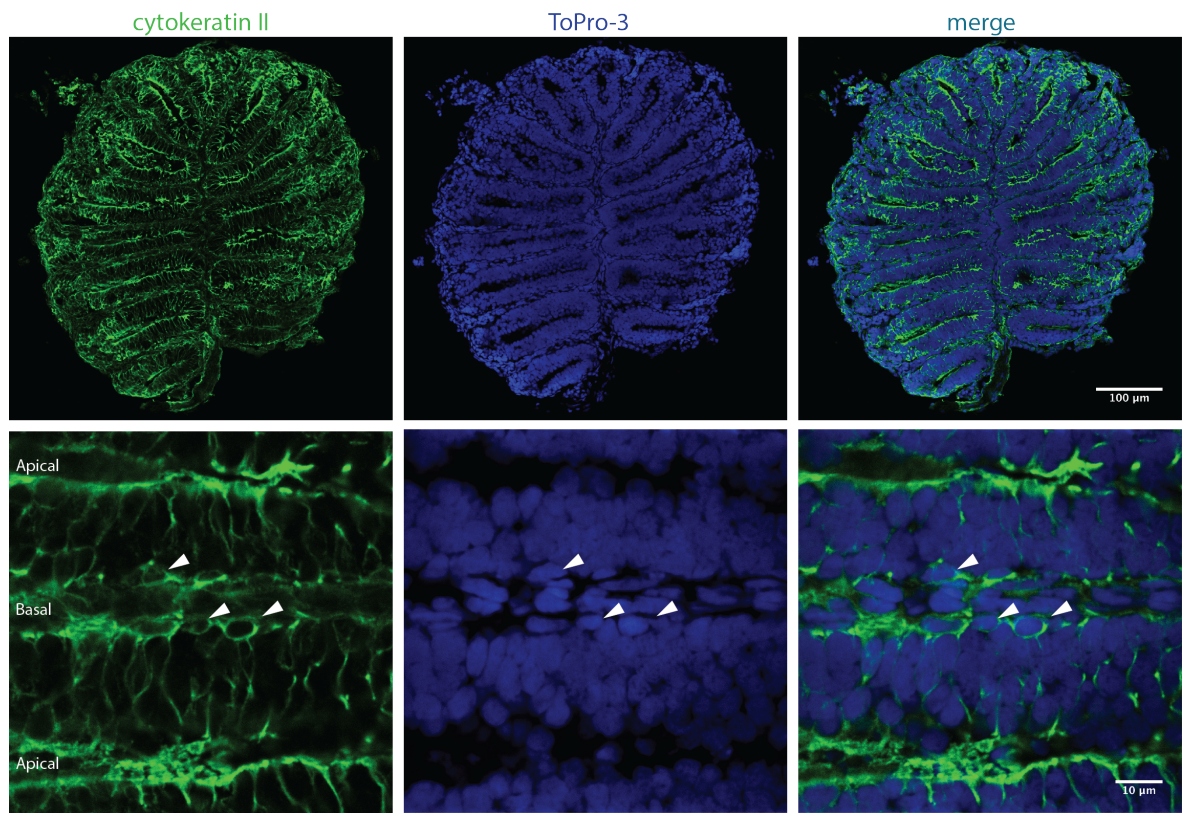


Figure 4.2. Cytokeratin II antibody labels zebrafish sustentacular cells. Confocal stacks of cryosections through the zebrafish olfactory epithelium labeled with anti-cytokeratin immunohistochemistry (green, left) and the nuclear stain ToPro-3 (blue, middle). The overlay is shown on the right. Top row: full sections through the olfactory epithelium, bottom row: detail of a middle section of a single lamella.

Thus, to better characterize Sus morphology, single-cell electroporation experiments were performed to label individual cells within the OE. To do so, 10 kDa dextran-conjugated Alexa488 was electroporetically applied from the apical border of hemi-lamella on 140 μ m vibratome sections. On occasion, single cells, which do not resemble any of the identified neuron types, were labeled by this technique. These cells display a columnar architecture that spans the apicobasal dimension of the OE. The cells fan out at their apical ends and have a prominent bulge at their basal end but do not possess axon-like processes that project outside the OE (Figure 4.3). Thus, zebrafish Sus appear to have an inverted morphology with respect to Sus described in the rodent OE, where the cell bodies and nuclei are located at the apical side of the OE. In zebrafish, the cell bodies and nuclei might be located close to the basal lamina.

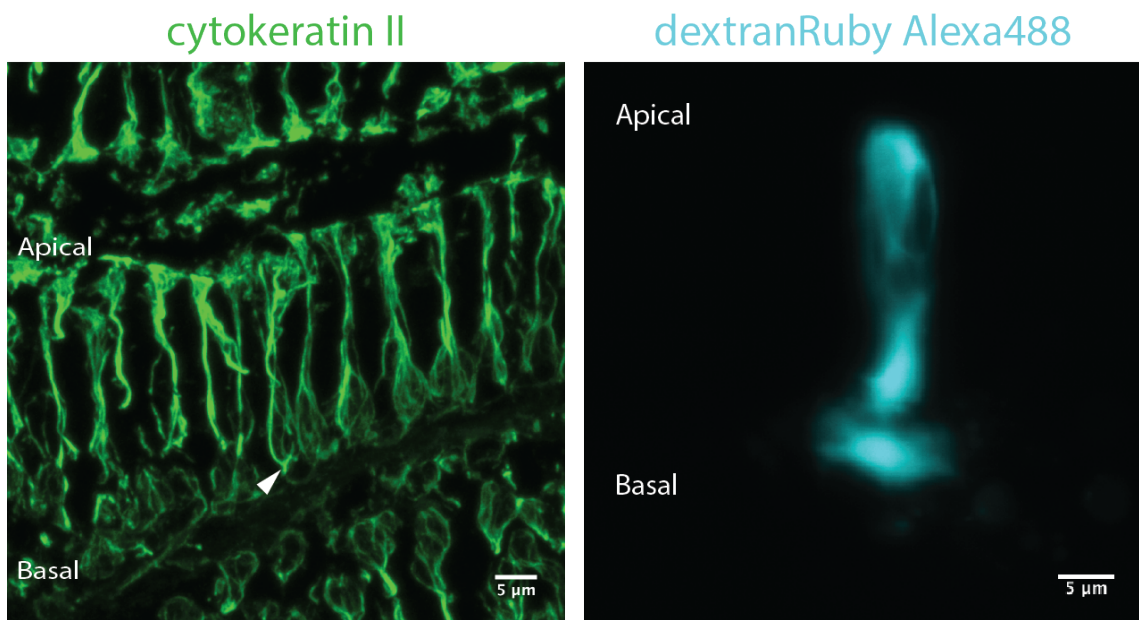


Figure 4.3. Detailed morphology of individual sustentacular cells. (A) IHC against CYKII (green, left) reveals a highly ordered array of labeled cells. The cells display extensive apical tufts and basal baskets (arrowhead) where either the nucleus of the cells or another cell body might sit. (B) AlexaFluor488-dextran electroporated single cell with cylindrical sustentacular cell morphology.

In addition to the pattern of immunoreactivity described above, the CYKII antibody appears to label another type of cells, which are located close to the interlamellar curves. In

contrast to the slender shape of Sus, those cells are large ($11.37 \mu\text{m} \pm 0.23 \mu\text{m} \times 6.26 \mu\text{m} \pm 0.15 \mu\text{m}$, $n = 54$ cells on 3 sections from 1 fish), located close to the apical surface of the tissue and have an elongated globose appearance (Figure 4.4). Interestingly, the immunoreactivity is stronger in those cells and within each cell two stacked compartments appear to be less immunoreactive. These cells most likely represent the zebrafish equivalent of Bowman's duct/gland cells, because it was shown that cytokeratin 18 labels both Sus and Bowman's duct/gland cells in the rodent OE in addition to other proteins such as Sox2, ezrin and Hes1 (Krolewski *et al.*, 2012).

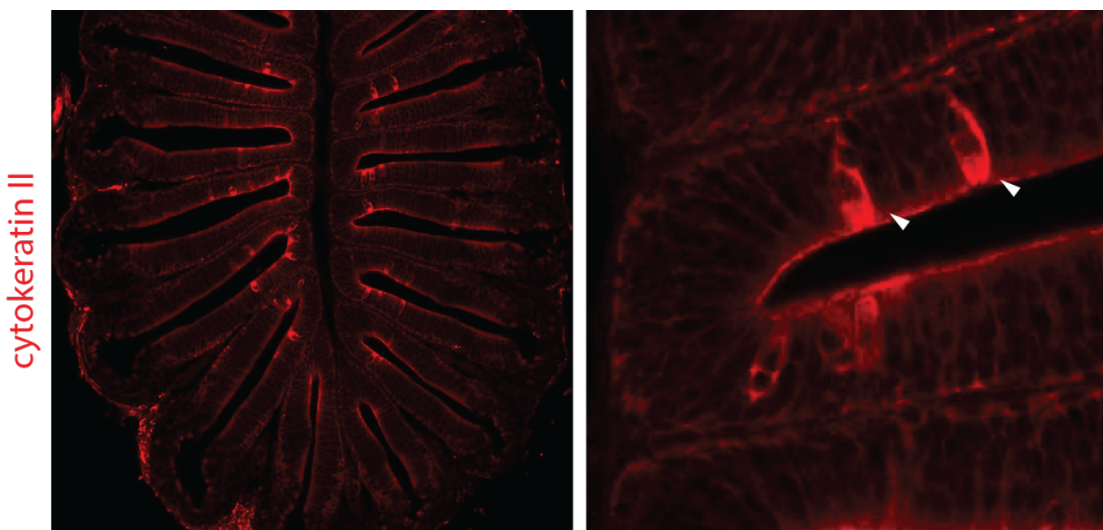


Figure 4.4. Cytokeratin II IHC marks a second cell population in the OE. Confocal stack through the zebrafish OE labeled with IHC of CYK II (left). Strongly immunoreactive cells are sparsely distributed, close to the ILC. Detail of the cells (arrowheads) around a single ILC. The cells are located apically but extend about halfway through the tissue and display two prominent unlabeled cavities.

Interestingly, on some sections immunohistochemistry against CYKII showed variable staining in different regions of a lamella. In the interlamellar curves and the non-sensory region, cytokeratin II might be more abundant because a stronger label could be observed in these regions. On the other hand, CYKII-positive cells in the sensory/non-sensory boundary showed a less regular horizontal spacing but had a stacked and layered appearance (Figure 4.5).

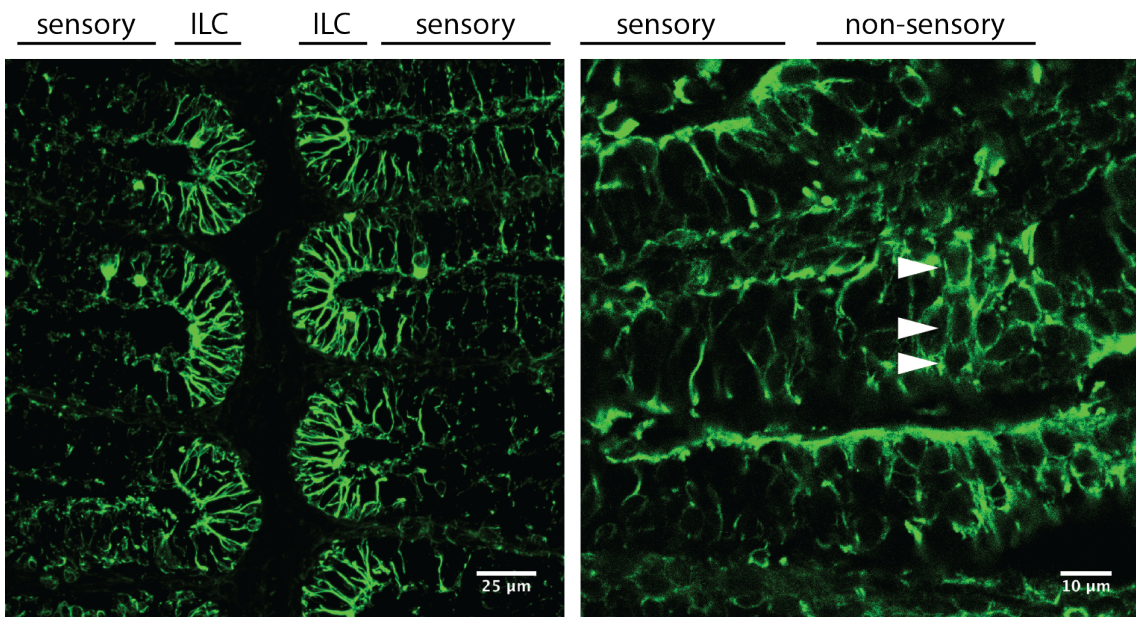


Figure 4.5. The pattern of CYKII-immunoreactivity varies across the lamella. Confocal stack of CYKII-positive cells in the center of the OE; strong label can be observed around the ILCs and sparse label within the sensory region (right panel). Left is the pattern of CYKII-ir around the s/ns boundary. In the ns region cells adopt a less regular appearance with multiple cells stacked on top of each other (arrowheads).

Thus, the 1h5 anti-CYKII antibody appears to reliably visualize Sus in the zebrafish OE as well. To our knowledge, this is the first direct visualization of this cell type by molecular means. Sus have been described in one EM study but the pattern of organization these cells had not been revealed (Hansen and Zeiske, 1998). Similar to the observations reported here, there was no obvious pseudo-stratification of Sus at the apical border in zebrafish OE, unlike the situation in the rodent OE. Instead, cell bodies of Sus and neurons are mixed within the OE. It is reasonable to assume that these cells are Sus as we also observed more basal basket-like structures by anti-CYKII immunohistochemistry (Figure 4.3). The second cell type identified by anti-CYKII immunohistochemistry consists of sparse (5.4 per lamella), globose cells that are located in and around the interlamellar curves. These cells possibly represent gland cells of the zebrafish OE (Figure 4.4). Lastly, CYKII-positive cells observed in the non-sensory region might represent yet another subtype of unknown identity and function (Figure 4.5).

4.3. Neuronal progenitor markers are expressed in sustentacular cells

To examine whether CYKII-positive Sus might also express neuronal progenitor markers, hinting at any progenitor potential of these cells, Sus were examined by co-labeling against CYKII with nestin and Sox2 separately on cross-sections through the OE. Intact OE showed immunoreactivity against Sox2 and nestin. However, complexity of the tissue hindered co-localization with CYKII. Hence, tissue dissociation assay followed by IHC was conducted.

4.3.1. Expression of nestin on zebrafish olfactory epithelium

Nestin is an intermediate filament protein and is often used as a selective marker for neuronal progenitors (Lendahl *et al.*, 1990). In the zebrafish nervous system, nestin-positive cells can be found in ventricular regions in the telencephalon and diencephalon, the midbrain hindbrain boundary (MHB), and the retinal ciliary marginal zone (CMZ) (Mahler and Driever, 2007), regions with neurogenic potential.

Interestingly, certain subsets of glia cells, such as a fraction of retinal Müller cells and radial glia, have also been shown to be nestin-positive (Hsieh, 2012; Murdoch and Roskams, 2008), which is considered to be a sign of progenitor capacity of these cells. Both cell types have been shown to undergo dedifferentiation into early precursors under certain conditions in zebrafish (Goldman, 2014; Götz *et al.*, 2002).

Nestin-positive structures could be observed close to the sensory/non-sensory border of the lamellae and within the interlamellar curves. In addition, the basal lamina also showed prominent immunoreactivity for the anti-nestin antibody where the labeling extends as a single ribbon of flattened cells along the base of each lamella (Figure 4.6). Since the sensory/non-sensory border and the interlamellar curves are proliferatively active and neurogenic zones in the zebrafish OE (Oehlmann *et al.*, 2002; Bayramli, unpublished), the nestin staining in these regions suggests that nestin immunoreactivity may demonstrate

the neurogenic niche. The role of the flattened cells along the basal lamina is less clear, but it may imply that a population of cells equivalent to horizontal basal cells could be located there.

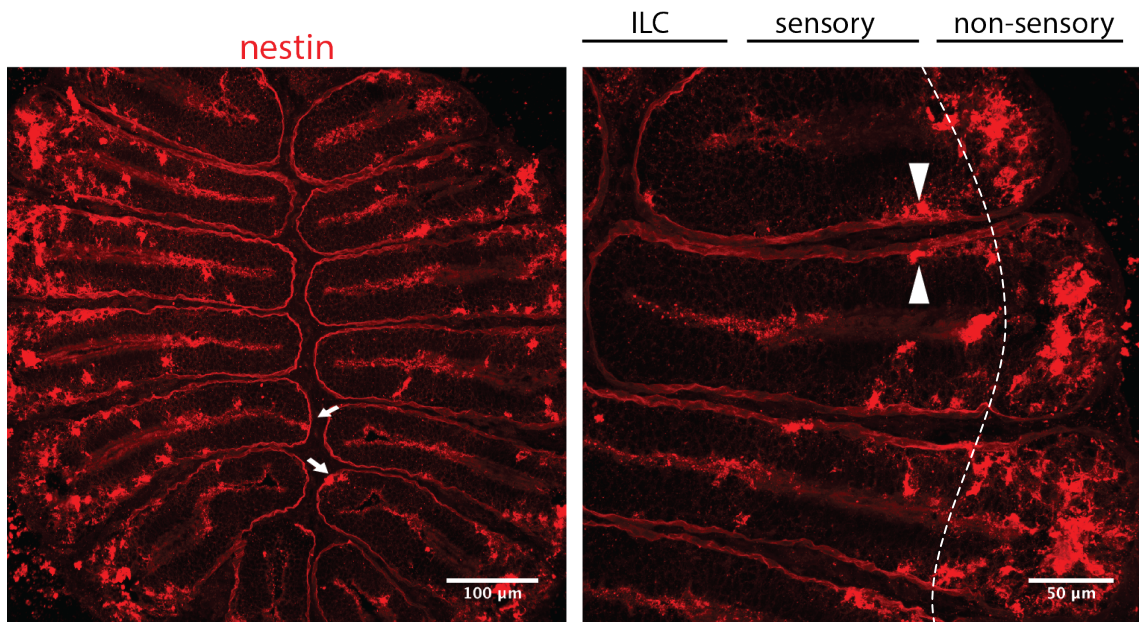


Figure 4.6. The expression motif of nestin on the OE. The progenitor marker (red) heavily labels non-sensory region and basal layer. Nestin+ cells are on ILC region (arrows, left) and on the S/NS border (arrowheads, right).

To investigate if these cells indeed represent a subpopulation of CYKII-positive cells, double label immunohistochemistry against nestin and cytokeratin II was performed. Interestingly, another pattern of nestin immunoreactivity could be observed within the sensory tissue. A population of sparsely distributed, nestin-positive cells (6 ± 0.46 cells per section) could be observed that resemble the morphology of CYKII-positive cells, suggesting that a sub-population of Sus are positive for nestin (Figure 4.7). These structures had approximate dimensions of $28.57 \mu\text{m} \pm 1.03 \mu\text{m}$ ($n = 37$ cells on 10 sections from 2 fish) in the apicobasal axis of the OE. The nestin-immunoreactive filaments of these cells form bulb-like structures at the basal OE resembling the ones observed for CYKII staining.

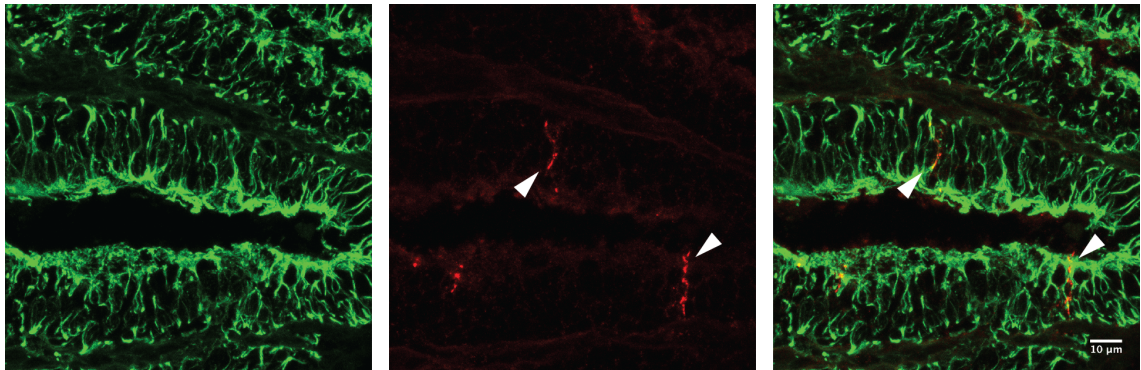


Figure 4.7. Nestin filaments also span the apicobasal axis and can be found in Sus. CYKII (green) and nestin (red) filaments predominantly exist in exclusive regions and span the apicobasal axis similarly.

4.3.2. Individual cells are both cytokeratin type II and nestin immunoreactive

Since the density of the OE tissue makes it difficult to clearly differentiate nestin-positive and CYKII-positive cells or, more importantly, to examine co-localization of the two staining, immunohistochemistry for CYKII and nestin was repeated on dissociated OE cells. To do so, OE tissue was minced, incubated in 1 U/ml papain in calcium-free Ringer's solution for 4-5 min at room temperature, and plated on glass slides. The mechanical disruption followed by chemical dissociation of the olfactory tissue resulted in larger cell clusters and single cells (Figure 4.8). After the treatment with 1 U/ml papain, several distinct cell morphologies, typical of ciliated cells with long protrusion and microvillous cells with more rounded cell bodies along with dendrites could be observed. However, most cells had a round profile, probably due to retraction of processes following the dissociation procedure. Thus, cells probably lost their shapes since the application was rigorous that might influence the cells negatively creating a stress condition for cells. Yet, cells were alive and attached to the slide making it feasible to visualize nestin and CYKII expression at the level of individual cells.

Since nestin and CYKII are both cytoskeletal proteins, they were co-localized surrounding DAPI-labeled nuclei in clusters of rounded cells (Figure 4.9). Cells that were

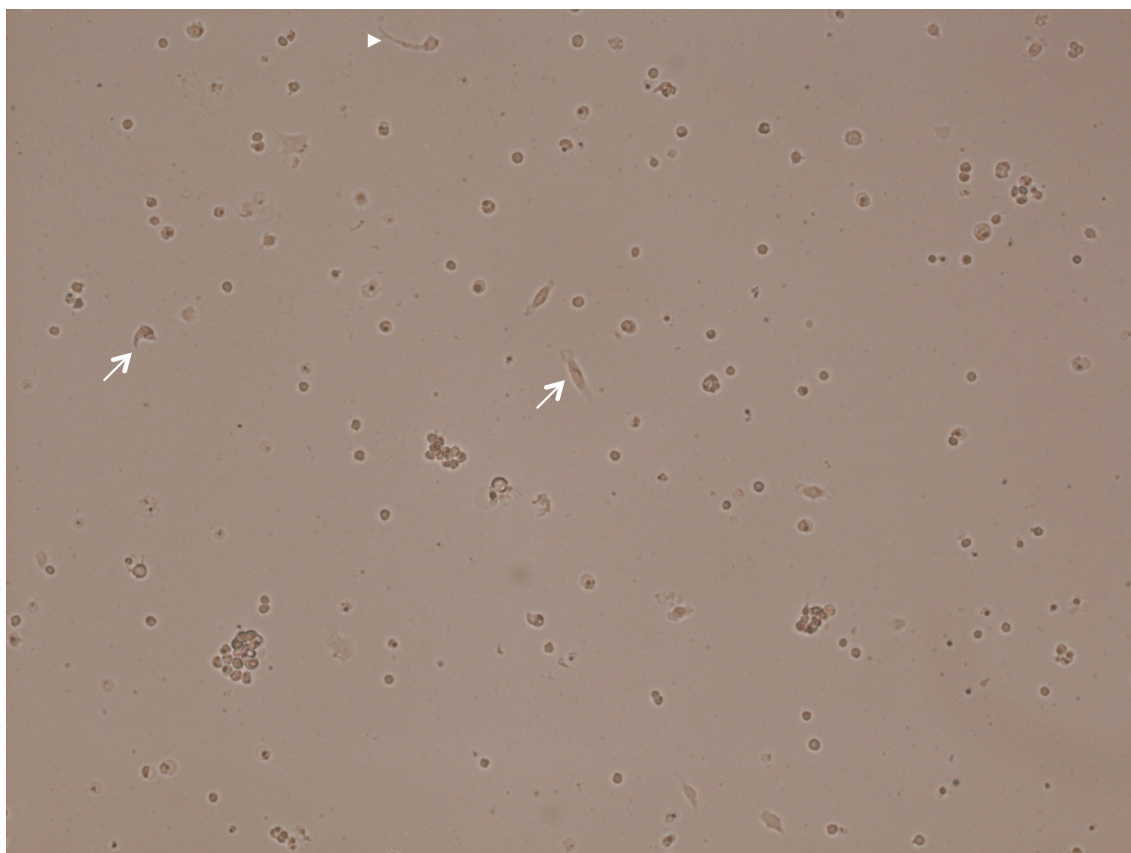


Figure 4.8. Cell morphologies in the dissociation assay. Rounded or typical single cells can be observed as well as the larger cell clusters attached to the poly-L-lysine coated glass slide. Arrowhead indicates the ciliated OSN with long protrusion and arrow indicates the microvillous OSN with rounded cell bodies and dendrites.

either nestin- or cytokeratin-positive could be observed in addition to double-positive cells, suggesting that not all CYKII-positive cells express nestin or vice versa. Therefore, the number of cytokeratin and nestin immunoreactive cells was analyzed to better understand the proportion of potentially neurogenic progenitor cytokeratin-positive cells. Of total 298 nuclei that could be visualized by DAPI in total, 113 stained positive for CYKII, thus on average $39\% \pm 4\%$ of dissociated DAPI-positive cells were CYKII positive and $44\% \pm 5\%$ of DAPI-positive cells stained positive for nestin immunohistochemistry. Of those, a total of $59\% \pm 8\%$ of CYKII positive cells were double positive for nestin and $54\% \pm 7\%$ of nestin-positive cells co-labeled for CYKII, and thus 22.1% of all cells are both nestin and CYKII-positive (Figure 4.14b). The abundance of CYKII and nestin positive cells seems to correlate with the results obtained by immunohistochemistry, where a large number of CYKII-positive cells across the entire OE were seen. However, the number of nestin-

positive cells appears to be higher than judged by immunohistochemistry, where only in the non-sensory region strong labeling was observed. It may be that different cell types were dissociated or attached to the glass slide with different efficiency, accounting for the disproportionately high number of nestin-positive cells.

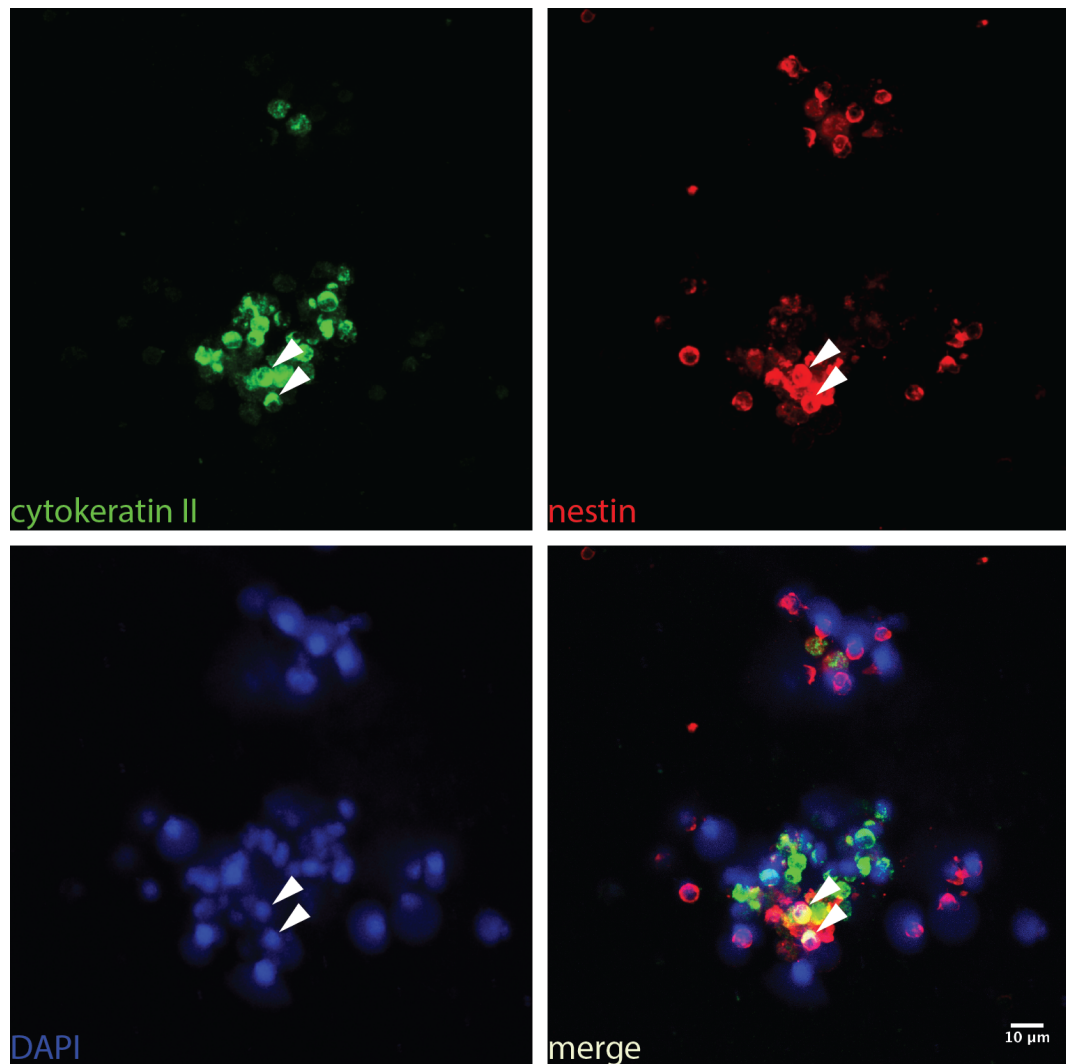


Figure 4.9. Cell dissociation assay to detect co-localization of CYKII and nestin. Confocal stacks of dissociated OE cells that were plated onto poly-L-lysine coated slides, subjected to IHC against CYKII (green, top left) and nestin (red, top right) and counterstained with the nuclear stain DAPI (blue, bottom left). Cells stained positive for both markers are indicated with arrowheads.

4.3.3. Expression of Sox2 on zebrafish olfactory epithelium

Another established neuronal progenitor marker is the transcription factor Sox2. In the rodent OE Sox2 is expressed in Sus, globose basal cells and horizontal basal cells (Guo *et al.*, 2010). In addition, other cell types with neurogenic potential, such as Müller and radial glia cells have also been shown to be Sox2-positive (Hsieh, 2012; Lenkowska and Raymond, 2014). Thus, we wanted to know whether progenitor marker Sox2 is expressed in CYKII immunoreactive cells including Sus.

Sox2-expressing cells in the zebrafish OE were visualized by immunohistochemistry using an anti-Sox2 antibody on tissue sections through the entire OE and counterstained with the nuclear stain TO-PRO 3 (Figure 4.10a). Most Sox2-positive cells were located within 18 μ m distance from the basal borderline where the maximum thickness of the hemi-lamella is 42 μ m and we observed no Sox2 immunoreactive cells within the range of 36-42 μ m from the apical frontier. Thus, Sox2-positive cells are basally located along the sensory region (Figure 4.10b).

Immunoreactivity against Sox2 was largely localized to the nucleus but weaker staining was noticeable in the perinuclear cytoplasm giving the cells a fuzzy appearance. Sox2-positive cells can be found along the entire lamella from the interlamellar curve to the sensory/non-sensory boundary. To better demonstrate the extension of Sox2-positive cells along the lamella, double immunohistochemistry against Sox2 and the neuronal marker HuC was performed (Figure 4.11). The co-labeling with the mature neuronal marker HuC/D revealed that HuC and Sox2 are never co-localized. Instead the staining was complementary and non-overlapping such that Sox2-positive cells and mature neurons occupy mutually exclusive territories. Because HuC is a marker of mature neurons suggesting that Sox2-positive cells constitute a non-neuronal population or are neuronal progenitor cells.

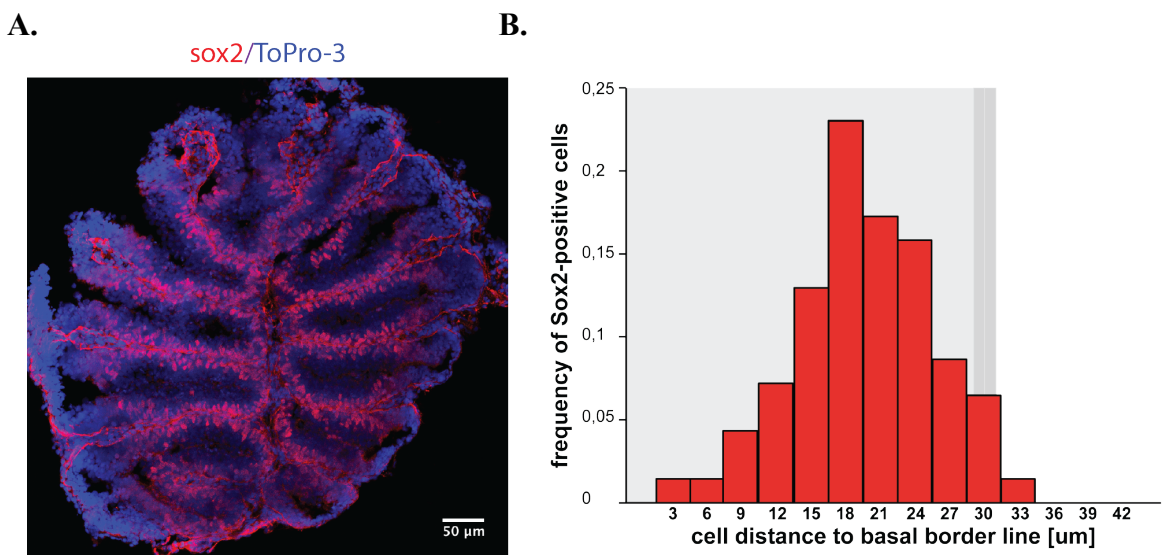


Figure 4.10. Expression motif of Sox2 on the OE. (A) Nuclear counter staining with DAPI (blue) shows that Sox2+ cells (red) extend all along hemi-lamella to the S/NS border and they were located basally. (B) Histogram of the frequencies of the cell according to their distance to apical border line. Shaded area represents average hemi-lamella thickness. The cells were concentrated more distantly from the apical border.

In rodent OE, Sox2 is expressed in Sus and neuronal progenitors (Guo *et al.*, 2010). CYKII immunohistochemistry revealed an inverted morphology of Sus with a basal cell body (Figure 4.2). Thus, a majority of Sox2-positive cells that were observed in the zebrafish OE could therefore be Sus in addition to precursors, yet both cell types occupy similar positions in the OE tissue. To investigate this possibility, cross-sections of the OE were co-labeled for Sox2 and CYKII. Double immunohistochemistry targeting CYKII and Sox2 showed that basal basket-like structures of the cytokeratin-positive cells surrounded the Sox2-positive structures. This compatibility between cytokeratin and Sox2 immunoreactivity supports the inverted morphology of the sustentacular cells expressing neuronal progenitor marker Sox2. Yet, more apically located Sox2-positive cells therefore may represent another cell type; most likely neuronal progenitor cells at different levels of differentiation (Figure 4.12). Similar to the considerations for Sus and nestin, however, it was difficult to unequivocally determine whether zebrafish Sus express Sox2 on tissue sections. Therefore colabeling by immunohistochemistry against Sox2 and CYKII was repeated on dissociated cells.

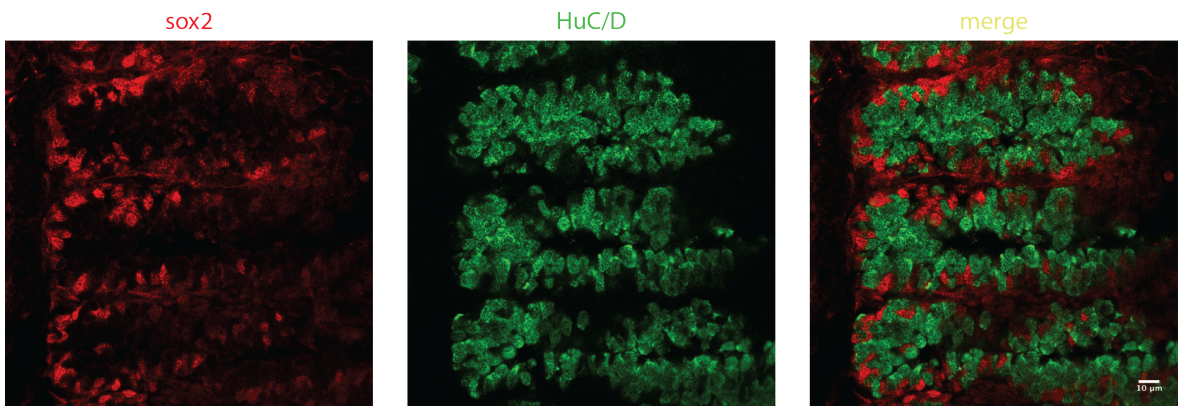


Figure 4.11. The expression motif of Sox2 on the OE. Sox2+ cells (red) are basally located and mature neurons labeled with anti-HuC/D (green) and cells labeled with anti-Sox2 antibodies are mutually exclusive.

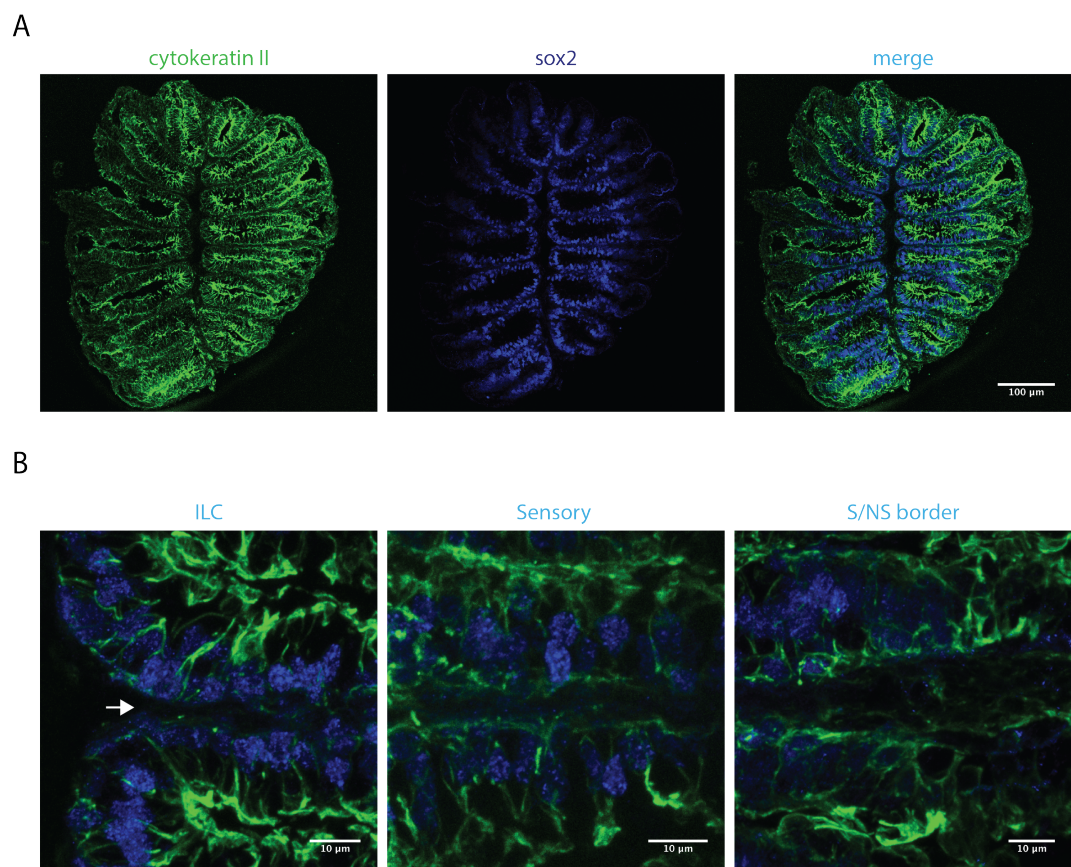


Figure 4.12. Sustentacular cells are Sox2-immunoreactive.
 (A) Confocal stack of the OE visualized with anti-CYKII (green) and anti-Sox2 (blue) IHC. (B) Detailed view of the ILC (left), Sensory region (center), and S/NS border. Arrow: basal lamina. Sox2⁺ cells are in direct contact with the bulbous basal structure of Sus in ILC and sensory region while the NS side of the border was fuzzier.

4.3.4. Individual cells are both cytokeratin type II and Sox2 immunoreactive

A cell dissociation assay was carried out to more clearly visualize co-localization of the CYKII and Sox2 proteins at the individual cell level. Both, only Sox2- as well as only cytokeratin-positive cells could be observed, suggesting that not all CYKII-positive cells are expressing the Sox2 progenitor marker (Figure 4.13). Therefore, the number of cytokeratin- and Sox2-immunoreactive cells was analyzed to understand the proportion of double-positive cells. Of 238 nuclei that could be visualized by DAPI in total, 125 stained positive for CYKII, thus on average $52\% \pm 8\%$ of DAPI- positive cells were also CYKII-positive. Similarly, $48\% \pm 7\%$ of DAPI- positive cells were also Sox2-positive. Of those a total of $63\% \pm 7\%$ of CYKII positive cells were double positive for Sox2 and $67\% \pm 5\%$ of Sox2-positive cells co-labeled for CYKII, and thus $31\% \pm 4\%$ of all cells are both Sox2 and CYKII-positive (Figure 4.14a). CYKII and Sox2 IHC in tissue dissociation assay exhibited similar proportions relative to the impression from immunohistochemistry on the whole OE.

4.4. Cytokeratin positive cells can divide

Because nestin and Sox2 could be shown to co-label cytokeratin-immunoreactive cells, we wanted to assess the ability of Sus to divide by using BrdU proliferation marker. Therefore, fish were incubated for 24 hours in BrdU and analyzed 1, 4 and 8 days later by immunohistochemistry against BrdU and CYKII. BrdU immunoreactivity that co-localized with basket-like structures of Sus was scored as a dividing Sus. BrdU incubation for 24h previously revealed two proliferative zones at the interlamellar curves and sensory/non-sensory boundary (Bayramli, unpublished). A significant increase in the number BrdU-positive cells within the sensory region is observed over the 8 day period (number of double-positive cells in sensory region on 1 day: 0.22 ± 0.11 to 8 day: 1.1 ± 0.3 ; Student's two-tailed t-test; p_{1d-8d} -value: 0.0031). This observation may imply that Sus could be born within the interlamellar curves and that they migrate towards the sensory region. On the other hand, the number of double positive cells in the non-sensory region was close to zero, which suggests that the sensory/non-sensory boundary may not contribute to Sus proliferation (1 day: 0.03 ± 0.03 8 day: 0.1 ± 0.1 ; p_{1-8} -value: 0.46).

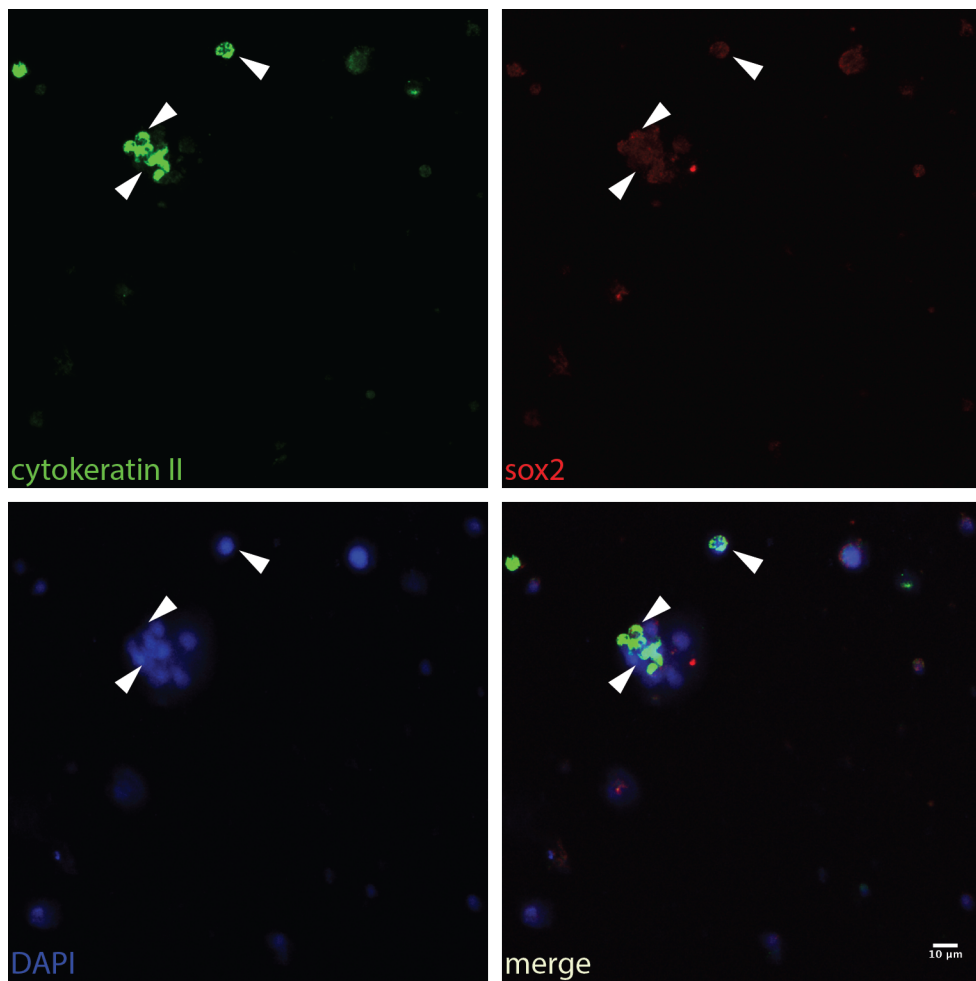


Figure 4.13. Cell dissociation assay to detect CYKII and Sox2 co-localization. Confocal stacks of dissociated OE cells that were plated onto poly-L-lysine coated slides, subjected to IHC against CYKII (green, top left) and Sox2 (red, top right) and counterstained with the nuclear stain DAPI (blue, bottom left). Cells stained positive for both markers are indicated with arrowheads.

In summary, visualization of the two neuronal progenitor markers nestin and Sox2 suggests that Sus, or a Sus subpopulation, may have stem cell capacity. Nestin is expressed in a certain subset of cytokeratin immunoreactive cells (56.9%), which, thus, may maintain the potential to de-differentiate into neural stem cells. On the other hand, distribution of Sox2 supports the inverted morphology of Sus in the sensory region. Sox2 is present in 66% of cytokeratin expressing cells implying a neurogenic progenitor capacity of a portion of Sus.

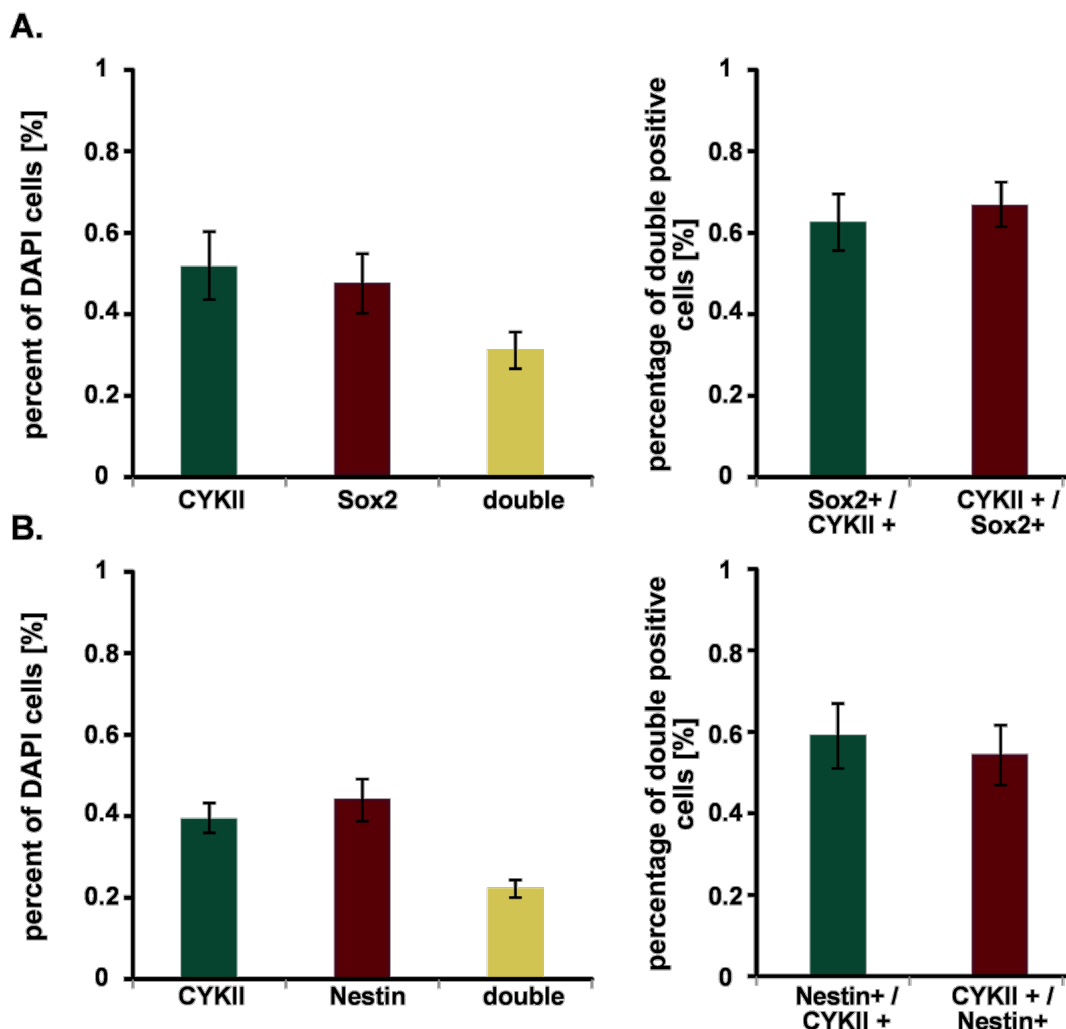


Figure 4.14. Profiling of the dissociated CYK II, nestin and Sox2-positive cells. (A) Percentage of the cells stained with CYKII (green) and Sox2 (red) normalized to DAPI (left) and proportion of CYKII and Sox2 to each other (right). (B) Percentage of the cells stained with CYKII (green) and nestin (red) normalized to DAPI (left) and proportion of CYKII and nestin to each other (right)

4.5. A pharmacological approach to sustentacular cell function

In addition to their potential neuronal progenitor function similar to other zebrafish glial cells, Sus might serve another function as a communication link that signals between the OE tissue and stem / progenitor cells. Sus have been implicated in conveying signals emerging from dead neurons to stem / progenitor cell populations to stimulate proliferation (Jia *et al.*, 2011). In particular, purine compounds, such as ATP have been

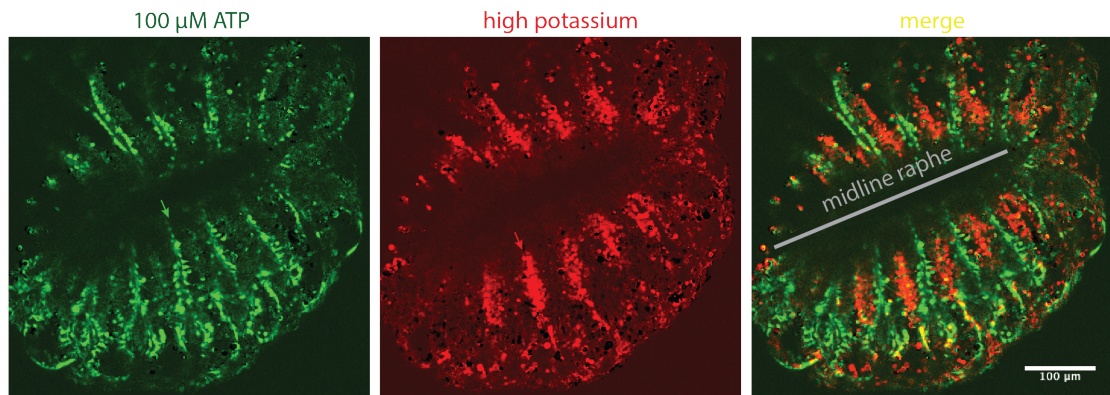
suspected to be active signaling molecules that stimulate Sus and eventually mediate communication between the tissue and Sus and between Sus and stem cells. It is assumed that dying cells release their cytoplasmic content and purines released by this process might activate nearby Sus (Hegg *et al.*, 2009). In rodent and amphibian models, Sus were shown to respond with intracellular Ca^{2+} signals upon purinergic activation (Hassenklöver *et al.*, 2008; Hegg *et al.*, 2009). Interestingly, this purinergic activation of Sus can induce cell proliferation in the OE through the release of FGF2 (Jia *et al.*, 2011).

To investigate the potential role of Sus in signaling in the zebrafish OE, responses of Sus and the pharmacology of this response to purine compounds was investigated by *in vitro* Ca^{2+} -imaging. To do so, OE vibratome sections were loaded with the Ca^{2+} indicator Fluo4-AM. Fluo4-AM is a membrane-permeable analog of the calcium indicator Fluo4, which becomes trapped inside cells after cytoplasmic cleavage of the acetoxyethyl ester moiety. This Ca^{2+} dye changes its fluorescence intensity upon binding to Ca^{2+} . Therefore, an increase in intracellular Ca^{2+} concentration results in an increase in fluorescence intensity in the cells that take up the dye.

To investigate whether cells in the zebrafish OE respond to purine compounds, the Fluo4-stained sections were stimulated with ATP by switching the perfusion stream from ACSF to ACSF containing 100 μM ATP. Stimulation with 100 μM ATP induced a strong calcium response across the OE. Application of the high potassium activates the neurons evoking a Ca^{2+} response more apical side. However, stimulation with 100 μM ATP resulted that at least two distinct cell populations appear to respond with changes in intracellular Ca^{2+} levels upon ATP stimulation. A row of basally located cells displayed a strong Ca^{2+} response. These responding cells form a densely packed monolayer along the lamina propria were not restricted to the sensory region (Figure 4.15a). These cells appear like a string of beads and have globular shapes of $5.71 \pm 0.09 \mu\text{m}$ diameter ($n = 185$ cells on 5 sections from 3 fish). Stimulation with 100 μM ATP also induced a calcium signal in cylindrical cells that span the apicobasal dimension of the tissue, the shape of which resembles Sus morphology (Figure 4.15b). Some of the prospective Sus are in direct contact with the ATP-responsive basally located cells, allowing for a flow of information

related to dead cells between the two. Morphometric measurements support the notion that these two cell populations cannot be the same. Average separation between two basal cells was $9.36 \mu\text{m} \pm 0.29 \mu\text{m}$ ($n = 80$ cells on 3 sections from 3 fish) and between two columnar cells $7.69 \mu\text{m} \pm 0.17 \mu\text{m}$ ($n = 171$ cells on 10 sections from 4 fish; p -value: 0.000000631).

A



B

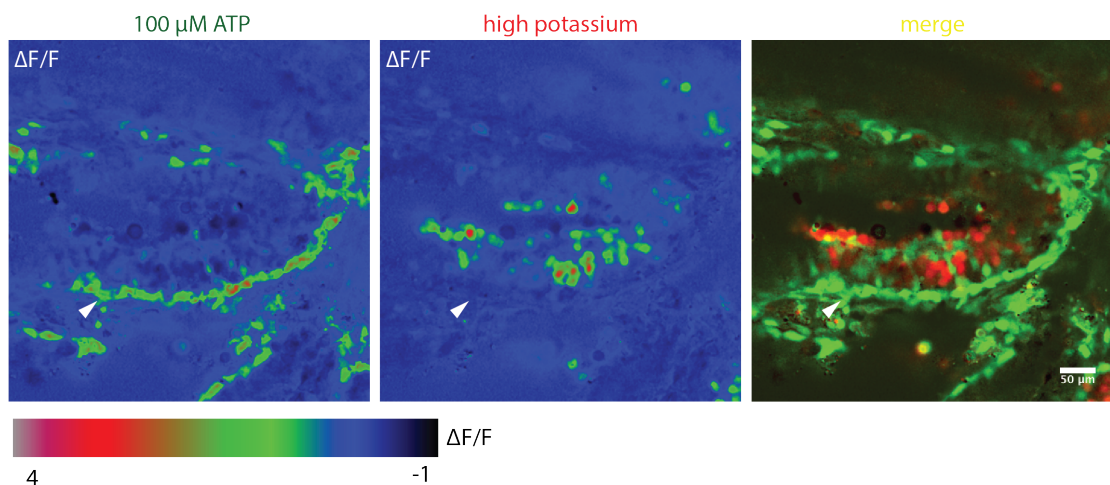


Figure 4.15. Ca^{2+} imaging on zebrafish OE vibratome sections. (A) Vibratome sections were loaded with the Ca^{2+} -sensitive dye Flu4-AM and stimulated with ATP (left, green) or high K^+ solution (center, green). Response was recorded over a 3 min / sec interval (B) Detailed and color coded view of the responses to ATP and high K^+ calculated as $\Delta\text{F/F}$.

In order to discriminate the observed responses to ATP from neuronal responses in the OE, a high K^+ -ion containing ACSF solution was applied which depolarizes the resting membrane potential of neurons and induces action potentials. Responses to high K^+

can be detected more apically compared to ATP-activated cells and the activation pattern is restricted to the sensory region of the OE as expected. On closer view neuronal responses to high K^+ fill the gaps between the columnar structures that respond to ATP (Figure 4.15a, b).

To understand whether the columnar cells responding to ATP are identical with Sus identified by CYKII immunohistochemistry a correlation analysis of cell distances was carried out. The space between two neighboring CYKII-positive cells was on average $6.9 \mu\text{m} \pm 0.14 \mu\text{m}$ ($n = 232$ pairs of cells), while the average distance between two columnar signals in response to $100 \mu\text{M}$ ATP was $7.69 \mu\text{m} \pm 0.17 \mu\text{m}$ ($n = 179$ pairs of cells). Thus, the similarity in intercellular distance supports the notion that cells responding to ATP may indeed be Sus (Figure 4.16).

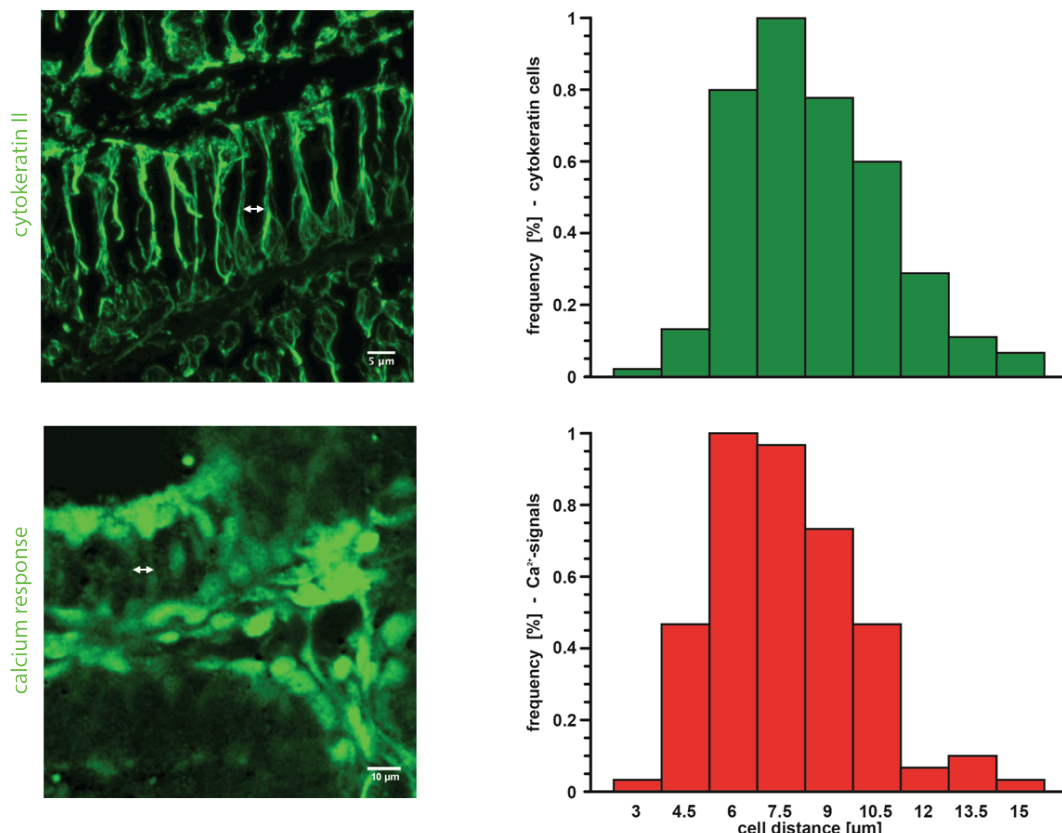


Figure 4.16. Activated columnar regions are possibly the Sus. Interstitial gap measured on CYKII confocal images (top row). Ca^{2+} response profile ones (bottom row) exhibit a similar distribution supporting that Sus respond to $100 \mu\text{M}$ ATP pulse.

4.5.1. Ca^{2+} signal is sourced from intracellular endoplasmic reticulum

To further characterize purinergic responses in the OE, it was investigated whether the source of the calcium signal is intra- or extracellular. For this purpose, Ca^{2+} release from intracellular sources was blocked by cyclopiazonic acid (CPA), a fungal toxin that blocks the Ca^{2+} -ATPases in the sarco-/endoplasmic reticulum. Thus, CPA can be used to deplete intracellular Ca^{2+} stores. Fluo4-AM-stained OE vibratome sections were continuously perfused with 10 μM CPA dissolved in ACSF. The OE was stimulated with 100 μM ATP at different time points (3, 6, and 9 min) following the onset of CPA perfusion. Blocking of endoplasmatic Ca^{2+} -ATPases abolished ATP-induced Ca^{2+} responses in a time-dependent fashion. After three minutes of CPA perfusion, calcium response to ATP of both cell populations decreased almost by half of the normalized ATP response before CPA application. After six minutes, Ca^{2+} was completely abolished for cells with Sus morphology, where basally located cells still showed small responses. After 9 min, Ca^{2+} response was still negligible for both cell types. To reestablish Ca^{2+} response, the OE sections were washed with ACSF solution resulting in a time-dependent recovery of the signal. Yet, even after 9 min wash the responses only reached about 20% of the normalized ATP response (Figure 4.17a; b). Thus, the source of the calcium signal is most likely calcium from intracellular stores.

4.5.2. Sus and basally located cells can express differential purinergic receptor subtypes

Suramin is a global antagonist of P2X and P2Y receptors, both of which are responsive to ATP. OE sections were constantly perfused with 100 μM suramin dissolved in ACSF solution. As for the CPA application, 100 μM ATP stimuli were presented after 3, 6 and 9 min to evoke a Ca^{2+} response on the OE (Figure 4.18a). After 3 min of suramin perfusion, a difference in the response profiles of Sus-like cells and basally located cells to 100 μM ATP was observed. Sus-like cells lost almost 20% of the Ca^{2+} response normalized to the pre-application ATP stimulus whereas basally located cells showed a slight decrease in response. After 6 min, for both cell types, the Ca^{2+} response was reduced significantly,

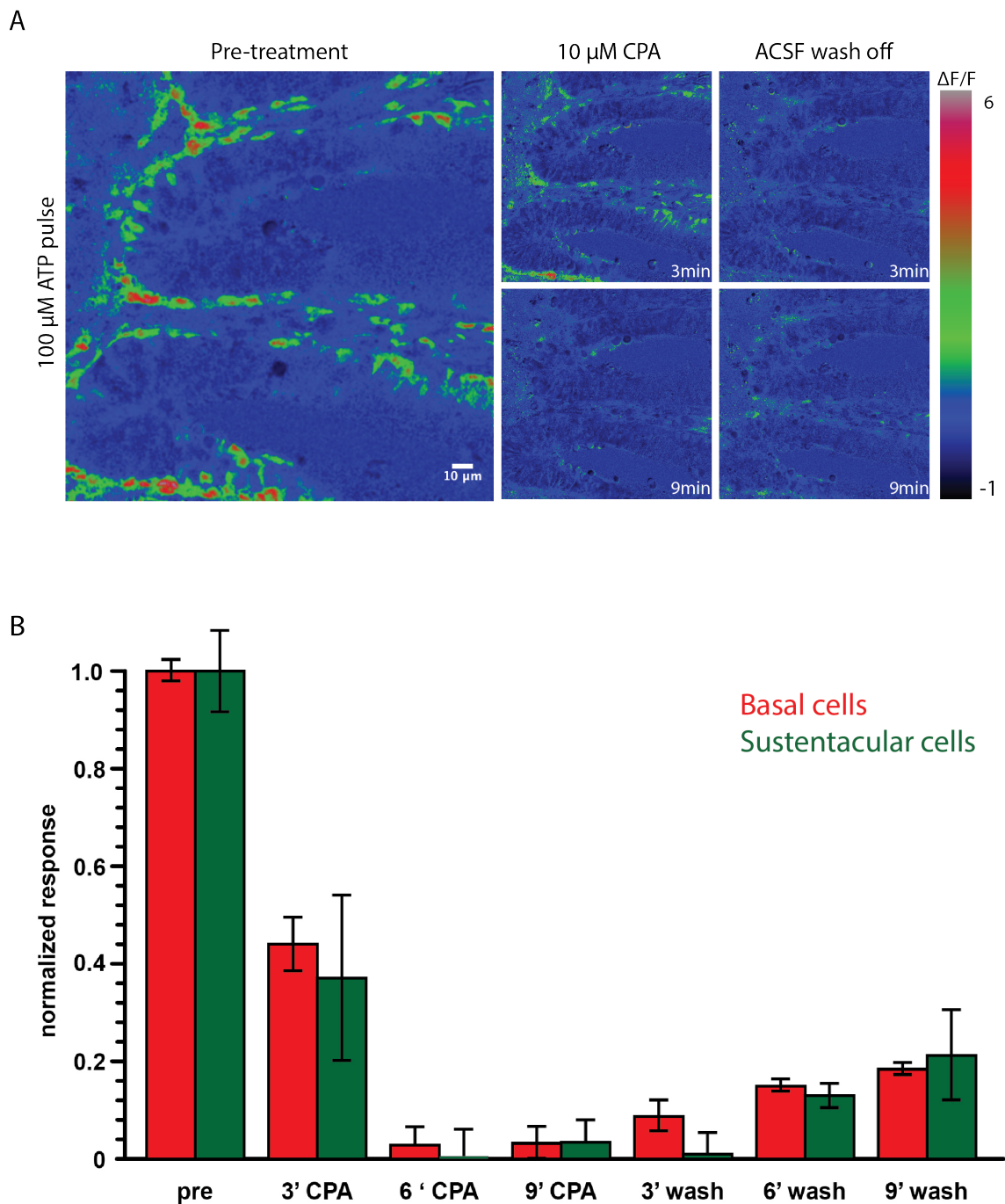


Figure 4.17. Ca^{2+} signal is mainly dependent on intracellular reservoirs.

(A) 9 min of CPA administration almost abolishes the response. Color scale represents the percent change in fluorescence. (B) Basal cells and Sus follow a similar response fashion.

dropping to 40% and 20% for basally located cells and Sus-like cells, respectively. After 9 min of suramin perfusion, Ca^{2+} response of both cell types was similar to 6 min suramin application with a slight increase in response (Figure 4.18b). This indicates that these two cell types might express different purinergic receptors that respond differently to the blocker suramin. Six minutes of washing-off with ACSF could not completely restore the lost Ca^{2+} response for both. These different response profiles of Sus-like cells and the basal cells might indicate that they can express different subsets of the purinergic receptor since the decrease in Ca^{2+} response on the onset of suramin perfusion differs between two cell types (Student's two-tailed t-test; $p_{3\text{min}}\text{-value}: 0.001$, $p_{6\text{min}}\text{-value}: 0.007$, $p_{9\text{min}}\text{-value}: 0.0033$).

4.5.3. Differential response to varying purine analogs supports the existence of two purinergically inducible cell types in zebrafish olfactory epithelium

As a final examination, the Ca^{2+} response pattern of the OE was scrutinized with respect to its activation by various purine compounds. 100 μM ATP, ADP, MeATP, MeADP, ATP γ S, UTP and UDP stimuli were applied in 3 min intervals onto OE cross-section, respectively. The consecutive administration of the analogs revealed that Sus-like cells and basal cells respond differently to the series of compounds and, thus, could have different purinergic receptors. For instance, responses of Sus-like cells to 100 μM ADP whereas are half the size as ATP responses, whereas basally located cells only respond with 20% of the signal compared to a 100 μM ATP pulse. When a 100 μM MeATP pulse was given, Sus-like cells responded with only 20% strength of the 100 μM ATP response while basal cell responses were nearly the same. 100 μM MeADP, on the other hand, evoked a nearly 60% Ca^{2+} signal in both cell populations. For ATP γ S, UTP and UDP, Sus and basal cells exhibited a decreasing response profile compared to MeADP response (Figure 4.19a; b).

Thus, the pharmacological analysis suggests that at least two different cell populations with different response properties towards purine compounds exist in the OE. Most likely, one of these populations is Sus, mainly based on comparison of morphometric

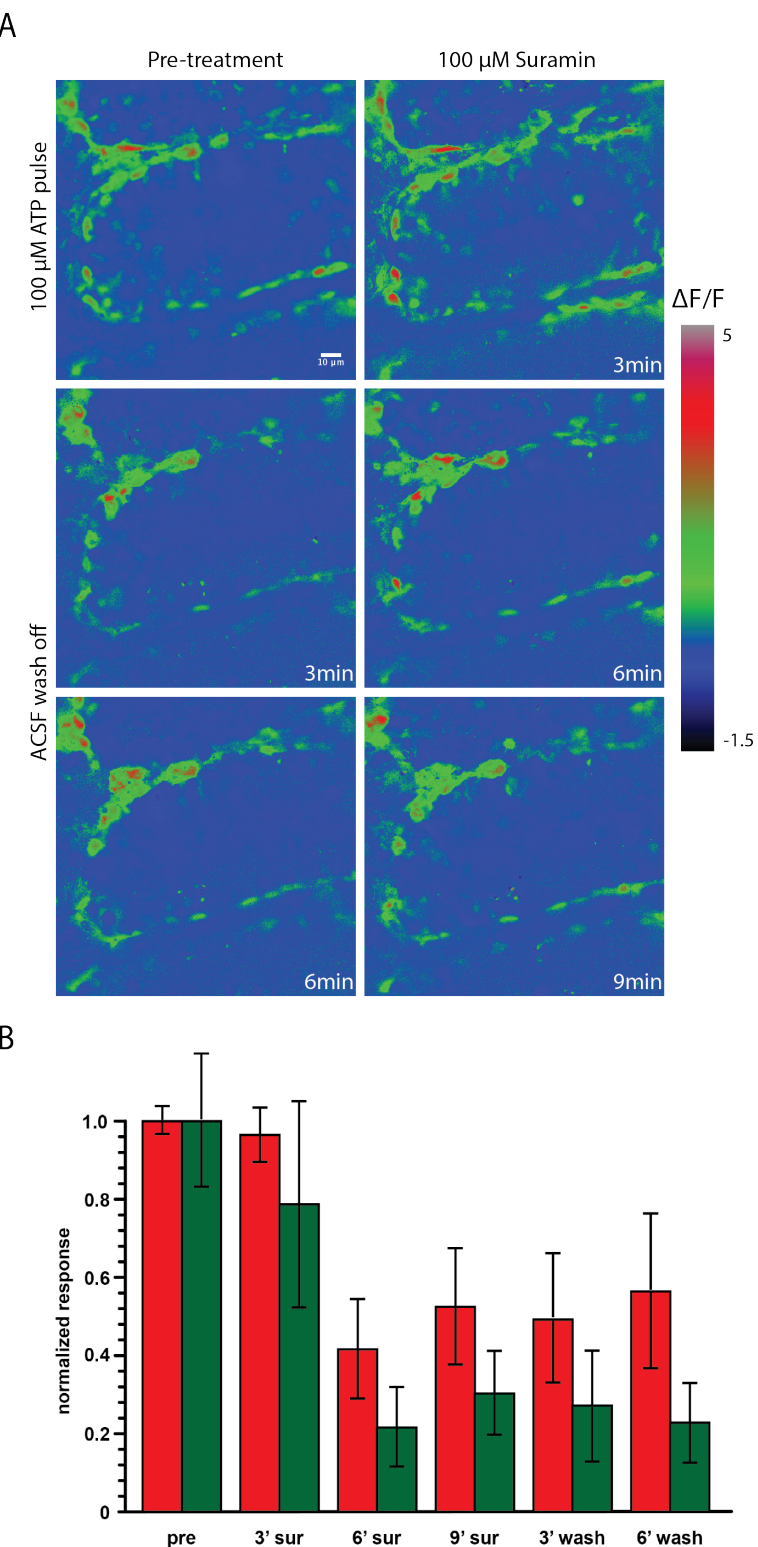


Figure 4.18. Two different cell populations with distinct purinergic receptor repertoire. (A) Suramin decreases the responsiveness of Sus and basal cells where Sus are more susceptible. Color scale represents the percent change in fluorescence. (B) Suramin revealed that Sus have a different set of receptors.

parameters, such as intercellular distance, distance across the basal lamina and lateral and vertical dimensions. Another cell population shows differential responses to purine analogs but the true identity of these cells remains unknown. Experiments with suramin also decreased the responsiveness of the two cell types differentially indicating that they express different P2-type purinergic receptors.

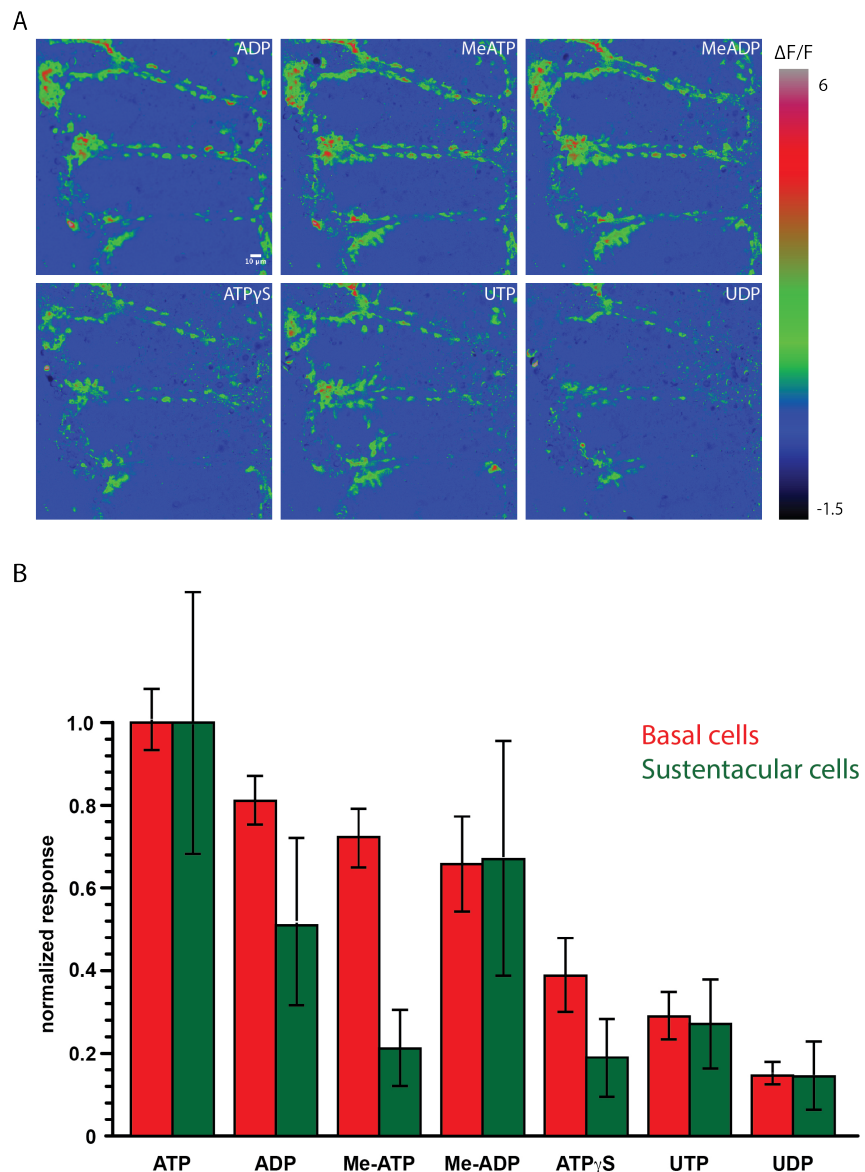


Figure 4.19. Varying analogs evoke different response. (A) UDP emerged as the least stimulating analog whereas ADP derivatives seem to be strong ligands after ATP. Color scale represents the percent change in fluorescence. (B) Differential inducibility of the two populations of cells underpins the differential expression of purinergic receptors on these two.

In summary, for the presented studies for the first time show that Sus in the zebrafish OE can be revealed by CYKII immunohistochemistry. Contrary to the rodent and amphibian counterparts, Sus are found to be in inverted orientation with basally located nuclei. CYKII immunohistochemistry also revealed a second cell population equivalent to duct/gland cells in the OE. Sus subsets appear to express the neuronal progenitor markers, nestin and Sox2. Immunohistochemistry against the two neurogenic progenitor marker proteins on intact and dissociated tissue showed that CYKII-immunoreactive cells are also immunoreactive to nestin and Sox2. This observation can suggest that Sus, or a subpopulation of Sus, may exhibit neurogenic progenitor capacity. BrdU incorporation assay suggests that Sus in the sensory region may divide occasionally but the proliferative zone of the interlamellar curves may be the major contributor to Sus in the sensory region. On the other hand, contribution of sensory/non-sensory border to the Sus population in sensory region may be sparse or not exist at all. Both features, neurogenic marker expression and being able to divide are prerequisites for any progenitor role of Sus. By pharmacological analyses, two distinct populations of purinergically inducible cells are could be revealed, one of which has Sus-like morphology, while the other one is more basally located. Both populations were shown respond differently to purine analogues and pharmacological inhibitors, suggesting that two different cell population respond to purines in the zebrafish OE.

5. DISCUSSION

The major aim of this study was the identification and initial characterization of sustentacular cells in the zebrafish olfactory epithelium. By analogy to the rodent OE, it was assumed that the zebrafish tissue also contains this olfactory-specific type of glia. However, cells with Sus morphology and tissue distribution have not been well characterized before. The only previous description of zebrafish Sus comes from electron microscopy studies in which those cells had been identified based on morphological features (Hansen and Zeiske, 1998).

Here, immunohistochemistry against the cytoskeletal filament cytokeratin II was used to highlight the population of Sus. Cytokeratin 18 is a commonly used Sus marker in the mouse and rat OE (Satoh and Yoshida, 2000; Holbrook *et al.*, 1995), but because of a recent third genome duplication in the teleost lineage (Woods *et al.*, 2000), functionally identical genes in zebrafish and mammals are not always easy to pinpoint. Nevertheless, an antibody raised against the *Xenopus* protein, which exclusively labels Sus in the *Xenopus* OE (Hassenklöver *et al.*, 2008), also marked a unique and extensive cell population that resembles Sus in the zebrafish OE.

Morphologically, at least two distinct cell populations have been revealed, of which the principal one shows Sus characteristics while the minor one consists of large elongated cells predominantly distributed around the interlamellar curves of the OE. By analogy to the mouse OE, in which Sus and gland/duct cells express the same cytokeratin (Krolewski *et al.*, 2012), it is reasonable to assume that these large globose cells are the zebrafish equivalent of olfactory gland cells. The cells are large, in contact with the apical border of the OE and appear to have two less densely stained intracellular compartments, one of which contains a nucleus, while the other one may be a mucus reservoir.

Over the recent years the concept has emerged that Sus are not simply structural cells that support the integrity and morphology of the OE but rather serve important functions

with respect to tissue maintenance and repair (Gokoffski *et al.*, 2010). In a wider sense, glia cells in zebrafish have been shown to bear neurogenic potential either through de- and trans-differentiation or by maintaining a neurogenic subpopulation (Hsieh, 2012; Lenkowski and Raymond, 2014). This capacity has been demonstrated extensively in the zebrafish retina, where the residing glia population, the Müller cells, contribute extensively to the generation of retinal neurons upon injury during adult life (Fausett and Goldman; 2006). Thus, it may be that Sus in the zebrafish OE serve related functions, either by direct proliferation and contribution to the pool of olfactory neurons or by conveying signals between the tissue and specialized stem cell populations located in the basal OE (Jia *et al.*, 2011).

In this light, it is interesting that established neuronal progenitor and stem cell markers, such as nestin and Sox2, co-localize with CYKII-positive cells in the zebrafish OE, which could be indicative of their potential to dedifferentiate to adopt stem cell function. Nestin has been widely used as a marker for neuronal stem cells (Lam and Strahle, 2009) and a small Sus subpopulation appears to be immunoreactive to an anti-nestin antibody. Sox2, on the other hand has a dual distribution in the rodent OE and specifies a subpopulation of globose basal cells (GBCs), which are believed to be early neuronal progenitors (Chen *et al.*, 2004) as well as Sus (Guo *et al.*, 2010). This dual expression of Sox2 in Sus and early neuronal progenitors could be a sign of the retained capacity of Sus to undergo dedifferentiation and/or proliferation under certain conditions, such as injury or tissue loss.

In addition, Sus might not only hold progenitor capacity *per se* but could be intermediates between the tissue and true stem cell populations located in the basal OE. In zebrafish, as in the rodent OE, Sus span the entire apicobasal dimension from the apical border of the OE to the basal lamina. It has been suggested by calcium imaging studies that Sus may respond to purines released from dying OSNs in the tissue and could release stimulating factors onto progenitor / stem cells at the base of the tissue that trigger proliferation and neurogenesis (Jia *et al.*, 2011). However, unlike in mouse and rat, where basal progenitors have been characterized extensively (Beites *et al.*, 2005), the population

of basal cells in the zebrafish OE awaits further investigation and characterization, mainly due to the lack of cross-reactive antibodies for established molecular markers.

In functional tissue imaging experiments using Ca^{2+} -indicator dyes, activation of Sus by purine compounds could be demonstrated in this thesis. It appears that two distinct cell populations, Sus and more basally located cells, respond to ATP and related compounds. Yet, these two cell populations show different temporal and pharmacological response profiles. The exact relationship between these two apparent cell populations still needs further examination but it could be that zebrafish Sus signal and stimulate onto as of yet undefined basal cell population or that the distinct profiles are physiological phenotypes of different compartments of the same Sus.

5.1. Zebrafish Sus show an inverted morphology

Sus in the mammalian and the amphibian OE are columnar cells with their cell bodies densely packed in the most apical layer of the OE, forming a dense Sus stratum (Hassenklöver *et al.*, 2008; Dittrich *et al.*, 2013; Farbman, 1992; Scwob *et al.*, 1995). Sus seal the OE tissue by forming a brush border, allowing only the dendritic knobs and cilia of OSNs to protrude above the apical border of the OE into the environment (Hassenklöver *et al.*, 2008). Rodent Sus extend slender cytoplasmic protrusions basally and are in direct contact with the basal lamina where they form feet-like endings that may form functional contacts with other cells in the basal OE (Hassenklöver *et al.*, 2008; Farbman, 1992).

Cytokeratin II staining on the zebrafish OE, however, revealed an inverted morphology of Sus. In the zebrafish, Sus extend apical tufts defining the apical border of the OE instead of the densely packed cell bodies characteristic of rodent and frog Sus. In the fish, CYKII-positive cells arborize at their basal end to form basket-like structures that surround a central nucleus. From the morphology alone it is difficult to conclude whether these nuclei are Sus nuclei or whether they belong to a second cell population, reminiscent of the contacts that Sus form in the rodent OE. The immunostaining against CYKII appears

to label only intracellular bundles of cytokeratin fibers but not the entire morphology of the cells. Thus, at least theoretically, Sus cell bodies and nuclei could be located anywhere along the apical to basal dimension of the OE.

One indication that Sus cell bodies may be located basally comes from the tissue distribution of Sox2-positive cells. As mentioned above, Sox2 is expressed in Sus and neuronal progenitors in the rodent OE (Guo *et al.*, 2010). Accordingly Sox2-expression is localized to the basal OE and to the apical-most layer where Sus cell bodies reside. In the zebrafish, however, Sox2-positive cells occupy basal positions exclusively. Immunohistochemistry on dissociated single cells revealed that at least a subpopulation of Sox2-positive cells is CYKII positive as well. Similarly, Sox2-positive cells in the basal side of zebrafish OE are very dense and appear to be more abundant than expected for the neuronal progenitor population.

In the zebrafish, proliferative activity and neurogenesis in the unperturbed OE occurs largely at two distinct zones located at the interlamellar curves and the sensory/non-sensory boundary, but not within the sensory region of the OE (Byrd and Brunjes, 2001; Oehlmann *et al.*, 2004; Bayramli, unpublished). Early neuronal progenitors transiently express Sox2 (Guo *et al.*, 2010), thus if Sox2-positive cells in the zebrafish OE were only neuronal precursors, a distribution of Sox2-positive cells closer to the proliferation zones should be expected. However, Sox2 staining reveals a dense cell population distributed along the entire sensory region of the OE as well. Thus, a subpopulation of Sox2-positive cells in the basal OE may be Sus in addition to GBCs.

This inverted orientation of Sus is surprising, the functional implication of which remains unexplored. It may be however, that Sus in zebrafish have a more prominent and more direct role in damage-induced neurogenesis when compared to higher vertebrates as outlined for Müller glia in the zebrafish retina (Fausett and Goldman; 2006) and that the basal OE provides an appropriate substrate for cell proliferation and neuronal differentiation.

5.2. Sus can potentially be neurogenic progenitors

To search for neuronal progenitor markers in the zebrafish OE, immunohistochemistry against nestin and Sox2 (Park *et al.*, 2010; Brazel *et al.*, 2005) was conducted. For both markers, the OE exhibits strong immunoreactivity, indicative of the presence of multipotent progenitor cells.

However, staining for nestin was quite variable and different cell populations were labeled. Among those, a basal continuous line of flat cells surrounding each lamella, individual cells located at the interlamellar curves and the sensory/non-sensory boundary, and occasional cells resembling Sus morphology could be observed. It remains speculative at best, which of these cell populations are truly nestin-positive and which ones are false-positive due to unspecific immunoreactivity of the anti-nestin antiserum. However, from a neurogenesis point of view all of the three cell populations could be involved in the process. Most likely, strongly nestin-immunoreactive cells at the interlamellar curves and sensory/non-sensory boundary are real stem cells, as intense neurogenesis is observed in these regions in unperturbed OE tissue (Byrd and Brunjes, 2001; Oehlmann *et al.*, 2004; Bayramli, unpublished). However, double label experiments with BrdU to demonstrate mitotic activity of these cells need yet to be performed.

Acute injury to the OE induces a robust injury response that is characterized by a unique tissue distribution of proliferating cells (Iqbal and Byrd-Jacobs, 2010; Capar, 2015). While proliferation is restricted to the ends of each lamella in intact tissue, mitotic activity is induced within the sensory region upon mechanical and chemical injury (Iqbal and Byrd-Jacobs, 2010; Capar, 2015). Proliferating cells are localized to the basal OE of injured tissue, thus the continuous line of nestin-immunoreactive cells could have functional significance as well.

Yet another possibility is that Sus directly contribute to injury-induced proliferation and tissue repair by de-differentiation and neuronal progenitor expansion. To investigate

this possibility, co-immunolocalization studies for CYKII and nestin or Sox2 were performed on intact and dissociated olfactory tissue. Co-localization of the neurogenic markers with CYKII may imply that a subpopulation of Sus may have neurogenic potential under injury conditions. Indeed, a certain fraction of cells was found to be double-positive for CYKII and nestin or Sox2 in these assays.

In the zebrafish central nervous system, radial glia cells remain active beyond early development and were associated with the reconstitution of damaged brain tissue (Becker and Becker, 2008; Chapouton *et al.*, 2007; Kizil *et al.*, 2012; Zupanc, 2001; 2006; Zupanc and Sirbulescu, 2011). In zebrafish radial glia cells represent a multipotent proliferating cell population expressing the unique markers GFAP, BLBP, vimentin (Chapouton *et al.*, 2007; Kizil *et al.*, 2012) in addition to markers of stem cell identity, such as nestin, Sox2, Musashi-1, and S100 in partially overlapping cell populations (Chapouton *et al.*, 2007; Kizil *et al.*, 2012).

In the mammalian brain, radial glia cells also express nestin and Sox2 markers (Hsieh, 2012; Lendahl *et al.*, 1990; Hockfield and McKay, 1985). In the rodent embryo, nestin-expressing radial glia-like progenitors are reported to create olfactory neurons (Murdoch and Roskams, 2008). As far as peripheral sensory tissue is concerned, the retinal equivalent of radial glia cells, the Müller glia, has been shown to proliferate upon retinal tissue damage giving rise to photoreceptor cells after molecular reprogramming (Fausett and Goldman, 2006; Ramachandran *et al.*, 2010; Wan *et al.*, 2012). In the mammalian and avian systems, Müller glia cells are proposed to be residual dormant progenitors with the capacity to recover the retinal neuroepithelium (Ooto, 2004; Fisher and Reh, 2001). Similar to Sus and radial glial cells, Müller glia cells express nestin and Sox2 (Das *et al.*, 2006; Walcott and Provis, 2003; Surzenko *et al.*, 2013).

In the rodent OE, Sus also express nestin and Sox2 markers, which could point to their direct neurogenic potential (Doyle *et al.*, 2001; Guo *et al.*, 2010). Interestingly, nestin is localized to the end-feet of Sus and hence near to the basal lamina (Doyle *et al.*, 2001). Sox2, on the other hand, is found within the somata of Sus (Guo *et al.*, 2010). Along with

those markers, Sus were also shown to express Hes1 and Pax6, which are found in GBCs, the presumed active progenitor population in the mammalian OE (Manglapus *et al.*, 2004; Guo *et al.*, 2010). Expression of the notch target Hes1 and the homeotic transcription factor Pax6 was reported for Müller glia cells as well (Tomita *et al.*, 1996; Furukawa *et al.*, 2000; Roesch *et al.*, 2008). In addition, another critical proliferation factor, TGF- α , is found in Sus (Schwob, 2002).

Localization of these proliferation markers might be the indicative of restricted neurogenic potential by de-differentiation of Sus. Yet, it could equally well reflect Sus potential to divide and generate new Sus rather than neurons in a lineage-restricted manner. Indeed, Sus were shown to predominantly generate new Sus in the murine OE (Mulvaney and Heist, 1971; Huard *et al.*, 1998; Chen *et al.*, 2004; Manglapus *et al.*, 2004).

Strong nestin-positive cells are predominantly found in the non-sensory region at the interlamellar curves and the sensory/non-sensory boundary, the predominant proliferation zones of the zebrafish OE (Byrd and Brunjes, 2001). Along the basal lining, we also observed a series of nestin-immunoreactive cells which can be basal progenitors or end-feet of Sus that orient cell migration and mobility (Doyle *et al.*, 2001). Besides, we observed a few nestin-positive structures spanning the apicobasal axis, reminiscent of Sus. The distributed localization of nestin-positive cells may be a reflection of the dual nature of olfactory neurogenesis in the zebrafish OE during maintenance and injury responses.

Sox2 expression, on the contrary, is restricted to the sensory region and interlamellar curves where Sus and mature neurons reside. Sox2-immunoreactive cells are basally located and coincide with the basket-like structures of cytokeratin basal termini. As for Sus in rodent OE (Guo *et al.*, 2010), Sox2 may be a marker of zebrafish Sus as well. However, Sox2 appears to label more than just the Sus population, as some Sox2-positive cells are more detached from the basal lamina and not surrounded by cytokeratin II filaments. Those cells may be the zebrafish equivalent of GBCs described in the rodent OE (Guo *et al.*, 2010). BrdU incorporation assays performed in this study revealed that Sox2-positive cells in the zebrafish are mitotically active. Yet, unless additional markers are at hand, the basal

cell population in the zebrafish OE remains largely undefined. The inverted morphology of Sus adds yet another layer of complication to clearly dissect the various cell populations in this part of the tissue.

5.3. The basal OE, which cells to expect?

In the rodent OE, two neurogenic progenitor cell populations have been described extensively and which are located basally within the pseudo-stratified epithelium. Based on their distinct morphology, they are known as globose basal cells (GBCs) and horizontal basal cells (HBCs; Holbrook *et al.*, 1995). HBCs are most basally located, have slow rate of cellular division and express the markers cytokeratin 5 and 14. They are thought to be injury responsive cells and to replenish the pool of GBCs following induced proliferation (Leung *et al.*, 2007). GBCs, on the other hand, have a higher rate of proliferation, form a layer above HBCs and express the neurogenic progenitor markers Sox2 and Pax6 (Guo *et al.*, 2010). They are thought to maintain the OE under normal cellular turnover conditions and can give rise to other cell types in lesioned tissue (Chen *et al.*, 2004). In the zebrafish OE, two possible counterparts of HBCs and GBCs have been described in this and related study (Bayramli, unpublished; Capar, 2015). Cells at the sensory/non-sensory border and interlamellar curves give rise to new cells under maintenance conditions (Byrd and Brunjes, 2001; Oehlmann *et al.*, 2004; Bayramli, unpublished). These cells might represent the main pool of GBCs in zebrafish and Sox2-positive cells are found in these positions. On the other hand, under injury conditions (Iqbal and Byrd-Jacobs, 2010; Capar, 2015), a second cell population responds with mitotic activity in the basal OE reminiscent of HBCs.

5.4. Sus and intraepithelial signaling

An exciting possible function of Sus may be to convey signals of tissue injury to basal stem cell populations (Jia *et al.*, 2010; 2011). This concept is straightforward in the rodent OE, where adult neurogenesis occurs all along the sensory epithelium. Sus are particularly suited for this process because they span the entire apicobasal dimension of the OE and, thus, could communicate between apically located OSNs and stem cells in the

basal layers. Yet, in zebrafish, neurogenesis in the unperturbed tissue occurs at concentrated regions located laterally to the sensory tissue. Zebrafish Sus are oriented perpendicular to this axis but are oriented in a fashion that is consistent with the observation that acute damage induces proliferation at the base of the sensory OE. Thus, in zebrafish, and in mammals, Sus may only contribute to damage responses but are not involved in monitoring the number of neurons in the intact OE. In particular purines have been proposed to play a role in this intraepithelial signaling (Jia *et al.*, 2010).

Throughout the central nervous and peripheral sensory systems, purinergic signaling has been demonstrated in glia cells and Sus (Abbracchio *et al.*, 2009; Housley *et al.*, 2009). In the murine and amphibian OE, it was reported that Sus, basal cells, and OSNs can be activated by purines as revealed by functional calcium imaging (Hassenklöver *et al.*, 2008; Hassenklöver *et al.*, 2009; Hegg *et al.*, 2003; Hegg *et al.*, 2009; Dittrich *et al.*, 2013).

5.5. ATP evokes Ca^{2+} responses in Sus

To investigate whether purinergic signaling may play a role in the zebrafish OE, a similar calcium imaging approach was followed. Similar to the murine and amphibian OE, ATP induces a strong Ca^{2+} response mainly in columnar cells that span the apicobasal dimension of the OE and in basal cells in the zebrafish OE. It remains to be shown which of these populations represent Sus or if different subpopulations of Sus exist.

To discriminate between different ATP-responding cells, high K^+ stimulation, which triggers a breakdown of the neuronal resting potential was used to highlight neurons. As expected, a few neurons also responded to ATP, which is a natural odorant for fish (Friedrich and Korschning, 1998). This indicates some zebrafish neurons also express purinergic receptors similar to sensory neurons in the mouse OE (Hegg *et al.*, 2003; Gayle *et al.*, 2005).

To understand whether Ca^{2+} signal emerges from intracellular calcium stores, CPA, an endo-/sarcoplasmic reticulum Ca^{2+} ATPase inhibitor, was applied constantly depleting the stores. CPA perfusion almost completely abolishes Ca^{2+} signals in columnar and basal cells, suggesting the dependency of the response on intracellular Ca^{2+} similarly to mouse and *X.laevis* (Hassenklöver *et al.*, 2008; Hegg *et al.*, 2003; Dittrich *et al.*, 2013).

5.6. Identification of purinergic receptor subtypes

To further analyze purinergic receptor subtypes, acute slices of zebrafish OE were treated with a general P2 purinergic receptor antagonist, suramin. Both, columnar and basal cells responded with a decrease in Ca^{2+} responses upon ATP stimulation. However, the decrease was not parallel in both cell types. Ca^{2+} response of basal cells remained stronger than responses of columnar cells during suramin application. This difference in the response profile may be indicative of a variation in purinergic receptors among these two cell populations. Basal cells, for instance, might be expressing the P2Y₄ purinergic receptor as the P2Y₄ subtype is known to be uninhibited by suramin (von Kügelgen, 2006). In the amphibian model, Sus are shown to be unaffected by suramin whereas basal cell's respond to suramin application (Hassenklöver *et al.*, 2008; Dittrich *et al.*, 2013). This apparent difference may indicate a difference between purinergic receptor subtypes across species.

Alternatively, the basal cell population that is unresponsive to suramin in the zebrafish OE may indeed be the Sus population. The distribution of responding cells, their cell diameters and density closely resemble CYKII-positive structures and Sox2-positive cells in the basal OE. Again, the inverted morphology of Sus prevents clear cut answers at this point and awaits further examination.

Purinergic receptor subtypes were further characterized with the application of different purine analogs. As expected from the suramin inhibition experiment, columnar apicobasal cells and basal cells showed different response profiles. The basal cell

population responded in the order ATP>ADP>MeATP>MeADP> ATP γ S>UTP>UDP whereas columnar cells responded in the order ATP>MeADP>ADP>UTP> MeATP=ATP γ S>UDP. ATP is the most potent activator of both cell types, which might suggest that P2Y2 and P2Y4 receptors are the most abundant receptors in columnar and basal cells. Additionally, second and third order of response to nucleoside diphosphates can indicate the presence of P2Y1, P2Y6, P2Y12 receptors in which P2Y6 might be the least in number because it is the highest responsive receptor for UDP. Finally, P2Y11 receptors can also be expressed in both cell populations due to ATP γ S responsiveness (von K \ddot{u} gelgen, 2006).

In this initial characterization of purinergic signaling in the zebrafish OE two different cell types responded to purine stimulation. Even though the pathway and significance of this stimulation still awaits further investigation, the observations reported here are consistent with a functional role of Sus in signaling between the tissue and an uncharacterized stem cell population.

5.7. Is there a role for purinergic signaling in response to injury?

Different parts of the zebrafish OE contribute to neurogenesis under maintenance and injury conditions, the sensory/non-sensory border and ILC (Byrd and Brunjes, 2001; Oehlmann *et al.*, 2004; Bayramli, unpublished), or basal cells within the sensory region (Iqbal and Byrd-Jacobs, 2010; Capar, 2015), respectively. This implies that two distinct progenitors/ stem cell populations exist, one of which is located close to the basal lamina of the OE. Those cells are activated by injury and divide to reconstitute the damaged tissue. How this population of the basal cells can “sense” dying epithelial cells remains to be answered. Purinergic signaling can have such a role in activating progenitor cells and Sus may act as intermediary messengers, due to their apicobasal orientation. Upon reception of purinergic cues from dying neurons, Sus close to the injury site respond with a Ca²⁺ wave that can cause release of purines or neuropeptides at their basal end and in turn stimulate progenitor cells located there. Moreover, differential expression of purinergic

receptors in the Sus and basal cells on zebrafish OE might be an indication of such a two-step process.

Taken together, here, for the first time, the population of Sus in the zebrafish OE is described with some detail. As in mammalian and amphibian counterpart, Sus are regularly spaced along the lamella and span the apicobasal dimension of the OE. Yet, instead of large and columnar apical cell bodies zebrafish Sus have an inverted orientation with basally located cell bodies and apical tufts. There are indications that zebrafish Sus could have progenitor capacity based on their glia-like properties and marker expression. Sox2 and nestin, two neurogenic progenitor markers, could be shown to co-localize with Sus. In line with this, BrdU incorporation assays showed that zebrafish Sus can divide. These two properties are no proof but basic prerequisites for Sus to be progenitor/stem cell. However, dividing Sus under maintenance conditions might only contribute to other Sus or Sus subtypes. Therefore, as in Müller glia, Sus might regain neurogenic progenitor capacity under injury conditions and give rise to other cell types including receptor neurons.

Finally, physiological experiments showed that Sus, in addition to a basal cell population, respond with Ca^{2+} signals upon purinergic stimuli. There are indications that these two populations express different subtypes of purinergic receptors, imply that the two can have different roles in neurogenesis. To better understand their functions, an injury experiment followed by BrdU incorporation protocol could be performed in which purinergic receptors are blocked to inhibit the signal from dying cells to be conveyed to basal stem cells.

APPENDIX A: EQUIPMENT

Table A.1. List of equipments.

4 °C Room	Birikim Elektrik, Turkey
Autoclaves	Astell Scientific, UK
Centrifuge	Eppendorf, Germany (5417R)
Confocal Microscope	Leica, USA (SP5-AOBS)
Electronic Balance	Sartorius, Germany (TE412)
Fluorescence Microscope	Leica Microsystems, USA (MZ16FA)
Freezer 1 -20 °C	Arçelik, Turkey
Freezer 2 -80 °C	Thermo Electron Corp., USA (Farma 723)
Glass Bottles	Isolab, Germany
Incubator 1	Weiss Gallenkamp, UK
Incubator 2	Nuve, Turkey
Incubating Shaker	Thermo Electron Corp., USA
Micropipetters	Eppendorf, Germany (Research)
Microinjector	Eppendorf, Germany (FemtoJet)
Refrigerator	Arçelik, Turkey
Vortex	Scientific Industries, USA
Stereo Microscope	Zeiss, Germany (2000-C)
Single cell electroporator	Molecular Devices, USA (Axoporator 800A)
Cryostat	Leica, Germany (CM3050S)
Inverted Microscope	Zeiss, Germany (Axio Vert.A1)
Coplin staining jars	Wheaton-VWR, The Netherlands (900520)
Ventilated oven	Thermo Scientific Hereaus, UK
Poly-L-Lysine Coated Slides	Electron Microscopy Sciences, USA (63410)
Microinjection needles	Warner Instruments USA (Nanoject II)
Confocal microscope	Zeiss, Germany, (LSM 780/Axio Examiner)
Vibratome	Leica, Germany (VT1200S)

APPENDIX B: SUPPLIES

Table B.1. List of supplies.

Ethanol Absolute	Sigma-Aldrich, U.S.A. (34870)
Paraformaldehyde	Sigma-Aldrich, U.S.A. (P6148)
Triton X-100	Sigma-Aldrich, U.S.A. (T8787)
Hydrochloric acid (HCl)	Sigma-Aldrich, U.S.A (H1758)
Optimum cutting temperature compound (OCT)	Sakura® Finetek, USA (4583)
MS-222 (Tricaine)	Sigma-Aldrich, U.S.A. (E10521)
Phosphate buffered saline tablet	Sigma-Aldrich, U.S.A. (P4417)
Mouse anti-cytokeratin type II	Developmental Studies Hybridoma Bank, USA (1h5)
Rabbit anti-nestin	Abcam, UK (ab27952)
Rabbit anti-Sox2	GeneTex, UK (CTX124477)
Mouse anti-HuC/D	Abcam, UK (ab78467)
Mouse anti-BrdU	Becton-Dickinson, USA (347580)
Rat anti-BrdU	Abcam, UK (ab6326)
BrdU	Sigma-Aldrich, USA (B5002)
Anti-mouse Alexa Fluor 488	Life Technologies, UK (A28175)
Anti-mouse Alexa Fluor 633	Life Technologies, UK (21146)
Anti-rabbit Alexa Fluor 633	Life Technologies, UK (A21072)
Anti-rat Alexa Fluor 633	Life Technologies, UK (21094)
TO-PRO®-3 Iodide	Molecular Probes, USA (T3605)
DAPI Nucleic Acid Stain	Molecular Probes, USA (D1306)
Dextran-coupled Alexa Fluor 488	Life Technologies, UK (D-22910)
Fluo-4, AM	Life Technologies, UK (F14201)
Cyclopiazonic acid (CPA)	Sigma-Aldrich, USA (C1530)
Suramin	Sigma-Aldrich, USA (S2671)
ATP	Sigma-Aldrich, USA (FLAAS)

Table B.1. List of supplies (cont.).

ADP	Sigma-Aldrich, USA (A2754)
2-MeSATP	Sigma-Aldrich, USA (A023)
2-MeSADP	Sigma-Aldrich, USA (M152)
ATP γ S	Sigma-Aldrich, USA (A1388)
UTP	Sigma-Aldrich, USA (U6875)
UDP	Sigma-Aldrich, USA (94330)

APPENDIX C: RESULTS FOR INDIVIDUAL EXPERIMENTS

Table C.1. Cell numbers expressing different markers using IHC on tissue dissociation assay.

Image #	Total Cell Number					Image #	Total Cell Number			
	DAPI +	CYKII +	Nestin +	Triple +			DAPI +	CYKII +	Sox2 +	Triple +
14_1	39	11	15	10		6_1	29	17	20	10
12_1	40	20	19	6		5_1	83	42	40	24
11_1	34	17	19	10		4_2	47	36	27	22
10_1	49	16	12	9		3_2	36	9	11	8
9_1	41	15	24	8		2_1	43	21	14	10
7_1	86	34	33	21		Average	47.6	25.00	22.4	14.8
Average	48.2	18.8	20.3	10.7		SD	20.94755	13.6565	11.58879	7.563068
SD	19.2	8.0	7.4	5.3		SE	9.368031	6.107373	5.182663	3.382307
SE	7.8	3.3	3.0	2.2						

Table C.2. CYKII and BrdU temporal profiling.

1day					
BrdU positive			Double positive		
Curve	Sensory	Nonsensory	Curve	Sensory	Nonsensory
6	5	6	0	1	0
2	2	7	0	0	0
4	1	4	0	0	0
2	6	8	0	0	0
3	0	7	0	0	0
4	3	7	0	2	0
5	2	6	0	1	0
0	2	3	0	0	0
0	4	5	0	0	1
3	4	5	0	0	0
1	4	6	0	0	0
3	6	7	0	0	0
6	2	6	0	0	0
3	6	8	0	0	0
7	3	8	0	0	0
5	1	5	0	0	0
4	1	5	0	0	0
15	3	7	0	2	0
13	0	6	0	0	0
13	1	3	0	0	0
11	2	4	0	0	0
8	2	6	0	0	0
8	3	5	1	0	0
20	0	11	0	0	0
20	5	6	0	0	0
9	0	7	0	0	0
7	2	4	0	0	0

Table C.2. CYKII and BrdU temporal profiling (cont.).

4day					
BrdU positive			Double positive		
Curve	Sensory	Nonsensory	Curve	Sensory	Nonsensory
5	6	5	0	0	0
4	7	2	0	0	0
5	6	0	0	0	0
5	4	2	0	0	0
3	1	1	0	0	0
7	1	3	1	0	0
6	3	3	0	0	0
4	3	4	0	0	0
4	4	0	0	0	0
3	1	1	0	0	0
9	5	5	1	0	0
8	1	5	1	0	0
7	5	2	1	0	0
3	3	3	0	0	0
2	2	0	0	0	0
3	4	5	0	0	0
1	3	3	0	0	0
2	0	4	0	0	0
0	0	6	0	0	0
3	4	1	0	0	0
4	0	5	0	0	0
4	9	6	0	0	0
5	0	1	0	0	1
1	1	1	0	0	0
8day					
3	10	2	1	3	0
5	12	4	1	1	1
5	16	2	0	1	0
2	4	2	1	0	0
2	6	4	0	0	0
0	5	2	0	1	0
3	8	0	0	3	0
14	15	1	1	1	0
6	19	0	0	1	0
2	17	4	0	0	0

Table C.2. CYKII and BrdU temporal profiling (cont.).

	Curve	Sensory	Nonsensory	
1 day	0.03703704	0.22222222	0.03703704	average
	0.19245009	0.57735027	0.19245009	SD
	0.03703704	0.11111111	0.03703704	SE
8 days	0.4	1.1	0.1	average
	0.51639778	1.10050493	0.31622777	SD
	0.16329932	0.34801022	0.1	SE
4 days	0.16666667	0	0.04166667	average
	0.38069349	0	0.20412415	SD
	0.07770873	0	0.04166667	SE

Table C.3. Abundance and thickness of the cells expressing nestin.

Fish1									
Nestin Cell	Thickness	Nestin Cell	Thickness	Nestin Cell	Thickness	Nestin Cell	Thickness	Nestin Cell	Thickness
1	26.474	1	30.68	1	28.325	1	20.441	1	30.177
2	32.763	2	28.293	2	25.8	2	18.164	2	35.824
3	33.397	3	18.3	3	21.997	3	18.037	3	28.206
				4	20.033	4	29.573	4	24.974
				5	22.892	5	25.037		
				6	16.947	6	25.939		
Fish2									
Nestin Cell	Thickness	Nestin Cell	Thickness	Nestin Cell	Thickness	Nestin Cell	Thickness	Nestin Cell	Thickness
1	36.705	1	35.88	1	36.853	1	26.948	1	33.761
2	30.995	2	35.508	2	31.577	2	29.22	2	32.273
		3	37.859	3	30.178			3	33.878
average	28.56984			4	22.629			4	40.547
sd	6.260984								
se	1.029299								
nestin cell abundance					average	6.00000			
Fish1		Fish2			sd	1.595448			
S5 N1-1	7	S9 N2-1		3	se	0.460566			
S4 N1-1	9	S8 N2-1		6					
S3 N2-1	7	S7 N2-1		6					
S2 N1-1	6	S6 N2-1		5					
S1 N1-1	7	S6 N1-1		4					
		S5 N1-1		7					
		S4 N1-1		5					

Table C.4. Distance of the basal and columnar cells to neighboring cells.

distance between 2 neighboring basal cells			
fish#1	fish#2	fish#3	
141216N1S206ATP	141210S1-8ATP	141208S1-3ATP	
8.177	11.276	10.279	12.768
7.311	9.596	12.838	12.003
5.863	6.831	11.095	8.816
8.463	10.801	7.743	10.318
8.102	3.780	10.883	13.196
11.916	5.278	8.548	11.200
9.790	6.720	5.939	12.344
5.863	5.977	8.255	13.219
5.794	7.697	12.425	11.699
4.490	12.502	5.185	9.924
5.895		9.669	12.409
10.210		11.679	7.997
8.342		12.395	12.263
6.152		13.659	9.160
6.846		9.816	11.665
6.007		12.734	13.867
7.948		10.944	10.974
7.560		4.643	7.591
12.614		7.296	9.957
10.072		8.271	8.063
			9.344
			11.665
			11.211
			14.166
			11.813
			6.202
			8.242
			8.652
			8.895
			7.083

Table C.4. Distance of the basal and columnar cells to neighboring cells (cont.).

distance between 2 neighboring coulumnar cells									
fish#1		fish#2		fish#3			fish#4		
1	2	3	4	5	6	7	8	9	10
11.307	8.722	8.467	9.673	6.119	5.786	7.25	5.152	9.513	13.22
4.903	5.205	6.17	8.177	9.126	8.853	5.067	5.443	7.241	7.169
4.505	11.364	6.265	4.847	5.216	3.209	6.959	6.25	7.892	7.256
5.365	8.433	7.669	5.429	10.172	8.917	6.758	5.069	10.523	5.402
6.226	13.716	10.47	7.201	5.082	12.081	7.069	5.615	9.693	8.711
4.659	9.8	8.155	7.094	7.916	5.97	7.722	9.748	9.127	6.993
5.746	10.625	8.502	5.977	9.415	5.293	14.315	7.799	7.892	
6.226	11.033	6.371	7.094	9.967	9.845	12.039	11.622	7.739	
8.676	11.146	9.01	7.466	6.412	7.332	6.707	6.831	8.398	
7.233	12.493	11.188	4.847	7.048	5.456	10.403	7.599	6.727	
4.614	5.717	7.313	5.691	6.267	10.27	9.105	7.173	8.271	
5.6	8.167	9.865	4.672	5.487	6.419	5.067	7.168	13.93	
9.39	8.662		3.672	7.76	3.351	11.888	4.128	5.557	
6.325	8.208		5.593	11.577	9.745	6.694	8.039	8.831	
7.482	9.176		6.339	7.345	5.856	6.044		9.301	
9.865			10.755	9.152	7.655			7.67	
11.281			6.804	8.059	5.175			11.594	
7.792			8.203	7.209	13.095			9.693	
6.658			4.975	7.867	8.182			3.008	
6.022			9.694	6.827	5.013				
2.884				6.364	4.365				
5.48				9.152	9.134				
				7.037	6.546				
				7.819	7.608				

Table C.5. Duct/gland cells morphometry.

Cell #	Apical Diameter	Basal Diameter	Cell #	Apical Diameter	Basal Diameter	Cell #	Apical Diameter	Basal Diameter
1	11.293	6.044	1	13.706	7.069	1	13.029	7.441
2	10.109	5.607	2	11.239	7.472	2	12.489	6.302
3	9.067	5.911	3	9.133	7.655	3	11.170	5.774
4	10.825	4.323	4	10.453	7.166	4	12.789	5.167
5	13.128	4.772	5	11.239	7.484	5	7.931	5.001
6	8.942	4.927	6	10.177	4.833	6	13.128	7.478
7	11.278	5.137	7	13.035	6.557	7	7.974	5.511
8	10.177	6.557	8	13.128	6.095	8	11.452	5.585
9	12.046	6.816	9	12.701	7.057	9	11.054	7.344
10	12.869	6.785	10	10.777	8.496	10	9.691	5.404
11	10.270	5.833	11	14.601	7.631	11	11.690	4.827
12	12.440	7.312	12	13.800	7.385	12	11.690	5.944
13	10.960	3.739	13	13.725	9.308	13	10.920	5.542
14	11.631	5.814				14	12.489	6.302
15	14.671	5.570	Average	11.145	5.911	15	8.757	4.430
16	9.485	5.088	sd	1.70	1.11	16	9.329	6.644
17	11.888	5.558	se	0.23	0.15	17	13.655	6.684
18	10.453	5.974		11.37	6.26	18	10.608	6.545
19	11.077	5.734						
20	12.735	7.177	total # of lamella	10				
21	7.426	6.997	total # of cell	54.00				
22	11.749	7.439	# of cell / lamella	5.40				
23	11.808	6.837						

Table C.6. Distance obtained from Ca^{2+} imaging.

Distances obtained from Calcium imaging data									
1	2	3	4	5	6	7	8	9	10
11.307	8.722	8.467	9.673	6.119	5.786	7.25	5.152	9.513	13.22
4.903	5.205	6.17	8.177	9.126	8.853	5.067	5.443	7.241	7.169
4.505	11.364	6.265	4.847	5.216	3.209	6.959	6.25	7.892	7.256
5.365	8.433	7.669	5.429	10.172	8.917	6.758	5.069	10.523	5.402
6.226	13.716	10.47	7.201	5.082	12.081	7.069	5.615	9.693	8.711
4.659	9.8	8.155	7.094	7.916	5.97	7.722	9.748	9.127	6.993
5.746	10.625	8.502	5.977	9.415	5.293	14.315	7.799	7.892	
6.226	11.033	6.371	7.094	9.967	9.845	12.039	11.622	7.739	
8.676	11.146	9.01	7.466	6.412	7.332	6.707	6.831	8.398	
7.233	12.493	11.188	4.847	7.048	5.456	10.403	7.599	6.727	
4.614	5.717	7.313	5.691	6.267	10.27	9.105	7.173	8.271	
5.6	8.167	9.865	4.672	5.487	6.419	5.067	7.168	13.93	
9.39	8.662		3.672	7.76	3.351	11.888	4.128	5.557	
6.325	8.208		5.593	11.577	9.745	6.694	8.039	8.831	
7.482	9.176		6.339	7.345	5.856	6.044		9.301	
9.865			10.755	9.152	7.655			7.67	
11.281			6.804	8.059	5.175			11.594	
7.792			8.203	7.209	13.095			9.693	
6.658			4.975	7.867	8.182			3.008	
6.022			9.694	6.827	5.013				
2.884				6.364	4.365				
5.48				9.152	9.134				
				7.037	6.546				
				7.819	7.608				

Table C.6. Distance obtained from Ca^{2+} imaging (cont.).

Distances obtained from CYKII staining data						
1		2	3		4	
3.164	8.576	11.896	5.642	6.012	9.224	4.474
4.490	4.847	6.845	2.983	7.650	5.273	5.469
9.231	3.356	8.143	7.457	8.066	8.337	2.983
7.979	5.338	9.433	7.839	8.736	3.786	3.480
5.002	5.273	8.066	3.964	6.328	6.463	4.996
5.895	5.836	8.279	3.964	5.895	7.066	10.249
6.855	8.379	10.005	3.964	4.551	6.007	6.149
4.505	6.250	9.351	4.348	4.551	6.366	6.149
5.429	6.607	5.836	6.339	4.033	5.668	9.905
6.206	6.149	3.964	5.895	4.716	6.463	5.819
5.071	7.172	6.845	6.711	5.016	4.716	5.558
8.379	5.836	9.171	4.474	7.354	5.798	12.106
8.279	7.901	5.002	4.904	7.504	6.068	14.956
9.209	4.861	5.691	5.338	7.839	8.466	7.066
6.936	8.949	4.251	6.415	7.074	9.843	8.451
4.551	3.802	6.070	5.593	8.177	12.024	9.943
6.855	3.729	9.321	6.024	4.169	12.429	9.955
8.502	3.075	9.231	6.436	4.033	12.518	6.482
7.035	6.206	9.410	3.839	8.863	8.949	7.605
5.377	5.836	10.019	4.904	7.201	7.766	7.391
8.006	5.605	10.095	3.729	5.071	6.670	5.118
7.466	4.847	7.123	5.895	7.429	6.539	5.118
5.220	5.543	7.466	3.335	6.115	11.595	6.633
4.474	6.804	6.250	4.251	6.875	7.605	7.970
3.786	5.977	5.543	4.775	6.875	4.474	10.054
5.285	9.694	8.049	6.875	7.678	10.249	9.167
5.986	8.502	6.711	4.505	6.670	6.463	7.718
5.354	8.203	12.506	5.605	10.177	6.762	7.066
5.668		10.761	6.711		7.589	7.718
5.798		13.572	6.349		8.451	8.809
4.583		10.177	7.927		9.498	7.605
4.277		9.321	12.099		9.905	9.446
5.377		8.203	6.371		10.249	4.716
5.624		8.956	4.251		7.474	11.005
		8.584	8.211		5.469	4.921
		6.722	7.901			

Table C.7. Ca^{2+} imaging data obtained from CPA treatment.

CPA treatment								
TREATMENT 1_141216_Nose1_Section2								
Basally located cells								
	Cell1	Cell2	Cell3	Cell4		Average intensities	Average intensities	SE
Before CPA	2.6082	3.5796	1.6115	3.1569	Before CPA	2.73905	1.5079	0.425207
3min CPA	0.3861	0.8704	1.3452	0.158	3min CPA	0.689925	-0.0177	0.264135
6min CPA	0.0345	0.3144	0.2375	0.0446	6min CPA	0.15775	0.039375	0.070055
9min CPA	0.137	0.297	0.2912	0.0235	9min CPA	0.187175	0.054675	0.065948
3min ACSF wash-off	0.2158	0.022	0.4097	0.0571	3min ACSF wash-off	0.17615	0.1843	0.088531
6min ACSF wash-off	0.0854	0.1152	0.2984	0.3134	6min ACSF wash-off	0.2031	0.042325	0.059741
9min ACSF wash-off	0.0621	0.1329	0.2279	0.1587	9min ACSF wash-off	0.1454	0.022975	0.034252
Sustentacular cells								
	Cell1	Cell2	Cell3	Cell4		Average intensities		SE
Before CPA	1.2418	1.7286	1.3952	1.666		1.5079		0.114461
3min CPA	-0.0978	0.1508	-0.1512	0.0274		-0.0177		0.067494
6min CPA	0.0282	0.1733	-0.1792	0.1352		0.039375		0.079067
9min CPA	0.0834	0.2259	-0.161	0.0704		0.054675		0.080055
3min ACSF wash-off	0.1597	0.2431	0.0139	0.3205		0.1843		0.065606
6min ACSF wash-off	-0.0708	-0.045	-0.13	0.4151		0.042325		0.125526
9min ACSF wash-off	-0.0632	-0.0666	-0.0674	0.2891		0.022975		0.088713
TREATMENT 2_141216_Nose2_Section1								
Basally located cells								
	Cell1	Cell2	Cell3	Cell4		Average intensities		SE
Before CPA	2.4147	2.4734	2.427	2.6856	Before CPA	2.500175	1.66835	0.063087
3min CPA	0.6913	1.1081	1.3409	1.2601	3min CPA	1.1001	0.61955	0.144559
6min CPA	-0.0033	-0.0729	-0.0012	0.3566	6min CPA	0.0698	0.008625	0.09704
9min CPA	0.0096	-0.0175	-0.0238	0.3471	9min CPA	0.07885	-0.0568	0.08971
3min ACSF wash-off	0.4591	0.1988	0.0589	0.15	3min ACSF wash-off	0.2167	0.017375	0.085843
6min ACSF wash-off	0.4709	0.2787	0.3634	0.3744	6min ACSF wash-off	0.37185	0.217425	0.039334
9min ACSF wash-off	0.5596	0.4052	0.4838	0.3916	9min ACSF wash-off	0.46005	0.35305	0.03891
Sustentacular cells								
	Cell1	Cell2	Cell3	Cell4		Average intensities		SE
Before CPA	1.3116	1.8086	1.5765	1.9767		1.66835		0.144469
3min CPA	0.9219	-0.0671	0.3905	1.2329		0.61955		0.287455
6min CPA	0.2738	-0.1306	-0.1467	0.038		0.008625		0.097763
9min CPA	0.119	-0.2352	-0.1406	0.0296		-0.0568		0.080218
3min ACSF wash-off	0.1972	-0.0583	-0.1495	0.0801		0.017375		0.076292
6min ACSF wash-off	0.2933	0.2591	0.2358	0.0815		0.217425		0.046822
9min ACSF wash-off	0.2929	0.0809	0.8114	0.227		0.35305		0.159075

Table C.8. Ca^{2+} imaging data obtained from suramin treatment.

Suramin treatment								
TREATMENT 1_141210								
Basally located cells								
	Cell1	Cell2	Cell3			Average intensity	SE	
Before Suramin	3.452	3.465	2.4524	Before Suramin		3.123133	0.8821	0.335388
3min Suramin	0.8499	1.3782	0.2828	3min Suramin		0.836967	0.1178	0.316281
6min Suramin	0.8999	1.7333	0.2611	6min Suramin		0.964767	-0.02433	0.426223
9min Suramin	2.3731	1.7782	1.3141	9min Suramin		1.8218	0.065567	0.306483
3min ACSF wash-off	1.5975	1.4132	1.6411	3min ACSF wash-off		1.5506	0.195567	0.069843
6min ACSF wash-off	2.0684	1.5542	1.4938	6min ACSF wash-off		1.705467	-0.00073	0.182302
9min ACSF wash-off	1.9473	1.7288	1.2152	9min ACSF wash-off		1.630433	0.024433	0.216987
Sustentacular cells								
	Cell1	Cell2	Cell3			Average intensity		
Before Suramin	0.6392	1.0765	0.9306			0.8821		0.128546
3min Suramin	0.0517	0.1023	0.1994			0.1178		0.043336
6min Suramin	-0.1268	0.1052	-0.0514			-0.02433		0.068326
9min Suramin	-0.0666	0.2625	0.0008			0.065567		0.100371
3min ACSF wash-off	0.0497	0.3678	0.1692			0.195567		0.092769
6min ACSF wash-off	-0.0845	0.1769	-0.0946			-0.00073		0.088865
9min ACSF wash-off	-0.0863	0.1625	-0.0029			0.024433		0.073111
TREATMENT 2_141125 Section1								
Basally located cells								
	Cell1	Cell2	Cell3	Cell4		Cell5	Cell6	Average intensity
Before Suramin	3.452	3.465	2.4524	3.452		3.465	2.4524	3.123133
3min Suramin	1.4606	1.1098	1.1608	1.6552		1.5802	1.1185	1.347517
6min Suramin	1.2128	0.4227	0.3642	0.1749		1.0753	0.2358	0.58095
9min Suramin	1.5158	0.7556	0.2305	0.3296		1.183	0.382	0.73275
3min ACSF wash-off	1.3829	1.3786	0.2197	0.1765		0.7378	0.222	0.68625
6min ACSF wash-off	1.5011	1.8156	0.3944	0.2864		0.4797	0.248	0.787533
Sustentacular cells								
	Cell1	Cell2	Cell3	Cell4		Average intensity		
Before Suramin	0.6528	0.419	0.3882	0.2668		0.4317		0.08069
3min Suramin	0.4976	0.2573	0.0519	0.552		0.3397		0.115334
6min Suramin	0.1777	-0.034	0.1295	0.0997		0.093225		0.045351
9min Suramin	0.2151	0.0371	0.0614	0.21		0.1309		0.047412
3min ACSF wash-off	0.2937	0.0239	0.032	0.1201		0.117425		0.062666
6min ACSF wash-off	0.2091	0.1309	0.0028	0.0506		0.09835		0.045401

Table C.9. Ca^{2+} imaging data obtained from purines treatment.

purines									
Basally located cells									
	Cell1	Cell2	Cell3	Cell4	Cell5		Average intensity	SE	
ATP	1.9436	1.5332	2.0319	2.5037	2.1383	ATP	2.03014	0.92028	ATP
ADP	1.5117	1.2462	1.7159	1.9931	1.769	ADP	1.64718	0.46892	ADP
Me-ATP	1.8634	1.1201	1.6428	1.1145	1.5948	Me-ATP	1.46712	0.19552	Me-ATP
Me-ADP	1.8179	1.1408	1.7438	0.5021	1.4699	Me-ADP	1.3349	0.61644	Me-ADP
ATPgammaS	1.2233	0.5453	0.9572	0.1791	1.0312	ATPgammaS	0.78722	0.17456	ATPgammaS
UTP	0.5557	0.5281	0.7388	0.1878	0.9231	UTP	0.5867	0.24968	UTP
UDP	0.3762	0.0854	0.3641	0.237	0.4223	UDP	0.297	0.1326	UDP
Sustentacular cells									
	Cell1	Cell2	Cell3	Cell4	Cell5		Average intensity	SE	
ATP	0.7127	2.0771	0.7458	0.6206	0.4452		0.92028		ATP
ADP	0.4891	0.8112	0.9132	0.2601	-0.129		0.46892		ADP
Me-ATP	0.1444	0.1808	0.5136	0.1623	-0.0235		0.19552		Me-ATP
Me-ADP	0.1323	0.7058	1.5729	0.5366	0.1346		0.61644		Me-ADP
ATPgammaS	0.0226	0.416	0.2248	0.2859	-0.0765		0.17456		ATPgammaS
UTP	0.119	0.604	0.0842	0.3552	0.086		0.24968		UTP
UDP	0.1187	0.0592	0.2153	0.3711	-0.1013		0.1326		UDP

Table C.10. Distance of the Sox2-positive cells to apical layer.

thikness of hemi-lamella		distance to apical border					
#1	#3	#1	#2	#3	#4	#5	#6
28.126	30.576	22.473	16.201	26.77	21.652	21.76	23.217
26.463	32.269	26.221	15.37	29.685	25.327	20.892	21.493
25.379	33.157	25.925	21.732	32.238	29.269	21.472	19.687
25.279	32.496	25.208	23.572	23.588	28.597	24.083	21.649
25.279	30.174	23.671	18.77	26.561	27.283	24.371	14.508
#2	28.47	24.373	17.062	12.819	25.485	24.378	21.975
34.345	28.725	22.937	23.331	16.662	31.645	17.118	19.616
34.648	29.304	29.05	22.133	26.306	30.1	22.647	19.21
37.426	25.533	22.37	12.97	19.806	29.654	31.336	17.57
42.325	23.211	14.822	18.9	23.357	25.504	15.087	17.533
38.325	#4	23.807	22.665	24.222	22.448	16.828	16.346
31.561	24.156	11.896	15.745	16.023	22.413	22.37	23.864
	29.429	20.028	16.006	19.782	23.275	16.54	23.481
	33.166	20.908	20.888	26.82	21.777	22.632	14.809
	34.747	12.766	22.835	28.9	20.43	18.914	14.121
	33.409		17.895	25.731	19.991	25.248	20.971
	32.938		15.895	23.646		11.025	11.008
			20.632	23.391		20.608	17.603
			18.742	24.661		10.735	12.462
			16.047	32.007		16.83	18.243
			11.737	34.058		8.124	21.226
			7.819	23.038		9.284	13.579
				28.581		13.056	11.448
				38.43		20.608	16.571
				34.188		25.532	23.555
				26.273		13.639	18.448
				31.18		11.315	11.417
				37.07		15.377	17.185
				28.646		13.636	18.698
				20.516		26.997	19.899
				29.188		24.663	

REFERENCES

Abbracchio MP., G. Burnstock, A. Verkhratsky, H. Zimmermann, 2009, “Purinergic Signalling In The Nervous System: An Overview”, *Trends in Neurosciences*, Vol. 32, No.1, pp. 19–29.

Adolf B., P. Chapouton, CS. Lam, S. Topp, B. Tannhäuser, U. Strähle, M. Götz, L. Bally-Cuif, 2006, “Conserved And Acquired Features Of Adult Neurogenesis In The Zebrafish Telencephalon”, *Developmental Biology*, Vol. 295, No.1, pp. 278–293.

Ahuja G., SB. Nia, V. Zapilko, V. Shiriagin, D. Kowatschew, Y. Oka, SI. Korschning, 2014, “Kappe Neurons, A Novel Population Of Olfactory Sensory Neurons”, *Science Reports*, Vol. 4, No. 1, pp. 4037.

Altman J., 1969, “Postnatal Neurogenesis And The Problem Of Neural Plasticity”, *Developmental Neurobiology*, Vol. 3, No. 1, pp. 197–257.

Alvarez-Buylla, A., JM. Garcia-Verdugo, AD. Tramontin, 2001, “A Unified Hypothesis On The Lineage Of Neural Stem Cells”, *Nature Review Neuroscience*, Vol. 2, No. 1, pp. 287–293.

Asson-Batres MA., WB. Smith, 2006, “Localization Of Retinaldehyde Dehydrogenases And Retinoid Binding Proteins To Sustentacular Cells, Glia, Bowman's Gland Cells, And Stroma: Potential Sites Of Retinoic Acid Synthesis In The Postnatal Rat Olfactory Organ”, *Journal of Comparative Neurology*, Vol. 496, No. 2, pp. 149-71.

Au E., AJ. Roskams, 2003, “Olfactory Ensheathing Cells Of The Lamina Propria *In Vivo* And *In Vitro*”, *Glia*, Vol. 41, No. 3, pp. 224-36.

Bauer S., S. Rasika, J. Han, C. Mauduit, M. Raccurt, G. Morel, F. Jourdan, M. Benahmed, E. Moyse, PH. Patterson, 2003, “Leukemia Inhibitory Factor Is A Key Signal For Injury-induced Neurogenesis In The Adult Mouse Olfactory Epithelium”, *Journal of Neurosciences*, Vol. 23, No. 5, pp. 1792–1803.

Becker CG., T. Becker, 2008, “Adult Zebrafish As A Model For Successful Central Nervous System Regeneration”, *Restorative Neurology and Neuroscience*, Vol. 26, No. 2, pp. 71-80.

Beites C.L., S. Kawauchi, CE. Crocker, AL. Calof, 2005, “Identification And Molecular Regulation Of Neural Stem Cells In The Olfactory Epithelium”, *Experimental Cell Research* Vol. 306, No. 2, pp. 309–316.

Bhardwaj RD., MA. Curtis, KL. Spalding, BA. Buchholz, D. Fink, T. Björk-Eriksson, C. Nordborg, FH. Gage, H. Druid, PS. Eriksson, J. Frisén, 2006, “Neocortical Neurogenesis In Humans Is Restricted To Development”, *Proceedings of the National Academy Sciences*, Vol. 103, No. 33, pp. 12564-8.

Bjornsson CS., M. Apostolopoulou, Y. Tian, S. Temple, 2015, “It Takes A Village: Constructing The Neurogenic Niche”, *Developmental Cell*, Vol. 32, No. 4, pp. 435-446.

Brazel CY., TL. Limke, JK. Osborne, T. Miura, J. Cai, L. Pevny, MS. Rao, 2005, “Sox2 Expression Defines A Heterogeneous Population Of Neurosphere-forming Cells In The Adult Murine Brain”, *Aging Cell*, Vol. 4, No. 4, pp. 197-207.

Byrd CA., PC. Brunjes, 2001, “Neurogenesis In The Olfactory Bulb Of Adult Zebrafish”, *Neuroscience*, Vol. 105, No. 4, pp. 793-801.

Caggiano M., JS. Kauer, DD. Hunter, 1994, "Globose Basal Cells Are Neuronal Progenitors In The Olfactory Epithelium: A Lineage Analysis Using A Replication-Incompetent Retrovirus", *Neuron*, Vol. 13, No: 2, pp. 339–352.

Calof AL., DM. Chikaraishi, 1989, "Analysis Of Neurogenesis In A Mammalian Neuroepithelium: Proliferation And Differentiation Of An Olfactory Neuron Precursor *In Vitro*", *Neuron*, Vol. 3, No:1, pp. 115–127.

Calof AL., JS. Mumm, PC. Rim, J. Shou, 1998, "The Neuronal Stem Cell Of The Olfactory Epithelium", *Journal Of Neurobiology*, Vol. 36, No. 2, pp. 190–205.

Calof AL., A. Bonnin, C. Crocker, S. Kawauchi, RC. Murray, J. Shou, HH. Wu, 2002, "Progenitor Cells Of The Olfactory Receptor Neuron Lineage", *Microscopic Research And Technique*, Vol. 58, No. 3, pp. 176–188.

Carr VM., AI. Farbman, 1992, "Ablation Of The Olfactory Bulb Upregulates The Rate Of Neurogenesis And Induces Precocious Cell Death In Olfactory Epithelium", *Experimental Neurology*, Vol. 115, No. 1, pp. 55–59.

Cau E., G. Gradwohl, C. Fode, F. Guillemot, 1997, "Mash1 Activates A Cascade Of Bhlh Regulators In Olfactory Neuron Progenitors", *Development*, Vol. 124, No. 1, pp.1611–1621.

Cau E, G. Gradwohl, S. Casarosa, R. Kageyama, F. Guillemot, C. Fode, 2000, "Hes Genes Regulate Sequential Stages Of Neurogenesis In The Olfactory Epithelium Mash1 Activates A Cascade Of Bhlh Regulators In Olfactory Neuron Progenitors", *Development*, Vol. 127, No. 2, pp. 2323–2332.

Carter LA., JL. MacDonald, AJ. Roskams, 2004, "Olfactory Horizontal Basal Cells Demonstrate A Conserved Multipotent Progenitor Phenotype", *Journal of Neurosciences*, Vol. 24, No. 3, pp. 5670–5683.

Carson C., B. Murdoch, AJ. Roskams, 2006, "Notch 2 And Notch 1/3 Segregate To Neuronal And Glial Lineages Of The Developing Olfactory Epithelium", *Developmental Dynamics*, Vol. 235, No. 6, pp. 1678-88.

Catania S., A. Germana, R. Laura, and J. Vega, 2003, "The Crypt Neurons In The Olfactory Epithelium Of The Adult Zebrafish Express Trka-like Immunoreactivity", *Neuroscience Letters*, Vol. 350, No. 7, pp. 5–8.

Chapouton P., R. Jagasia, L. Bally-Cuif, 2007, "Adult Neurogenesis In Non-mammalian Vertebrates", *Bioessays*, Vol. 29, No. 8, pp. 745-57.

Chen, X., H. Fang, JE. Schwob, 2004, "Multipotency Of Purified, Transplanted Globose Basal Cells In Olfactory Epithelium", *Journal of Comparative Neurology*, Vol. 469, No. 8, pp. 457–474.

Chuah MI., R. Teague, 1999, "Basic Fibroblast Growth Factor In The Primary Olfactory Pathway: Mitogenic Effect On Ensheathing Cells", *Neuroscience*, Vol. 88, No. 4, pp. 1043-50.

Das AV., KB. Mallya, X. Zhao, F. Ahmad, S. Bhattacharya, WB. Thoreson, GV. Hegde, I. Ahmad, 2006, "Neural Stem Cell Properties Of Müller Glia In The Mammalian Retina: Regulation By Notch And Wnt Signaling", *Developmental Biology*, Vol. 299, No. 1, pp. 283-302.

Davis JA., RR. Reed, 1996, "Role Of Olf-1 And Pax-6 Transcription Factors In Neurodevelopment", *Journal of Neurosciences*, Vol. 16, No. 16, pp. 5082-5094.

Dahlstrand J., M. Lardelli, U. Lendahl, 1995, "Nestin Mrna Expression Correlates With The Central Nervous System Progenitor Cell State In Many, But Not All, Regions Of Developing Central Nervous System", *Brain Research: Developmental Brian Research*, Vol. 84, No. 1, pp. 109-129.

Deng W., JB. Aimone, FH. Gage, 2010, "New Neurons And New Memories: How Does Adult Hippocampal Neurogenesis Affect Learning And Memory?" *Nature Review Neuroscience*, Vol. 11, No. 2, pp. 339-350.

Dittrich K, A. Sansone, T. Hassenklöver, I. Manzini, 2014, "Purinergic Receptor-induced Ca2+ Signaling In The Neuroepithelium Of The Vomeronasal Organ Of Larval *Xenopus Laevis*" *Purinergic Signalling*, Vol. 10, No. 2, pp. 327-36.

Doetsch F., 2003, "The Glial Identity Of Neural Stem Cells", *Nature Neurosciences*, Vol. 6, No. 11, pp. 1127-1134.

Doyle KL., M. Khan, AM. Cunningham, 2001, "Expression Of The Intermediate Filament Protein Nestin By Sustentacular Cells In Mature Olfactory Neuroepithelium", *Journal Of Comparative Neurology*, Vol. 437, No. 2, pp. 186-195.

Eriksson PS., E. Perfilieva, T. Björk-Eriksson, AM. Alborn, C. Nordborg, DA. Peterson, FH. Gage, 1998, "Neurogenesis In The Adult Human Hippocampus", *Nature Medicine*, Vol. 4, No. 5, pp. 1313-1317.

Ekström P., CM. Johnsson, LM. Ohlin, 2001, "Ventricular Proliferation Zones In The

Brain Of An Adult Teleost Fish And Their Relation To Neuromeres And Migration (Secondary Matrix) Zones”, *Journal Of Comparative Neurology*, Vol. 436, No. 13, Pp. 92–110.

Ever L., N. Gaiano, 2005, “Radial ‘Glial’ Progenitors: Neurogenesis And Signaling”, *Current Opinion on Neurobiology*, Vol.15, No. 11, Pp. 29–33.

Ezeh PI., AI. Farbman, 1998, “Differential Activation Of Erbb Receptors In The Rat Olfactory Mucosa By Transforming Growth Factor-Alpha And Epidermal Growth Factor *In Vivo*”, *Journal of Neurobiology*, Vol. 37, No. 2, pp. 199-210.

Farbman AI., 1990, “Olfactory Neurogenesis: Genetic Or Environmental Controls?” *Trends in Neurosciences*, Vol. 13, No. 1, pp. 362–365.

Farbman AI., 1992, “Cell Biology Of Olfaction”, *Cambridge: Cambridge University Press*.

Farbman AI., JA. Buchholz, 1996, “Transforming Growth Factor-Alpha And Other Growth Factors Stimulate Cell Division In Olfactory Epithelium *In Vitro*”, *Journal of Neurobiology*, Vol. 30, No. 2, pp. 267-280.

Fausett BV., D. Goldman, 2006, “A Role For Alpha1 Tubulin-expressing Müller Glia In Regeneration Of The Injured Zebrafish Retina”, *Journal of Neurosciences*, Vol. 26, No. 23, pp. 6303-6313.

Fischer AJ., TA. Reh, 2001, “Müller Glia Are A Potential Source Of Neural Regeneration In The Postnatal Chicken Retina”, *Nature Neurosience*, Vol. 4, No. 3, pp. 247-252.

Friedrich RW., SI. Korschning, 1997, "Combinatorial And Chemotopic Odorant Coding In The Zebrafish Olfactory Bulb Visualized By Optical Imaging", *Neuron*, Vol. 18, No. 5, pp. 737-52.

Furukawa T., S. Mukherjee, ZZ. Bao, EM. Morrow, CL. Cepko, 2000, "Rax, Hes1, And Notch1 Promote The Formation Of Müller Glia By Postnatal Retinal Progenitor Cells", *Neuron*, Vol. 26, No. 2, pp. 383-394.

Gage FH., 2000, "Mammalian Neural Stem Cells", *Science*, Vol. 287, No. 5457, pp. 1433-1438.

Gayle S., G. Burnstock, 2005, "Immunolocalisation Of P2X And P2Y Nucleotide Receptors In The Rat Nasal Mucosa", *Cell and Tissue Research*, Vol. 319, No. 1, pp. 27-36.

Getchell ML., MA. Boggess, SJ. Pruden, SS. Little, S. Buch, TV. Getchell, 2002, "Expression Of TGF-Beta Type II Receptors In The Olfactory Epithelium And Their Regulation In TGF-Alpha Transgenic Mice", *Brain Research*, Vol. 945, No. 2, pp. 232-41.

Gokoffski KK., S. Kawauchi, HH. Wu, R. Santos, PLW. Hollenbeck, AD. Lander, A. Calof, 2010, "Feedback Regulation Of Neurogenesis In The Mammalian Olfactory Epithelium: New Insights From Genetics And Systems Biology, The Neurobiology Of Olfaction", CRC Press; Chapter 10.

Goldman D., 2014, "Müller Glial Cell Reprogramming And Retina Regeneration", *Nature Review Neuroscience*, Vol. 15, No. 7, pp. 431-442.

Goldshmit Y., F. Frisca, J. Kaslin, AR. Pinto, JK. Tang, A. Pébay, R. Pinkas-Kramarski, PD. Currie, 2015, "Decreased Antiregenerative Effects After Spinal Cord Injury In

Spry4-/- Mice”, *Neuroscience*, Vol. 287, No. 1, pp. 104-112.

Goldstein BJ., JE. Schwob, 1996, “Analysis Of The Globose Basal Cell Compartment In Rat Olfactory Epithelium Using GBC-1, A New Monoclonal Antibody Against Globose Basal Cells”, *Journal of Neurosciences*, Vol. 16, No. 12, pp. 4005–4016.

Goldstein BJ., BL. Wolozin, JE. Schwob, 1997, “FGF2 Suppresses Neuronogenesis Of A Cell Line Derived From Rat Olfactory Epithelium”, *Journal of Neuorbiology*, Vol. 33, No. 4, pp. 411-428.

Gordon MK., JS. Mumm, RA. Davis, JD. Holcomb, AL. Calof, 1995, “Dynamics Of MASH1 Expression *In Vitro* And *In Vivo* Suggest A Non-stem Cell Site Of MASH1 Action In The Olfactory Receptor Neuron Lineage”, *Molecular and Cellular Neuroscience*, Vol. 6, No. 1, pp. 363–379.

Götz M., YA. Barde, 2005, “Radial Glial Cells Defined And Major Intermediates Between Embryonic Stem Cells And CNS Neurons”, *Neuron*, Vol. 46, No. 29, pp. 369–372.

Grandel H., J. Kaslin, J. Ganz, I. Wenzel, M. Brand, 2006, “Neural Stem Cells And Neurogenesis In The Adult Zebrafish Brain: Origin, Proliferation Dynamics, Migration And Cell Fate”, *Developmental Biology*, Vol. 295, No. 1, pp. 263–277.

Graziadei PP., GA. Graziadei, 1979, “Neurogenesis And Neuron Regeneration In The Olfactory System Of Mammals. I. Morphological Aspects Of Differentiation And Structural Organization Of The Olfactory Sensory Neurons”, *Journal of Neurocytology*, Vol. 8, No. 1, pp.1–18.

Guillemot F., LC. Lo, JE. Johnson, A. Auerbach, DJ. Anderson, AL. Joyner, 1993,

“Mammalian Achaete-Scute Homolog 1 Is Required For The Early Development Of Olfactory And Autonomic Neurons”, *Cell*, Vol. 75, No. 1, pp. 463–476.

Guo Z., A. Packard, RC. Krolewski, MT. Harris, GL. Manglapus, JE. Schwob, 2010, “Expression Of Pax6 And Sox2 In Adult Olfactory Epithelium”, *Journal of Comparative Neurology*, Vol. 518, No. 21, pp.4395-418.

Götz M., E. Hartfuss, P. Malatesta, 2002, “Radial Glial Cells As Neuronal Precursors: A New Perspective On The Correlation Of Morphology And Lineage Restriction In The Developing Cerebral Cortex Of Mice”, *Brain Research Bulletin*, Vol. 57, No. 6, pp. 777-788.

Hansen A., E. Zeiske, 1998, “The Peripheral Olfactory Organ Of The Zebrafish, Danio Rerio: An Ultrastructural Study”, *Chemical Senses*, Vol. 23, No. 1, pp. 39-48.

Hansen A, TE. Finger, 2000, “Phyletic Distribution Of Crypt-Type Olfactory Receptor Neurons In Fishes” *Brain Behaviour and Evolution*, Vol. 55, No.1, pp. 100-110.

Hassenklöver T., S. Kurtanska, I. Bartoszek, S. Junek, D. Schild, I. Manzini, 2008, “Nucleotide-Induced Ca^{2+} Signaling In Sustentacular Supporting Cells Of The Olfactory Epithelium”, *Glia*, Vol. 56, No. 1, pp.1614–1624.

Hassenklöver T., P. Schwartz, D. Schild, I. Manzini, 2009, “Purinergic Signaling Regulates Cell Proliferation Of Olfactory Epithelium Progenitors”, *Stem Cells*. Vol. 27, No. 1, pp. 2022–2031.

Hayoz S., C. Jia, C. Hegg, 2012, “Mechanisms Of Constitutive And ATP-Evoked ATP Release In Neonatal Mouse Olfactory Epithelium”, *BioMedCentral Neurosience*,

Vol. 28, No. 11, pp. 13-53.

Hegg CC., D. Greenwood, W. Huang, P. Han, MT. Lucero, 2003, "Activation Of Purinergic Receptor Subtypes Modulates Odor Sensitivity", *Journal of Neurosciences* Vol. 23, No. 23, pp. 8291–8301.

Hegg CC., M. Irwin, MT. Lucero, 2009, "Calcium Store-mediated Signaling In Sustentacular Cells Of The Mouse Olfactory Epithelium", *Glia*, Vol. 15, No. 6, pp. 634-44.

Hempstead JL., JL. Morgan, 1985, "A Panel Of Monoclonal Antibodies To The Rat Olfactory Epithelium", *Journal of Neuroscience*, Vol. 5, No. 2, pp. 438-49.

Hockfield S, RD. McKay, 1985, "Identification Of Major Cell Classes In The Developing Mammalian Nervous System", *Journal of Neuroscience*, Vol. 5, No. 12, pp. 3310-3328.

Holbrook EH., KE. Szumowski, JE. Schwob, 1995, "An Immunochemical, Ultrastructural, And Developmental Characterization Of The Horizontal Basal Cells Of Rat Olfactory Epithelium", *Journal of Comparative Neurology*, Vol. 363, No. 3, pp. 129-146.

Housley GD., A. Bringmann, A. Reichenbach, 2009, "Purinergic Signaling In Special Senses", *Trends in Neurosciences*, Vol. 32, No. 6, pp. 128–141.

Huard JM., SL. Youngentob, BJ. Goldstein, MB. Luskin, JE. Schwob, 1998, "Adult Olfactory Epithelium Contains Multipotent Progenitors That Give Rise To Neurons And Non-neural Cells", *Journal of Comparative Neurology*, Vol. 400, No. 1, pp.

469–486.

Hsieh J., 2012, “Orchestrating Transcriptional Control Of Adult Neurogenesis”, *Genes And Development*, Vol. 26, No. 10, pp. 1010-1021.

Hsu P., F. Yu, F. Feron, JO. Pickles, K. Sneesby, A. Mackay-Sim, 2001, “Basic Fibroblast Growth Factor And Fibroblast Growth Factor Receptors In Adult Olfactory Epithelium”, *Brain Research*, Vol. 896, No. 2, pp. 188–197.

Illing N., S. Boolay, JS. Siwoski, D. Casper, MT. Lucero, AJ. Roskams, 2002, “Conditionally Immortalized Clonal Cell Lines From The Mouse Olfactory Placode Differentiate Into Olfactory Receptor Neurons”, *Molecular and Cellular Neuroscience*, Vol. 20, No. 2, pp. 225-243.

Iqbal T., C. Byrd-Jacobs, 2010, “Rapid Degeneration And Regeneration Of The Zebrafish Olfactory Epithelium After Triton X-100 Application”, *Chemical Senses*, Vol. 35, No. 5, pp. 351-61.

Iwema CL., JE. Schwob, 2003, “Odorant Receptor Expression As A Function Of Neuronal Maturity In The Adult Rodent Olfactory System”, *Journal of Comparative Neurology*, Vol. 459, No. 3, pp. 209-222.

Jang W., SL. Youngentob, JE. Schwob, 2003, “Globose Basal Cells Are Required For Reconstitution Of Olfactory Epithelium After Methyl Bromide Lesion”, *Journal of Comparative Neurology*, Vol. 460, No. 4, pp. 123–140.

Jia C., JP. Doherty, S. Crudginton, CC. Hegg, 2009, “Activation Of Purinergic Receptors Induces Proliferation And Neuronal Differentiation In Swiss Webster Mouse Olfactory Epithelium”, *Neuroscience*, Vol. 29, No. 1, pp. 120-163.

Jia C., C.Roman, CC. Hegg, 2010, "Nickel Sulfate Induces Location-dependent Atrophy Of Mouse Olfactory Epithelium: Protective And Proliferative Role Of Purinergic Receptor Activation", *Toxicology Science*, Vol. 115, No. 2, pp. 547-556.

Jia C., AR. Cussen, CC. Hegg, 2011, "ATP Differentially Upregulates Fibroblast Growth Factor 2 And Transforming Growth Factor A In Neonatal And Adult Mice: Effect On Neuroproliferation", *Neuroscience*, Vol. 17, No. 177, pp. 335-346.

Kaslin J., V. Kroehne, F. Benato, F. Argenton, M. Brand, 2013, "Development And Specification Of Cerebellar Stem And Progenitor Cells In Zebrafish: From Embryo To Adult", *Neural Development*, Vol. 8, No. 1, pp. 9.

Kaslin J., J. Ganz, M. Brand, 2008, "Proliferation, Neurogenesis And Regeneration In The Non-mammalian Vertebrate Brain." *Philosophical transactions of the Royal Society of London. Series B, Biological Sciences*, Vol. 363, No. 1489, pp. 101-122.

Kizil C., N. Kyritsis, S. Dudczig, V. Kroehne, D. Freudenreich, J. Kaslin, M. Brand, 2012 "Regenerative Neurogenesis From Neural Progenitor Cells Requires Injury-induced Expression Of Gata3", *Developmental Cell*, Vol. 23, No. 6, pp. 1230-1237.

Kizil C., A. Iltzsche, J. Kaslin, M. Brand, 2013, "Micromanipulation Of Gene Expression In The Adult Zebrafish Brain Using Cerebroventricular Microinjection Of Morpholino Oligonucleotides", *Journal of Visualized Experiments*, Vol. 75, No. 1, pp. 50415.

Kokoeva MV., H. Yin, and JS. Flier, 2005, "Neurogenesis In The Hypothalamus Of Adult Mice: Potential Role In Energy Balance", *Science*, Vol. 310, No. 1, pp. 679-683.

Krishna NS., SS. Little, TV. Getchell, 1996, "Epidermal Growth Factor Receptor Mrna

And Protein Are Expressed In Progenitor Cells Of The Olfactory Epithelium”, *Journal of Comparative Neurology*, Vol. 373, No. 3, pp. 297–307.

Krolewski RC., A. Packard, W. Jang, H. Wildner, JE. Schwob, 2012, “Ascl1 (Mash1) Knockout Perturbs Differentiation Of Nonneuronal Cells In Olfactory Epithelium”, *Public Library of Science One*, Vol. 7, No. 12, pp. 51737.

Lam CS, M. März, U. Strähle, 2009, “GFAP And Nestin Reporter Lines Reveal Characteristics Of Neural Progenitors In The Adult Zebrafish Brain”, *Developmental Dynamics*, Vol. 238, No. 1, pp. 475–486.

Lee DA, JL. Bedont, T. Pak, H. Wang, J. Song, A. Miranda-Angulo, V. Takiar, V. Charubhumi, F. Balordi, H. Takebayashi, 2012, “Tanycytes Of The Hypothalamic Median Eminence Form A Diet-responsive Neurogenic Niche”, *Nature Neuroscience*, Vol. 15, No. 5, pp. 700-702.

Lendahl U., LB. Zimmerman, RD. McKay, 1990, “CNS Stem Cells Express A New Class Of Intermediate Filament Protein”, *Cell*, Vol. 60, No. 4, pp. 585-595.

Lenkowski JR., PA. Raymond, 2014, “Müller Glia: Stem Cells For Generation And Regeneration Of Retinal Neurons In Teleost Fish”, *Progress in Retina and Eye Research*, Vol. 40, No. 3, pp. 94-123.

Lepousez G., MT. Valley, PM. Lledo, 2013, “The Impact Of Adult Neurogenesis On Olfactory Bulb Circuits And Computations”, *Annual Reviews of Physiology*, Vol. 75, No. 1, pp. 339-363.

Leung CT., PA. Coulombe, RR. Reed, 2007, “Contribution Of Olfactory Neural Stem

Cells To Tissue Maintenance And Regeneration”, *Nature Neuroscience*, Vol. 10, No. 4, pp. 720–26.

Luskin MB., 1993, “Restricted Proliferation And Migration Of Postnatally Generated Neurons Derived From The Forebrain Subventricular Zone”, *Neuron*, Vol. 11, No. 14, pp. 173–189.

Mackay-Sim A., P. Kittel, 1991, “Cell Dynamics In The Adult Mouse Olfactory Epithelium: A Quantitative Autoradiographic Study”, *Journal of Neuroscience*, Vol. 11, No. 1, pp. 979–84.

Mahler J, W. Driever, 2007, “Expression Of The Zebrafish Intermediate Neurofilament Nestin In The Developing Nervous System And In Neural Proliferation Zones At Postembryonic Stages”, *BioMedCenter Developmental Biology*, Vol. 7, No. 1, pp. 89.

Manglapus GL., SL. Youngentob, JE. Schwob, 2004, “Expression Patterns Of Basic Helix-Loop-Helix Transcription Factors Define Subsets Of Olfactory Progenitor Cells”, *Journal of Comparative Neurology*, Vol. 479, No. 2, pp. 216-233.

Murdoch B., AJ. Roskams, 2008, “A Novel Embryonic Nestin-expressing Radial Glia-like Progenitor Gives Rise To Zonally Restricted Olfactory And Vomeronasal Neurons”, *Journal of Neurosciences*, Vol. 28, No. 16, pp. 4271-4282.

Murray RC., D. Navi, J. Fesenko, AD. Lander, AL. Calof, 2003, “Widespread Defects In The Primary Olfactory Pathway Caused By Loss Of Mash1 Function”, *Journal of Neurosciences*, Vol. 23, No. 15, pp. 1769–1780.

Mulvaney BD., HE. Heist, 1971, "Regeneration Of Rabbit Olfactory Epithelium", *American Journal of Anatomy*, Vol. 131, No. 2, Pp. 241-251.

Nan B, ML. Getchell, JV. Partin, TV. Getchell, 2001, "Leukemia Inhibitory Factor, Interleukin-6, And Their Receptors Are Expressed Transiently In The Olfactory Mucosa After Target Ablation", *Journal of Comparative Neurology*, Vol. 435, No. 1, pp. 60-77.

Oehlmann VD., H. Korte, C. Sterner, SI. Korschning, 2002, "A Neuropeptide FF-Related Gene Is Expressed Selectively In Neurons Of The Terminal Nerve In Danio Rerio", *Mechanisms of Development*, Vol. 117, No. 2, pp. 357-361.

Oehlmann VD., S. Berger, C. Sterner, SI. Korschning, 2004, "Zebrafish Beta Tubulin 1 Expression Is Limited To The Nervous System Throughout Development, And In The Adult Brain Is Restricted To A Subset Of Proliferative Regions", *Gene Expression Patterns*, Vol. 4, No. 2, pp. 191-198.

Ooto S., T. Akagi, R. Kageyama, J. Akita, M. Mandai, Y. Honda, M. Takahashi, 2004, "Potential For Neural Regeneration After Neurotoxic Injury In The Adult Mammalian Retina", *Proceedings of the National Academy of Sciences*, Vol. 101, No. 37, pp. 13654-13659.

Parent JM., GG. Murphy, 2008, "Mechanisms And Functional Significance Of Aberrant Seizure-induced Hippocampal Neurogenesis", *Epilepsia*, Vol. 49, No. 5, pp. 19-25.

Parisi V., MC. Guerrera, F. Abbate, O. Garcia-Suarez, E. Viña, JA. Vega, A. Germanà, 2014, "Immunohistochemical Characterization Of The Crypt Neurons In The Olfactory Epithelium Of Adult Zebrafish", *Annals of Anatomy*, Vol. 196, No. 4, pp.

178-82.

Park D., AP. Xiang, FF. Mao, L. Zhang, CG. Di, XM. Liu, Y. Shao, BF. Ma, JH. Lee, KS. Ha, N. Walton, BT. Lahn, 2010, “Nestin Is Required For The Proper Self-renewal Of Neural Stem Cells”, *Stem Cells*. Vol. 28, No. 12, pp. 2162-2171.

Paschaki M., L. Cammas, Y. Muta, Y. Matsuoka, SS. Mak, M. Rataj-Baniowska, V. Fraulob, P. Dollé, RK. Ladher, 2013, “Retinoic Acid Regulates Olfactory Progenitor Cell Fate And Differentiation”, *Neural Development*, Vol. 8, No. 13, pp. 13-23.

Piras E., A. Franzén, EL. Fernández, U. Bergström, F. Raffalli-Mathieu, M. Lang, EB. Brittebo, 2003, “Cell-specific Expression Of CYP2A5 In The Mouse Respiratory Tract: Effects Of Olfactory Toxicants”, *Journal of Histochemistry and Cytochemistry*, Vol. 51, No. 11, pp. 1545-1555.

Ramachandran R, BV. Fausett, D. Goldman, 2010, “Ascl1a Regulates Müller Glia Dedifferentiation And Retinal Regeneration Through A Lin-28-Dependent, Let-7 Microrna Signalling Pathway”, *Nature Cell Biology*, Vol. 12, No. 11, pp. 1101-1107.

Ramer LM., E. Au, MW. Richter, J. Liu, W. Tetzlaff, AJ. Roskams, 2004, “Peripheral Olfactory Ensheathing Cells Reduce Scar And Cavity Formation And Promote Regeneration After Spinal Cord Injury”, *Journal of Comparative Neurology*, Vol. 473, No. 1, pp. 1-15.

Ramón y Cajal, S., 1913, “Estudios Sobre La Degeneración Y Regeneración Del Sistema Nervioso. Tomo I. Degeneración Y Regeneración De Los Nervios” Moya, Madrid.

Pellegrini E., K. Mouriec, I. Anglade, A. Menuet, YLE. Page, M. Gueguen, NE.

Marmignon, 2007, “Identification Of Aromatase-positive Radial Glial Cells As Progenitor Cells In The Ventricular Layer Of The Forebrain In Zebrafish”, *Journal of Comparative Neurology*, Vol. 167, No. 1, pp. 150–167.

Roesch K., AP. Jadhav, JM. Trimarchi, MB. Stadler, B. Roska, BB. Sun, CL. Cepko, 2008, “The Transcriptome Of Retinal Müller Glial Cells”, *Journal of Comparative Neurology*, Vol. 509, No. 2, pp. 225-38.

Roskams AJ., DS. Bredt, TM. Dawson, GV. Ronnett, 1994, “Nitric Oxide Mediates The Formation Of Synaptic Connections In Developing And Regenerating Olfactory Receptor Neurons”, *Neuron*, Vol. 13, No. 2, pp. 289-299.

Roskams AJ., MA. Bethel, KJ. Hurt, GV. Ronnett, 1996, “Sequential Expression Of Trks A, B, And C In The Regenerating Olfactory Neuroepithelium”, *Journal of Neuroscience*, Vol. 16, No. 1, pp.1294–1307.

Roskams AJ., X. Cai, GV. Ronnett, 1998, “Expression Of Neuron-Specific Beta-III Tubulin During Olfactory Neurogenesis In The Embryonic And Adult Rat”, *Neuroscience*, Vol. 83, No. 1, pp. 191-200.

Rothenaigner I., M. Krecsmarik, JA. Hayes, B. Bahn, A. Lepier, G. Fortin, M. Götz, R. Jagasia, L. Bally-Cuif, 2011, “Clonal Analysis By Distinct Viral Vectors Identifies Bona Fide Neural Stem Cells In The Adult Zebrafish Telencephalon And Characterizes Their Division Properties And Fate”, *Development*, Vol. 138, No. 1, pp. 1459–1469.

Sato Y, N. Miyasaka, Y. Yoshihara, 2005, “Mutually Exclusive Glomerular Innervation By Two Distinct Types Of Olfactory Sensory Neurons Revealed In Transgenic

Zebrafish”, *Journal Neuroscience*, Vol. 25, No. 20, pp. 4889-4897.

Satoh M, T. Yoshida, 1997, “Promotion Of Neurogenesis In Mouse Olfactory Neuronal Progenitor Cells By Leukemia Inhibitory Factor *In Vitro*”, *Neuroscience Letters*, Vol. 225, No. 3, pp. 165-168.

Satoh M., T. Yoshida, 2000, “Expression Of Neural Properties In Olfactory Cytokeratin-positive Basal Cell Line”, *Brain Research: Developmental Brain Research*, Vol. 121, No. 2, pp. 219-222.

Sahay A., R. Hen, 2007, “Adult Hippocampal Neurogenesis In Depression” *Nature Neuroscience*, Vol. 10, No. 6, pp. 1110-1115.

Sambrook, J., DW. Russell, 2001, “Molecular Cloning: A Laboratory Manual”, New York, USA, Cold Spring Harbor Laboratory.

Schindelin J., I. Arganda-Carreras, E. Frise, V. Kaynig, M. Longair, T. Pietzsch, S. Preibisch, C. Rueden, S. Saalfeld, B. Schmid, JY. Tinevez, DJ. White, V. Hartenstein, K. Eliceiri, P. Tomancak, A. Cardona, 2012, “Fiji: An Open-source Platform For Biological-Image Analysis”, *Nature Methods*, Vol. 9, No. 7, pp. 676-682.

Schmidt R., U. Strahle, U. Scholpp, 2013, “Neurogenesis In Zebrafish – From Embryo To Adult”, *Neural Development*, Vol. 8, No. 1, pp. 3-16.

Schwob JE., SL. Youngentob, RC. Mezza, 1995, “Reconstitution Of The Rat Olfactory Epithelium After Methyl Bromide-induced Lesion”, *Journal of Comparative Neurology*, Vol. 359, No. 1, pp. 15–37.

Schwob JE., 2002, “Neural Regeneration And The Peripheral Olfactory System” *Anatomical Records*, Vol. 269, No. 14, pp. 33–49.

Shou J., RC. Murray, PC. Rim, AL. Calof, 2000, “Opposing Effects Of Bone Morphogenetic Proteins On Neuron Production And Survival In The Olfactory Receptor Neuron Lineage”, *Development*, Vol. 127, No. 7, pp. 5403–5413.

Suzuki Y., M. Takeda, 1991, “Basal Cells In The Mouse Olfactory Epithelium After Axotomy: Immunohistochemical And Electron-microscopic Studies”, *Cell and Tissue Research*, Vol. 266, No. 2, pp. 239-245.

Tietjen I., JM. Rihel, Y. Cao, G. Koentges, L. Zakhary, C. Dulac, 2003, “Single-cell Transcriptional Analysis Of Neuronal Progenitors”, *Neuron*, Vol. 38, No. 8, pp. 161–175.

Tomita H., S. Ishiguro, T. Abe, M. Tamai, 1998, “Increased Expression Of Low-affinity NGF Receptor In Rat Retinal Müller Cells After Ischemia And Reperfusion”, *Cell Structure and Function*, Vol. 23, No. 4, pp. 201-207.

Tsai L., G. Barnea, 2014, “A Critical Period Defined By Axon-targeting Mechanisms In The Murine Olfactory Bulb”, *Science*, Vol. 344, No. 6180, pp. 197-200.

von Kügelgen I., 2006, “Pharmacological Profiles Of Cloned Mammalian P2Y-receptor Subtypes”, *Pharmacology and Therapeutics*, Vol. 110, No. 1, pp. 415–432.

Walcott JC., JM. Provis, 2003, “Müller Cells Express The Neuronal Progenitor Cell Marker Nestin In Both Differentiated And Undifferentiated Human Foetal Retina”, *Clinical Experiment Ophthalmology*, Vol. 31, No. 13, pp. 246-249.

Wan J., R. Ramachandran, D. Goldman, 2012, "HB-EGF Is Necessary And Sufficient For Müller Glia Dedifferentiation And Retina Regeneration", *Developmental Cell*, Vol. 22, No. 2, pp. 334-347.

Weissman TA., PA. Riquelme, L. Ivic, AC. Flint, AR. Kriegstein, 2004, "Calcium Waves Propagate Through Radial Glial Cells And Modulate Proliferation In The Developing Neocortex", *Neuron*, Vol. 43, No. 5, pp. 647-661.

Westerfield M., 2007, "THE ZEBRAFISH BOOK; A Guide For The Laboratory Use Of Zebrafish (Danio Rerio), 5th Edition.", Eugene: University of Oregon Press.

Woods IG., PD. Kelly, F. Chu, P. Ngo-Hazelett, YL. Yan, H. Huang, JH. Postlethwait, WS. Talbot, 2000, "A Comparative Map Of The Zebrafish Genome" *Genome Research*, Vol. 10, No. 12, pp. 1903-1914.

Zhao C, W. Deng, FH. Gage, 2008, "Mechanisms And Functional Implications Of Adult Neurogenesis", *Cell*, Vol. 132, No. 1, pp. 645-660.

Zupanc GK., I. Horschke, 1995, "Proliferation Zones In The Brain Of Adult Gymnotiform Fish: A Quantitative Mapping Study", *Journal of Comparative Neurology*, Vol. 353, No.1, pp. 213–233.

Zupanc GK., 2001, "Adult Neurogenesis And Neuronal Regeneration In The Central Nervous System Of Teleost Fish", *Brain, Behavior and Evolution*, Vol. 58, No. 5, pp. 250-275.

Zupanc GK., K. Hinsch, FH. Gage, 2005, "Proliferation, Migration, Neuronal Differentiation, And Long-term Survival Of New Cells In The Adult Zebrafish

Brain”, *Journal of Comparative Neurology*, Vol. 488, No. 1, pp. 290–319.

Zupanc GK., 2006, “Neurogenesis And Neuronal Regeneration In The Adult Fish Brain”, *Journal of Comparative Physiology. A, Neuroethology, Sensory, Neural, and Behavioral Physiology*, Vol. 192, No. 6, pp. 649-670.

Zupanc GK., RF. Sîrbulescu, 2011, “Adult Neurogenesis And Neuronal Regeneration In The Central Nervous System Of Teleost Fish”, *European Journal of Neuroscience*, Vol. 34, No. 6, pp. 917-929.